UNCLASSIFIED

SECURITY CLASSIFICATION OF THIS PAGE

AD-A235 454

REPORT

1a. REPORT SECURITY CLASSIFICATION

2a. SECURITY CLASSIFICATION AUTHORITY

2b. DECLASSIFICATION / DOWNGRADING SCHEDULE

3. DISTRIBUTION / AVAILABILITY OF REPORT
Approved for public release; distribution unlimited.

4. PERFORMING ORGANIZATION REPORT NUMBER(S)
AFOSR-88-0086-FT

5. MONITORING ORGANIZATION REPORT NUMBER(S)
AFOSR-TR- 91 0494

6a. NAME OF PERFORMING ORGANIZATION
State of Oregon, acting by and through the State Board of Higher Education, on behalf of the University of Oregon

6b. OFFICE SYMBOL (If applicable)

7a. NAME OF MONITORING ORGANIZATION
AFOSR/NP

6c. ADDRESS (City, State, and ZIP Code)
P. O. Box 3237
Eugene, OR 97403-0237

7b ADDRESS (City, State, and ZIP Code)
Dr. Howard R. Schlossberg
Building 410
Bolling AFB, DC 20332-6448

8a. NAME OF FUNDING / SPONSORING ORGANIZATION
Same as 7a

8b. OFFICE SYMBOL (If applicable)
NP

9. PROCUREMENT INSTRUMENT IDENTIFICATION NUMBER
AFOSR-88-0086

8c. ADDRESS (City, State, and ZIP Code)
Same as 7b

10. SOURCE OF FUNDING NUMBERS

PROGRAM ELEMENT NO.	PROJECT NO.	TASK NO.	WORK UNIT ACCESSION NO
61102F	2301	A1	

11 TITLE (Include Security Classification)
Experimental Studies of Fundamental Problems in Quantum Optics

12. PERSONAL AUTHOR(S)
Mossberg, Thomas W.

13a. TYPE OF REPORT	13b. TIME COVERED	14. DATE OF REPORT (Year, Month, Day)	15. PAGE COUNT
Final Technical	FROM 12/1/87 TO 1/31/91	91/4/15	43

16. SUPPLEMENTARY NOTATION

17. COSATI CODES		
FIELD	GROUP	SUB-GROUP

18. SUBJECT TERMS (Continue on reverse if necessary and identify by block number)
Quantum Optics
Electromagnetic Vacuum
Cavity QED
Two-Photon Laser

19. ABSTRACT (Continue on reverse if necessary and identify by block number)

An extensive study of the dynamical properties of laser driven atoms in optical cavities has been completed. The presence of a cavity is found to produce behavior dramatically different from that exhibited by driven atoms in free space. In the case of mode-degenerate optical cavities, it is found that a laser may drive two-level atoms into steady-state inversion. This has been considered impossible.

20. DISTRIBUTION / AVAILABILITY OF ABSTRACT
☒ UNCLASSIFIED/UNLIMITED ☒ SAME AS RPT ☐ DTIC USERS

21. ABSTRACT SECURITY CLASSIFICATION
UNCLASSIFIED

22a. NAME OF RESPONSIBLE INDIVIDUAL
Dr Howard Schlossberg

22b. TELEPHONE (Include Area Code) 202/767-4906

22c. OFFICE SYMBOL
NP

DD FORM 1473, 84 MAR

83 APR edition may be used until exhausted.
All other editions are obsolete.

SECURITY CLASSIFICATION OF THIS PAGE
UNCLASSIFIED

Report AFOSR-88-0086-FT

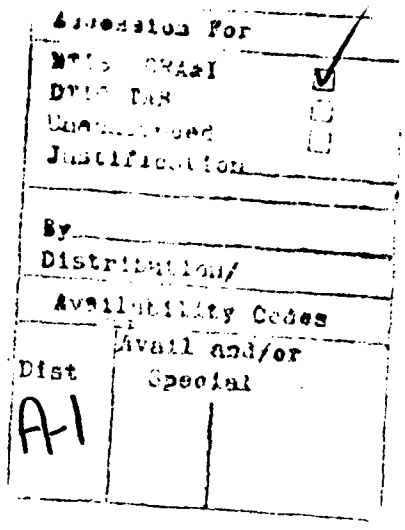

Experimental Studies of Fundamental Problems in Quantum Optics

Thomas W. Mossberg
Department of Physics
University of Oregon
Eugene, Oregon 97403
(503) 346-4779

April 14, 1991

Final Technical Report for Period 1 December 1987 - 31 January 1991

Prepared for:
Air Force Office of Scientific Research
Building 410
Bolling AFB DC 20332-6448

Summary

An extensive study of the dynamical properties of laser driven atoms in optical cavities has been completed. The presence of a cavity is found to produce behavior dramatically different from that exhibited by driven atoms in free space. In the case of mode-degenerate optical cavities, it is found that a laser field may drive two-level atoms into steady-state inversion. This has been considered impossible. Such cavities are also found to perturb fundamental strong-field atomic spectra. These perturbations indicate novel and previously unseen atomic dynamics. Inasmuch as any small structure may produce effects similar to those produced by a cavity, the results of the present experiments demonstrate that small optical devices may be operable in heretofore totally unanticipated regimes. We have also found that driven atoms in a cavity exhibit two-photon gain and may form the basis of the first cw two-photon laser. Already the first measurements of cw two-photon gain have been completed. We have theoretically analyzed to behavior of both one and two-photon driven atom lasers, and find that both may exhibit bright squeezing. In other words, these lasers have a squeezed-state output field rather than a coherent-state output.

Discoveries

1. The steady-state inversion of driven atoms was shown to be influenced by the spectral structure of the electromagnetic vacuum to which the atoms are coupled. In some cases, steady-state positive inversions arise. Heretofore, positive inversions in optically driven two-level atoms have been considered impossible. Using a cavity to perturb the vacuum, we have experimentally demonstrated increases in steady-state atomic excitation.

2. We have shown that depending on the precise configuration of walls and boundaries, driven atoms may exhibit dynamics radically different than in the well studied case of atoms in free space.

3. We have demonstrated one-photon lasing with cavity-confined optically driven **two-level** atoms as the gain medium.

4. We have made the world's first observation of cw two-photon gain.

5. We have theoretically demonstrated that driven two-level atoms may be employed as a gain medium to realize the first two-photon laser.

6. We have experimentally demonstrated that the effect of quantum fluctuations on a strong atomic transition can be suppressed in three-level atoms through the optical excitation of a weak transition coupled to the strong one.

7. We have experimentally demonstrated for the first time that atoms driven by a bichromatic excitation field exhibit a spectrum dramatically different from that known in the case of monochromatic excitation.

Description of Results

Original Statement of Work:

> We propose to undertake a comprehensive program of experimental studies aimed at the elucidation of fundamental problems in quantum optics. This program will include studies of the production of squeezed light using second harmonic generation, the interaction of squeezed light with two-level atoms under clean experimental conditions, the coupling of atoms to vacuum fluctuations of the electromagnetic field, the spectra of atoms in cavities, the creation of steady-state samples of atoms in pure dressed states, and the creation of squeezed atoms.

Throughout the three years of support provided by AFOSR, we obtained results in most of the areas specified. As is the nature of basic research, however, we discovered a number of unanticipated effects as important or more important than those mentioned in the original statement of work. Some of the available effort was therefore diverted to their study. As a result of AFOSR support, we produced 10 publications in refereed journals. Four of these publications have appeared in Phys. Rev. Lett. and a fifth is currently under consideration. Another three of the publications appeared in the Rapid Communications section of Physical Review A. A brief description of results obtained is given below.

Environmental Effects on Driven-Atom Dynamics

Driven two-level atoms in free space eventually come to a steady-state with the laser field that is driving them, and it is considered a fundamental result that the steady-state achieved can never be one displaying positive inversion. In the asymptotic case of an infinitely strong driving field, the atomic inversion approaches zero as an upper limit, indicating that the two atomic states become equally populated. In our theoretical and experimental studies, we have found that the situation can be dramatically different when

the driven atoms are not in free space, but rather are contained inside some structure reminiscent of an optical cavity.

In the traditional treatments of driven-atom dynamics, the steady-state condition of driven atoms is determined by the atom-field detuning, the strength of the driving field (conveniently expressed in terms of the driving-field Rabi frequency), and the density of electromagnetic modes at the atomic transition frequency. The latter quantity, the electromagnetic mode density, enters via the use of Fermi's Golden Rule in determining the rate of spontaneous emission. We have pointed out that in cavity-like structures, the rapid variation of electromagnetic mode density as a function of frequency leads to a failure of Fermi's Golden Rule and thus opens up entirely new vistas of atomic behavior. Using a particular type of optical cavity, a confocal one, we have experimentally demonstrated that the steady-state condition of driven atoms within the cavity can be modified simply by tuning the resonance frequency of the cavity in the vicinity of the atomic resonance frequency. In these situations, the driving field propagates orthogonal to the cavity axis so that tuning the cavity has no effect on the atom-laser field coupling. The cavity only affects the spontaneous decay of the atoms.

We experimentally demonstrated (Phys. Rev. Lett. **61**, 1946 (1988)) that the steady-state atomic inversion is enhanced for some cavity tunings and suppressed for others. Experimental limitations prevented us from demonstrating the creation of a positive steady-state inversion, but our theoretical analysis indicates that in suitable cavities, nearly 100 percent inversions can be achieved.

Our work demonstrates that the behavior of driven atoms in optical cavities can be qualitatively different from that of atoms in free space. In the world of optical devices, atoms are often exposed to strong fields and confined within cavity-like structures. One can not help but speculate that the new behavior we have predicted and demonstrated will lead to the possibility of previously unexpected device properties. By controlling the physical structure of small optical devices, the electromagnetic reservoir and hence atom response can be controlled and even made to exhibit features heretofore considered impossible.

These effects are intimately related to those discussed in relation to Photonic Bandgaps. Unfortunately, there have been no experimental demonstrations of perturbed driven atom dynamics in that area

Spectra of Driven Atoms in Cavities

In an area closely related to that described in the previous section, we have studied cavity-induced perturbations of the strong-field atomic fluorescence spectra. In these experiments the atoms were driven by a laser oriented orthogonal to an open-sided confocal cavity, and fluorescence emitted out the sides of the cavity was detected. The confining cavity affected the driven atoms only through its modification of the electromagnetic vacuum.

Normally, the strong field spectrum consists of a symmetric triplet. We found that by tuning the cavity into resonance with one of the sidebands of this spectrum a spectral asymmetry was introduced. On analysis, one can show that the observed asymmetry indicates that the cavity has created an imbalance in the populations of the atom-field dressed states. These states are eigenstates of the combined atom-field system and in the case of resonant excitation they are equally populated. An unbalancing of the dressed-state levels modifies, for example, the gain exhibited by the system. In some regimes, this effect leads to a squeezing of the atomic wavefunction. The results of our experimental observations have been published in the Rapid Communications section of Physical Review A.

One-Photon Lasing in an Ensemble of Driven Two-level Atoms

Again exploring the system comprised of driven two-level atoms confined within a cavity, we have explored the effects of gain on the atomic emission spectrum. We have studied the spectrum of atomic fluorescence emitted into the cavity modes as a function of

the number of atoms confined within the cavity. In situations in which the driving field is detuned from the atomic resonance by an amount comparable to the resonant Rabi frequency, we find that two-level-atom gain distorts the emission spectrum by strongly enhancing it at certain emission frequencies.

At higher atomic densities, the threshold for lasing is crossed and the ensemble of driven two-level atoms lases into the cavity modes. It should be noted that this lasing occurs in a two-level atomic system in which an inversion of the upper state relative to the lower state is never achieved. In many respects, the gain observed in this system is similar to the "inversionless" gain reported recently in other model systems. The lasing in the driven two-level atom system is true lasing in the sense that phase matching and wave mixing play no role.

The dynamics of lasing of this system can be best understood in the dressed-atom picture. In the case of non-zero laser-atom detuning, an inversion between certain pairs of dressed levels exists, and the lasing we observe occurs on such an inverted transition. Dressed levels form ladder of doublets and the lasing process drives the system down this ladder. On analysis it is found that cascading down this ladder of dressed doublets results in an increase in population of the atomic excited state. **In other words, lasing in the two-level atom occurs from the ground to the excited state - increasing atomic energy.** Of course the energy necessary to increase the atomic energy while simultaneously undergoing lasing is provided by the pump field. The dynamics of this laser are unique and rich in novel features. The two-level laser action occurs in an experimental regime relatively unexplored (strongly driven two-level atoms in cavities), and as this work and the work of the two previous sections indicates a wealth of fundamental new phenomenology associated with this regime is waiting to be discovered.

Two-Photon Gain and Lasing in Systems of Driven Two-Level Atoms

In our work on one-photon lasing in an ensemble of two-level atoms, it became clear to us that **two-photon** lasing could be produced in the same system. In fact, the driven atom system is nearly an ideal two-photon amplifier. The eigenstates of the driven atom form a ladder of equally spaced doublets. Two-photon transitions between these states are inverted, and possess nearly resonant intermediate states. There are essentially no competing one-photon processes to overwhelm the two-photon gain. It is to be noted that two-photon lasers are expected to display characteristics very different than those of the well-known one-photon laser. Regarding threshold conditions in particular, the two-photon laser is expected to stay off until it is started by a trigger field, i. e. its off-state is stable even though the two-photon inversion may be large enough to support lasing. The two-photon laser is bistable in the sense that once triggered it will stay on. We have already made the first observation of cw two-photon gain, and were on the verge of achieving two-photon oscillation at the end of our three-year funding cycle. Unfortunately, AFOSR has decided not to renew our support so that work along these lines and several others may have to come to a stop.

Coherent Stabilization of Quantum Fluctuations

We have studied the effect of a strong laser field on the coherence properties of V-type three-level atoms. In the case when one of the atomic transitions is weak and one is strong, we have shown that the application of a strong laser field to the weak transition acts to stabilize the atom with respect to quantum fluctuations acting on the strong atomic transition. This effect is observed by monitoring the natural linewidth of fluorescence emitted on the strong atomic transition as a function of the strength of the laser field driving the weak atomic transition. It is found that the natural linewidth of the strong transition narrows and eventually becomes significantly narrower than its normal, free-space, undriven value. These work demonstrates as do several of the sections above that many of the parameters affecting atom-field interactions are not the fixed constants they were once

invariably taken to be.

Summary

We have conducted a vigorous investigation into a number of fundamental aspects of the interaction of light with atoms. Our work has revealed that many of the most fundamental aspects of our understanding of the dynamics of even the simple driven two-level atom are incomplete. It is unfortunate that continued funding for this work is not available, because it would seem that entirely new regimes of atom-photon interactions remain to be elucidated - regimes that may lead to optical devices and phenomena previously unknown or thought to be impossible.

Publications

1. Vacuum-Field Dressed-State Pumping, Y. Zhu, A. Lezama, and T. W. Mossberg, Phys. Rev. Lett. **61**, 1946 (1988)

2. Cavity-Perturbed Strong-Field Resonance Fluorescence, A. Lezama, Y. Zhu, S. Morin, and T. W. Mossberg, Phys. Rev. A (Rapid Communications) **39**, 2754 (1989).

3. Effect of Optical Gain on the Fluorescence of Two-Level Atoms into the Modes of an Optical Cavity, Y. Zhu, A. Lezama, and T. W. Mossberg, Phys. Rev. A (Rapid Communications) **39**, 2268 (1989).

4. Radiative Emission of Driven Two-Level Atoms into the Modes of an Enclosing Optical Cavity: The transition from fluorescence to lasing, A. Lezama, Y. Zhu, M. Kanskar, and T. W. Mossberg, Phys. Rev. A **41**, 1576 (1990).

5. Two-Photon Gain and Lasing in Strongly Driven Two-Level Atoms, M. Lewenstein, Y. Zhu, and T. W. Mossberg, Phys. Rev. Lett. **64**, 3131 (1990).

6. Resonance Fluorescence of Two-Level Atoms Under Strong Bichromatic Excitation, Y. Zhu, Q. Wu, A. Lezama, T. W. Mossberg, Phys. Rev. A (Rapid Communications) **41**, 6574 (1990).

7. Vacuum Rabi Splitting as a Feature of Linear Dispersion Theory: Analysis and Experimental Observations, Y. Zhu, D. J. Gauthier, S. E. Morin, Q. Wu, H. J. Carmichael, and T. W. Mossberg, Phys. Rev. Lett. **64**, 2499 (1990).

8. Observation of a Two-Photon Gain Feature in the Strong Probe Absorption Spectrum of Driven Two-Level Atoms, Y. Zhu, Q. Wu, w. Morin, and T. W. Mossberg, Phys. Rev. Lett. **65**, 1200 (1990).

9. Spectrum of Radiation from Atoms under Intense Bichromatic Excitation, G. S. Agarwal, Yifu Zhu, D. J. Gauthier, and T. W. Mossberg, accepted for publication in J. Opt. Soc. Am. B.

10. Observation of Linewidth Narrowing due to Coherent Stabilization of Quantum Fluctuations, D. J. Gauthier, Yifu Zhu, and T. W. Mossberg, submitted to Phys. Rev. Lett.

Presentations

Work supported by this grant has been presented at a number of scientific meetings. Only those given as invited talks are listed here.

QELS '89 - Baltimore Apr. 23-28 (2 invited talks).
6th Rochester Conf. on Coherence and Quantum Optics - June '89.
1989 Atomic Physics Gordon Conference.
ILS conference 1989 at Stanford University.
International School on Quantum Electronics, Polish Academy of Sciences, Sept. 1989.
U. S. - Japan Seminar on Quantum Electronics, 1990, Kyoto, Japan.
International Quantum Optics Conference, 1991, Hyderabad, India.
IQEC '91, Baltimore, May 1991.

Research Staff

Prof. Thomas W. Mossberg
Dr. D. J. Gauthier
Dr. Arturo Lezama
Dr. Yifu Zhu
Ms. Qilin Wu
Mr. Steven Morin
Mr. Manoj Kanskar

Vacuum-Field Dressed-State Pumping

Yifu Zhu, A. Lezama, and T. W. Mossberg
Department of Physics, University of Oregon, Eugene, Oregon 97403

M. Lewenstein
Institute for Theoretical Physics, Polish Academy of Sciences, 02-668 Warsaw, Poland
(Received 27 July 1988)

The steady-state behavior of two-level atoms, driven by a strong field and relaxing into a frequency-dependent vacuum reservoir, has been studied in an experiment involving Ba atoms in a confocal cavity. Enhancement or suppression of the atomic excitation is observed when the cavity is tuned to either of the strong-field fluorescence sidebands. These effects result from a redistribution of the population among the dressed atom-field states induced by the cavity-modified vacuum field. The enhancement effect may be useful in achieving significant steady-state inversion.

PACS numbers: 42.50.Hz, 32.80.−t, 42.80.Jr

The influence of environment on spontaneous radiative decay properties has attracted considerable attention in recent years. It has been predicted[1] that cavity-confined atoms may experience an inhibition of spontaneous emission because of a cavity-induced reduction in resonant electromagnetic-mode density. The veracity of this prediction has been demonstrated in a number of experiments in the microwave,[2,3] infrared,[4] and optical[5–8] regimes. The opposite effect in which the spontaneous decay rate is enhanced over its free-space value because of a cavity-induced increase in mode density has also been reported.[6,8,9] These results have stimulated a number of theoretical works related to modified spontaneous emission under various special circumstances.[10–14]

In all of the work above, with the exception of the recent radiative line-shift measurements,[6] the spectral structure of the cavity-modified electromagnetic-mode density (i.e., of the vacuum reservoir) has not played a significant role. Entirely new phenomena including dynamical suppression of spontaneous emission,[15,16] non-Lorentzian radiative line shapes,[17] dressed-state pumping,[16] and atomic squeezing[18] have been predicted to occur in cases where the vacuum reservoir is frequency dependent on a scale comparable to or finer than the atomic resonance width. These effects are especially interesting because they can be viewed as resulting from the existence of a finite memory time in the cavity-modified vacuum reservoir.

We report here the first experimental study of atomic relaxation dynamics as perturbed by a frequency-dependent vacuum reservoir. Specifically, we have studied the modification of excited-state population in strongly driven atoms induced by tuning a cavity resonance, which corresponds to a peak in the vacuum-mode density, across the atomic fluorescence line shape. It is found that atomic excitation can be enhanced or suppressed depending on the spectral location of the vacuum-mode-density peak relative to the center of the atomic fluorescence line.

A simple theoretical description of the basic phenomena involved can be obtained by consideration of a two-level atom having a transition frequency ν_0 and a ground (excited) state $|g\rangle$ ($|e\rangle$) with population n_g (n_e) that is driven by a strong optical field of frequency ν_l. Let $\Delta=(\nu_l-\nu_0)$. The atom-field system is assumed to decay via coupling to a frequency-dependent vacuum reservoir. We describe our system in terms of the atom-field dressed states,[19,20] which consist of a ladder of doublets separated in frequency by ν_l and split by the generalized Rabi frequency (see Fig. 1). In the dressed-atom picture, the spontaneous-emission process consists of transitions between levels of adjacent doublets and the creation of reservoir photons. At steady state, we must have[19]

$$\Gamma_{12}\Pi_1=\Gamma_{21}\Pi_2, \tag{1}$$

where Π_1 (Π_2) represents the total population, summed over the photon number, of the upper (lower) component of the dressed-state doublet and Γ_{12} and Γ_{21} are spon-

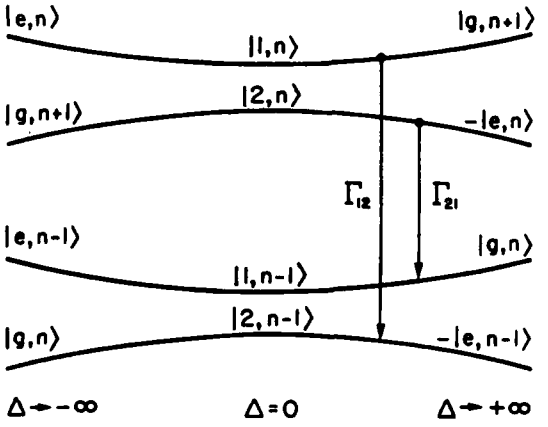

FIG. 1. Schematic energy diagram of two atom-field dressed-state doublets. The product states at the right (left) represent asymptotic forms at large positive (negative) Δ.

taneous decay rates (see Fig. 1). We may write the decay rates in the form

$$\Gamma_{ij} = \rho_{ij} d_{ij} \quad (i,j = 1,2); \tag{2}$$

here d_{ij} is proportional to the square of the atomic dipole matrix element between the considered dressed states and ρ_{ij} is a factor proportional to the photon-mode density at the corresponding transition frequency. After evaluation of the atomic dipole matrix elements, one can immediately deduce the steady-state values of Π_1 and Π_2, and, consequently, of n_e:

$$n_e = \frac{\rho_{21}\cos^2\theta\sin^4\theta + \rho_{12}\cos^4\theta\sin^2\theta}{\rho_{21}\sin^4\theta + \rho_{12}\cos^4\theta}, \tag{3}$$

where $\tan(2\theta) = -\Omega_R/\Delta$ $(0 \le \theta \le \pi/2)$ and Ω_R is the on-resonance Rabi frequency. Equation (3) states that we can control the excited-state atomic population by changing the relative values of ρ_{12} and ρ_{21}. The imbalance between the mode densities at the frequencies corresponding to the 12 and 21 transitions results in an optical pumping of the dressed state and consequently of the bare atomic states. This effect, which one might term *vacuum-field dressed-state pumping*, was predicted by Lewenstein and Mossberg.[16] Significantly, note that for

$$\rho_{12}/\rho_{21} < \tan^4\theta \quad (\Delta < 0),$$

or

$$\rho_{12}/\rho_{21} > \tan^4\theta \quad (\Delta > 0),$$

a steady-state positive atomic inversion can be realized. If $\rho_{ij}/\rho_{ji} = 10$, a maximum steady-state inversion $(n_e - n_g)$ of $\simeq 0.15$ is predicted. In our experiment, ρ_{ij} and ρ_{ji} differed by only 5% and no attempt was made to ascertain whether or not the small positive inversion expected did in fact occur.

In our experiment, a beam of atomic Ba was made to pass through the center and normal to the axis of a 1-cm symmetric confocal optical cavity. The mode degeneracy of this type of cavity is known[5] to give rise to a frequency-dependent photon-mode density. The atomic beam was 200 μm in diameter and had a collimation of 1:280. The cavity mirrors were spherical with 1-cm radius of curvature and had a specified reflectivity of 99.3%. Cavity finesse measured with a collimated 1-mm-diam laser beam was typically 180. The cavity mirrors were mounted in an Invar holder which was equipped with a piezoelectric transducer for cavity tuning and temperature stabilized to 10 mK. The reflecting surface of one of the 5-mm-diam mirrors was limited by an intracavity aperture of 2.2 mm in diameter. The 553.5-nm $6s^2\,{}^1S_0$-$6s6p\,{}^1P_1$ barium resonance line was driven by the output of a cw ring dye laser propagating normal to both the cavity axis and the barium beam. With a saturation resonance in an auxiliary Ba vapor cell, the laser frequency could be actively locked anywhere within ± 500 MHz of ν_0. Laser-field inhomogeneity was minimized by our passing the beam through an aperture and then imaging the aperture into the laser-atom interaction region. In the interaction region, the laser beam had a 150 μm diameter and $\simeq 10$ mw power. At any instant, approximately 50 atoms were within the interaction volume. The magnetic field at the interaction region was minimized with the help of external magnetic coils so that the residual Zeeman splitting was smaller than $\frac{1}{10}$ of the $\simeq 19$-MHz natural linewidth. The excitation laser was linearly polarized perpendicular to the cavity axis.

Atomic fluorescence was simultaneously monitored along the cavity axis and nearly perpendicular to it. In the latter case, imaging optics and spatial filtering were employed to collect only those photons that were emitted by atoms in a 130-μm-diam spot within the interaction region and which propagated along a direction 10° away from antiparallel with the laser beam and normal to the atomic beam. Light detected out the cavity's side was not frequency selected and thus provided a direct measure of the excited-state population of the atoms.[19] The total solid angle collected to the side was 2.5×10^{-3} sr. The two signal directions described above are referred to as the axial and side fluorescence signals, respectively.

Figure 2 shows the variation in the side fluorescence signal, generated by weak resonant excitation, as the spacing between the cavity mirrors (and hence the cavity resonance frequency) is swept. The drop in side fluorescence intensity results from a reduction in the steady-state, excited-state, and atomic population, which in turn results from a cavity-induced enhancement in the atomic spontaneous decay rate. The change in the atomic decay rate occurs because the intracavity mode density is frequency dependent (being maximum near the cavity resonance frequency) and tunes with the cavity. Importantly for the analysis that follows, in the weak excitation limit, the side fluorescence intensity is proportional to the inverse square of the mode density.[6]

Quantitative calculations concerning vacuum-field dressed-state pumping in our cavity require complete knowledge of the cavity's spatial and spectral mode distribution. Rather than attempt to calculate this distribution, we directly deduce, using the inverse square depen-

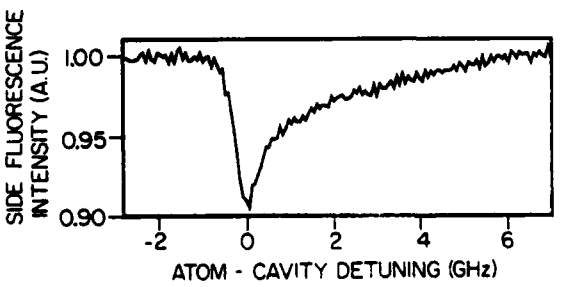

FIG. 2. Side fluorescence intensity vs atom-cavity detuning in the case of weak resonant excitation.

dence mentioned above, the spatially averaged spectral mode distribution from the cavity-modified fluorescence data of Fig. 2. Interestingly, the 10% dip in side fluorescence intensity indicates only a 5% variation in cavity-mode density as a function of frequency. The asymmetric structure of the cavity-mode distribution deduced from Fig. 2 can be qualitatively understood in terms of the geometric properties of the spherical mirror resonator.[21] Note that in the case of a weak excitation field, our vacuum reservoir is essentially constant over the atomic resonance line. This is not true in the strong-excitation-field regime reported below.

In Figs. 3(a)–3(c) (heavy solid lines), we show the measured side fluorescence intensity as a function of cavity tuning in the case of excitation by a strong laser field ($\Omega_R \simeq 600$ MHz) and with $\Delta = 320$, 0, and -320 MHz, respectively. Figure 3(d) shows the axial fluorescence signal recorded simultaneously with the side fluorescence signal of Fig. 3(a). The familiar Mollow resonance fluorescence triplet is observed.[19,20,22] The behavior of the side fluorescence in Fig. 3(b) is strikingly different from that observed in Fig. 2 in that the dip observed in Fig. 2 is completely absent. Furthermore, in Figs. 3(a) and 3(c), we see not only reductions in the side fluorescence intensity, but also enhancements. The presence of both reductions and enhancements of side fluorescence intensity indicate cavity-mediated increases in excited-state atomic population as well as decreases. It is clear that the modifications of the excited-state atomic population occur when the cavity is tuned to resonance with the sidebands of the Mollow triplet [and hence enhances the mode density at the 12 or 21 dressed-state transition frequency (see Fig. 1)]. For $\Delta > 0$ ($\Delta < 0$), *enhanced* atomic excitation occurs when the cavity is tuned to increase the mode density at the higher-frequency (lower-frequency) sideband of the resonance fluorescence triplet.

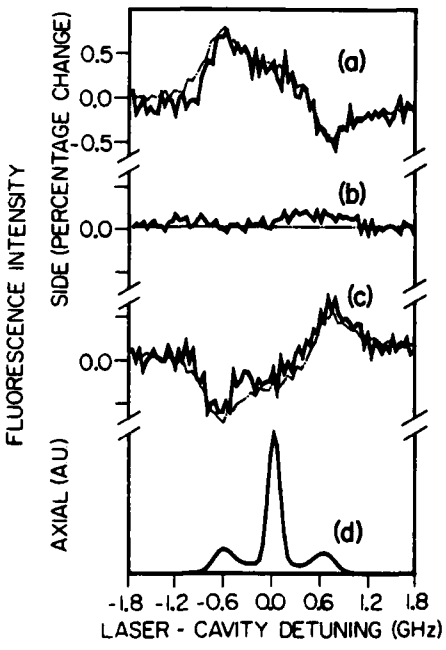

FIG. 3. (a)–(c) Side and (d) axial fluorescence intensity vs laser-cavity detuning in the case of strong excitation. Laser-atom detunings, Δ, are fixed and equal to $+320$, 0, -320, and $+320$ MHz in (a)–(d), respectively. The vertical axis for parts (a)–(c) represents percentage change relative to the average side fluorescence intensity observed for large laser-cavity detunings. In each case (a)–(c), one division represents 0.5% change. (a) and (d) were recorded simultaneously.

Interestingly, our model predicts that dressed-state pumping occurs for all three detunings studied in Fig. 3. Because of the detuning-dependent decomposition of the dressed states in terms of bare atomic states, however, at $\Delta = 0$ the expected dressed-state pumping does not lead to a change in atomic excited-state population. Note, however, that in an entirely different regime, a two-level atom interacting with a single resonant cavity mode has been predicted[23] to display a positive inversion provided that the mode is occupied by only a few photons.

To test the hypothesis that vacuum-field dressed-state pumping is responsible for the effects shown in Figs. 3(a)–3(c), we have employed Eq. (3) together with the spatially averaged spectral mode density as deduced from Fig. 2 to predict the magnitude and shape of the pumping resonance. The results of the simulation are shown as thin dash-dotted lines in Figs. 3(a)–3(c). The fluctuations in the dash-dotted line result from the use of the unsmoothed data from Fig. 2 to deduce the spectral mode density. The simulation is in excellent agreement with the observed results both in terms of magnitude and shape.

In summary, we have provided the first experimental demonstration of vacuum-field, dressed-state pumping, an effect whose existence depends on the modification of free-space spontaneous decay by a *frequency-dependent*, finite-correlation-time vacuum reservoir. By substituting highly corrected large-diameter optical components for the spherical mirrors employed in our cavity, one could reasonably expect to increase the cavity-induced change in mode density by 1 to 2 orders of magnitude compared to that observed here.[24] In this case, vacuum-field dressed-state pumping may provide for the establishment of a significant steady-state positive inversion in samples of two-level atoms.

We gratefully acknowledge financial support from the Air Force Office of Scientific Research (Grant No. AFOSR-88-0086) and the National Science Foundation (Grant No. PHY-8718518). One of us (A.L.) acknowledges support from the Conselho Nacional de Desenvolvimento Cientifico e Tecnologico (Brazil). We thank Y. S. Bai for assistance in the early stages of this experiment and acknowledge conversations with M. Feld.

[1]D. Kleppner, Phys. Rev. Lett. 47, 233 (1981).

[2]G. Gabrielse and H. Dehmelt, Phys. Rev. Lett. **55**, 67 (1985).

[3]R. G. Hulet, E. S. Hilfer, and D. Kleppner, Phys. Rev. Lett. **55**, 2137 (1985).

[4]W. Jhe, A. Anderson, E. A. Hinds, D. Meschede, L. Moi, and S. Haroche, Phys. Rev. Lett. **58**, 666 (1987).

[5]D. J. Heinzen, J. J. Childs, J. E. Thomas, and M. S. Feld, Phys. Rev. Lett. **58**, 1320 (1987).

[6]D. J. Heinzen and M. S. Feld, Phys. Rev. Lett. **59**, 2623 (1987).

[7]F. De Martini, G. Innocenti, G. R. Jacobovitz, and P. Mataloni, Phys. Rev. Lett. **59**, 2955 (1987).

[8]F. De Martini and G. R. Jacobovitz, Phys. Rev. Lett. **60**, 1711 (1988).

[9]P. Goy, J. M. Raimond, M. Gross, and S. Haroche, Phys. Rev. Lett. **50**, 1903 (1983).

[10]E. Yablonovitch, Phys. Rev. Lett. **58**, 2059 (1987).

[11]E. J. Bochove, Phys. Rev. Lett. **59**, 2547 (1987).

[12]A. M. Cetto and L. de la Pena, Phys. Rev. A **37**, 1960 (1988).

[13]J. Parker and C. R. Stroud, Jr., Phys. Rev. A **35**, 4226 (1987).

[14]H. F. Arnoldus and T. F. George, Phys. Rev. A **37**, 761 (1988).

[15]M. Lewenstein, T. W. Mossberg, and R. J. Glauber, Phys. Rev. Lett. **59**, 775 (1987).

[16]M. Lewenstein and T. W. Mossberg, Phys. Rev. A **37**, 2048 (1988).

[17]M. Lewenstein, J. Zakrzewski, and T. W. Mossberg, Phys. Rev. A **38**, 808 (1988).

[18]M. Lewenstein and T. W. Mossberg, Phys. Rev. A **38**, 1075 (1988).

[19]C. Cohen-Tannoudji and S. Reynaud, J. Phys. B **10**, 345 (1977); C. Cohen-Tannoudji, in *Frontiers in Laser Spectroscopy*, Les Houches Lectures, Session XXVII, edited by R. Balian, S. Haroche, and S. Liberman (North-Holland, New York, 1977).

[20]P. L. Knight and P. W. Milonni, Phys. Rep. **66**, 21 (1980).

[21]M. Hercher, Appl. Opt. **7**, 951 (1968).

[22]B. R. Mollow, Phys. Rev. **188**, 1969 (1969).

[23]C. M. Savage, Phys. Rev. Lett. **60**, 1828 (1988).

[24]Cavity-induced mode-density modifications larger than those observed in the present experiment have been reported (Ref. 6) by use of concentric spherical mirror cavities. The spatial volume over which this modified mode density exists, however, is considerably smaller than in confocal cavities.

PHYSICAL REVIEW A VOLUME 39, NUMBER 5 MARCH 1, 1989

Rapid Communications

The Rapid Communications section is intended for the accelerated publication of important new results. Since manuscripts submitted to this section are given priority treatment both in the editorial office and in production, authors should explain in their submittal letter why the work justifies this special handling. A Rapid Communication should be no longer than 3½ printed pages and must be accompanied by an abstract. Page proofs are sent to authors, but, because of the accelerated schedule, publication is not delayed for receipt of corrections unless requested by the author or noted by the editor.

Cavity-perturbed strong-field resonance fluorescence

A. Lezama, Yifu Zhu, S. Morin, and T. W. Mossberg
Department of Physics and Chemical Physics Institute, University of Oregon, Eugene, Oregon 97403
(Received 3 October 1988)

The spectrum of light emitted out the sides of a confocal mode-degenerate optical cavity by Ba atoms driven by a strong, resonant, excitation field has been studied. The cavity is found to induce asymmetries in the classic three-peaked Mollow spectrum. These asymmetries are explained primarily in terms of a spectral structure introduced into the electromagnetic vacuum reservoir by the cavity.

A two-level atom relaxing only via coupling to the electromagnetic vacuum reservoir constitutes a fundamental system whose study provides important insight into the light-matter interaction.[1-3] Of special interest over the last several years have been situations in which atoms are coupled to a vacuum reservoir that is different from the vacuum reservoir characteristic of free space. Such situations generally arise when the free-space vacuum is perturbed by the imposition of various types of special boundary conditions.[4-16] Already, several radiative properties, e.g., spontaneous emission rates,[5-9,11,12] natural radiative line shapes,[13] and radiative level shifts,[13] have been experimentally investigated in the presence of perturbed vacuum reservoirs. A newer aspect of this problem involves the properties of *strongly driven* two-level atoms in the presence of a perturbed vacuum.[17] A number of interesting effects including vacuum-field dressed-state pumping and modifications of the strong-field resonance spectrum (Mollow spectrum[18-21]) have been predicted. An experimental observation of the former effect has just been reported.[22]

We report here on the first experimental study of strong-field resonance fluorescence under conditions designed to highlight the effect of a perturbed vacuum reservoir on its spectrum. Atoms are observed as they pass through a mode-degenerate optical cavity which introduces relatively narrow, tunable, peaks in the spectral density of electromagnetic modes.[12,13] The mode-density peaks occur at frequencies corresponding to cavity resonances. Measuring the spectrum of atomic fluorescence emitted out the side of the cavity, we find that either of the Mollow fluorescence sidebands can be reduced in amplitude by tuning the cavity into resonance with it. Simultaneously, the sideband on the opposite side of the spectrum, which is not resonant with the cavity, is enhanced. The changes in sideband amplitude, while small, are clearly observable and are in reasonable agreement with recent theoretical predictions.[17] It should be noted that an early measurement[20] of the Mollow spectrum was accomplished using the axial emission of atoms contained within a confocal optical cavity. This experiment, which was analyzed in the context of a free-space experiment, employed a substantially larger cavity. As a result, the cavity perturbed the vacuum reservoir to a significantly smaller extent than the cavity employed in the present experiment,[12] and no effects specifically related to the cavity's presence were discerned.

A schematic of the experimental apparatus is shown in Fig. 1. A cw single-mode ring dye laser (≈1 MHz linewidth) is actively locked to the $6s^2\,{}^1S_0$–$6s6p\,{}^1P_1$ resonance of ^{138}Ba and sent through a sharp-edged aperture which is imaged into the center of a confocal optical cavity. The laser enters the cavity from the side and passes through its center with a diameter of 300 μm. A collimat-

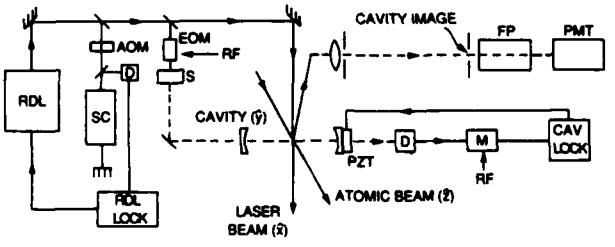

FIG. 1. Experimental schematic. RDL, single-mode ring dye laser; AOM, acousto-optic modulator; SC, barium saturation resonance vapor cell (to lock RDL); D, photodetector; EOM, electro-optic phase modulator; S, shutter; RF, radio-frequency signal used in the FM-spectroscopic locking of the cavity; PZT, piezoelectric transducer used to tune the cavity; M, radio-frequency mixer used in FM detection of the cavity resonance; FP, 7.5-GHz free-spectral-range scanning confocal Fabry-Perot interferometer; PMT, photomultiplier tube to detect fluorescence signal.

ed barium beam of natural isotopic composition and 200-μm diam also enters the cavity from the side and intersects the laser beam at the cavity center. The laser, atomic beam, and cavity axis are mutually orthogonal. The cavity, actively locked at controllable detunings relative to the laser frequency, is 1 cm in length and has spherical mirrors of 5-mm diam. The cavity displays a finesse of 200–300 when measured using restricted mirror apertures. Experiments similar to those reported elsewhere,[13,22] reveal that the cavity produces 600-MHz full width at half maximum (FWHM) mode-density peaks having a maximum mode density $\simeq$4%–6% above the free-space value. The mode-density peaks are asymmetric with a sharp rise (gentle falloff) on the low- (high-) frequency side. Fluorescence, originating from within a small spatial region $\simeq 150\,\mu$m across and emitted into a fractional solid angle of $\simeq 3\times10^{-5}$ in a direction normal to the atomic beam and nearly antiparallel to the laser beam, was collected and passed through a 1-cm, temperature-stabilized, confocal, Fabry-Perot spectrum analyzer. The excitation field was linearly polarized with the E vector normal to the cavity axis, and coils were employed to reduce the ambient magnetic field to the order of 1 G or less. At the highest atomic densities employed, the weak-signal, line-center, ^{138}Ba beam absorption was $\simeq$1%.

In Fig. 2, we show two Mollow spectra recorded in the case of resonant excitation of zero nuclear spin ^{138}Ba (72% natural isotopic abundance). The spectra, which are actually centered at the same frequency, were shifted along the frequency axis in order to make their differences more apparent. In the case of the solid (dashed) curve, the cavity, and hence the vacuum-mode-density peak, was tuned to resonance with the lower- (higher-) frequency Mollow sideband. Note that the adjacent cavity modes are separated by 7.5 GHz, the cavity-free spectral range, and are thus well removed from the atomic resonance.

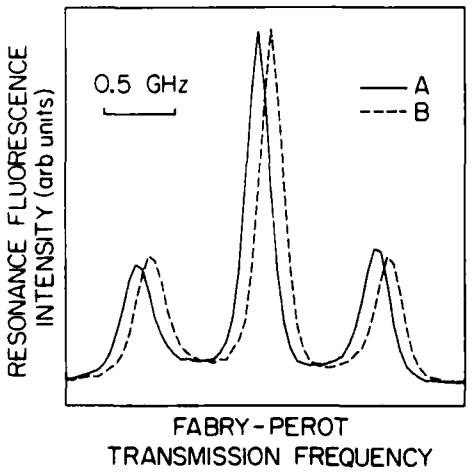

FIG. 2. Strong-field resonance fluorescence spectra observed out the side of a 1-cm confocal mode-degenerate optical cavity. The spectra actually coincide in frequency but were shifted relative to one another along the frequency axis for clarity. For the solid (dashed) trace, the cavity is tuned to the lower (higher) frequency sideband. Frequency increases to the right.

Considerable care was taken to ensure that the spectral modification apparent in Fig. 2 resulted from the tuning of the vacuum mode-density peak to one sideband or to the other and not from one of the many interesting but basically extraneous experimental factors that are known to create asymmetries in the free-space Mollow spectrum.[23] In fact, spectra observed in our experiments frequently displayed small asymmetries apparently unrelated to the influence of the cavity. To isolate the cavity effect, the spectra of Fig. 2 were obtained in the following manner. With the cavity tuned to one Mollow sideband, the transmission frequency of the Fabry-Perot spectrum analyzer was repeatedly swept across the resonance, and the Mollow spectrum obtained during each sweep recorded. After every five sweeps, the cavity was retuned, by changing the voltage applied to the cavity piezoelectric transducer, into resonance with the opposite Mollow sideband. This process continued until roughly 600 spectral sweeps had been recorded. All spectra corresponding to a particular cavity tuning were translated along the frequency axis until their peak values coincided (to compensate for spectrum analyzer drift over the long data acquisition period) and then averaged. The data acquisition scheme employed assures that the difference between the spectra obtained is a good indication of the cavity effect even though spurious asymmetries may mask the effect in the individual spectra.

While the difference between the spectra shown in Fig. 2 is among the largest of those observed, the same basic effect appeared in numerous repetitions of the experiment. On the other hand, when two spectra are obtained in the same manner described above, but with the cavity resonance frequency fixed no significant differences between the spectra are observed. A number of factors including Fabry-Perot resolution ($\simeq$70 MHz), residual Doppler effect, and excitation field inhomogeneity prevent us from resolving the intrinsic linewidths ($\simeq$20 MHz) of the Mollow components.

The difference between the two traces of Fig. 2 can be attributed primarily to the vacuum-field dressed-state pumping effect recently reported.[17,22] In the dressed-atom model, the three-peaked Mollow spectrum is seen to arise from transitions between equally split doublets of atom-field eigenstates. On resonance, the sublevels of the dressed-state doublets are equally populated and the relevant transition strengths are equal so that a symmetric triplet is expected whose spectrally integrated sidebands each have a height equal to half the height of the central peak. In the present case, the intracavity frequency-dependent vacuum-reservoir creates an imbalance in the populations of the dressed-state doublet sublevels by enhancing the decay of one sideband transition relative to the other. In particular, when the cavity is resonant with a given Mollow sideband, the density of electromagnetic modes coupled to the corresponding dressed-state transition is enhanced, and the population of the upper dressed-state doublet component is depressed.

The cavity's effect on the electromagnetic mode density is anisotropic. In particular, the open-sided confocal cavity used in the present experiments is not expected to significantly modify the density of vacuum modes associ-

ated with emission out the sides of the cavity; therefore, the vacuum-mode density contributing to emission out the cavity sides is the same at each of the Mollow sideband transition frequencies, and the area of the resonant-excitation Mollow sidebands should directly reflect the population imbalance between the dressed-state sublevels.

The spectral properties of light emitted out the side of a cavity such as the one employed in the present experiment have been calculated[17] and we have compared these predictions with our observed spectra. In doing so, we assume that the cavity mode-density peaks are Lorentzian (600 MHz FWHM) and exceed the free-space mode density by 5%. The predicted spectra, convolved with a Lorentzian function simulating our instrumental width, are shown in Fig. 3. The qualitative similarity between the predicted and observed spectra is apparent. Quantitatively, however, the predicted difference in area between corresponding solid and dashed sidebands is only 4.4% as compared to the 7.5% actually observed in Fig. 2. We believe that the difference between the magnitudes of the predicted and the observed effects is reasonable in light of the statistical reliability of the data and the difficulty involved in accurately assessing the effective enhancement in vacuum-mode density seen by atoms contributing to the spectra. Accurate assessment of the mode density is difficult because of the strong spatial dependence of the vacuum-mode density existing within the cavity and the likelihood that the experimental arrangements intended for mode-density and spectral measurements will sample atoms in slightly different spatial regions. The data of Fig. 2 indicates a peak mode density of $\simeq$8% above the free-space value. In the weak-excitation-field experiments,[12,13] which were explicitly designed to measure the cavity mode density, peak mode densities of $\simeq$6% above the free-space value were observed.

It is useful to consider the possible importance of atomic gain and loss[24–26] in the context of the present experiment. Atomic gain on a particular Mollow sideband will enhance the cavity's effect on the corresponding dressed-state transition by further increasing the transition rate and thereby further depleting the population of the upper dressed-state doublet sublevel. Atomic absorption should do the reverse. Using the results of Ref. 26 and including the effects of all barium isotopes weighted according to their observed weak-field absorption strengths, we find a small net gain (loss) at the frequency of the lower (higher) frequency Mollow sideband. Our calculations indicate further that atomic gain or loss will affect the spectral difference observed here at the level of at most 10%–20%. Furthermore, owing to the largeness of the loss term, the net effect of atomic gain or loss is, in the present instance, to reduce the difference in sideband area observed. We conclude that the observed spectral differences are for the most part generated by the vacuum-field dressed-state pumping effect. Signal size considerations prevented the repetition of the experiment at lower Ba densities.

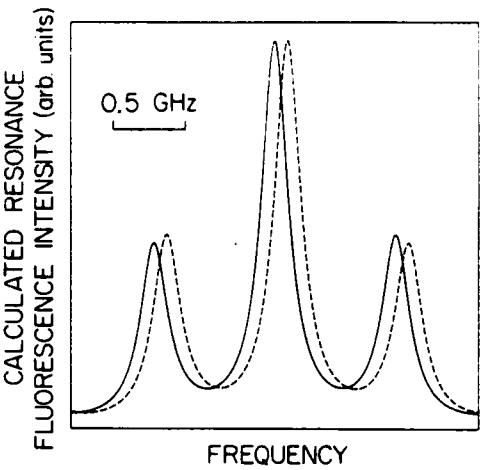

FIG. 3. Predicted strong-field resonance fluorescence spectra under conditions appropriate to the present experiment. For the solid (dashed) trace, the cavity is tuned to the lower- (higher-) frequency sideband. Frequency increases to the right.

In summary, we have reported the first experimental study of the strong-field resonance fluorescence spectrum characteristic of atoms coupled to a frequency-dependent vacuum reservoir. A distinctive modification of the free-space Mollow spectrum is observed and explained in terms of vacuum-field dressed-state pumping. Our results may be taken as indicative of the wealth of new spectral features that may be revealed in studies of atoms relaxing into perturbed vacuum reservoirs.

We gratefully acknowledge stimulating interactions with M. Lewenstein, and financial support from the Air Force Office of Scientific Research under Contract No. AFOSR-88-0086 and from the National Science Foundation under Grant No. PHY-8718518. One of us (A.L) acknowledges support from the Conselho Nacional de Desenvolvimento Cientifico e Tecnologico (Brazil).

[1] J. D. Cresser, Phys. Rep. **94**, 47 (1983).
[2] C. Cohen-Tannoudji, in *Frontiers in Laser Spectroscopy*, Les Houches Session XXVII, edited by R. Balian, S. Haroche, and S. Liberman (North-Holland, Amsterdam, 1977).
[3] P. L. Knight and P. W. Milonni, Phys. Rep. **66**, 21 (1980).
[4] D. Kleppner, Phys. Rev. Lett. **47**, 233 (1981).
[5] R. G. Hulet, E. S. Hilfer, and D. Kleppner, Phys. Rev. Lett. **55**, 2137 (1985).
[6] W. Jhe, A. Anderson, E. A. Hinds, D. Meschede, L. Moi, and S. Haroche, Phys. Rev. Lett. **58**, 666 (1987).
[7] P. Goy, J. M. Raimond, M. Gross, and S. Haroche, Phys. Rev. Lett. **50**, 1903 (1983).
[8] F. DeMartini, G. Innocenti, G. R. Jacobovitz, and P. Mataloni, Phys. Rev. Lett. **59**, 2955 (1987).
[9] F. DeMartini and G. R. Jacobovitz, Phys. Rev. Lett. **60**, 1711 (1988).
[10] M. Lewenstein, J. Zakrzewski, and T. W. Mossberg, Phys. Rev. A **38**, 808 (1988).
[11] G. Gabrielse and H. Dehmelt, Phys. Rev. Lett. **55**, 67 (1985).
[12] D. J. Heinzen, J. J. Childs, J. E. Thomas, and M. S. Feld,

Phys. Rev. Lett. **58**, 1320 (1987).
[13]D. J. Heinzen and M. S. Feld, Phys. Rev. Lett. **59**, 2623 (1987).
[14]H. J. Carmichael, A. S. Lane, and D. F. Walls, Phys. Rev. Lett. **58**, 2539 (1987).
[15]G. S. Agarwal, Phys. Rev. Lett. **53**, 1732 (1984).
[16]J. J. Sanchez-Mondragon, N. B. Narozhny, and J. H. Eberly, Phys. Rev. Lett. **51**, 550 (1983).
[17]M. Lewenstein and T. W. Mossberg, Phys. Rev. A **37**, 2048 (1988); M. Lewenstein, T. W. Mossberg, and R. J. Glauber, Phys. Rev. Lett. **59**, 775 (1987).
[18]B. R. Mollow, Phys. Rev. **188**, 1969 (1969).
[19]F. Schuda, C. R. Stroud, Jr., and M. Hercher, J. Phys. B **7**, L198 (1974).
[20]W. Hartig, W. Rasmussen, R. Schieder, and H. Walther, Z. Phys. A **278**, 205 (1976).
[21]R. E. Grove, F. Y. Wu, and S. Ezekiel, Phys. Rev A **15**, 227 (1977).
[22]Y. Zhu, A. Lezama, T. W. Mossberg, and M. Lewenstein, Phys. Rev. Lett. **61**, 1946 (1988).
[23]M. G. Prentiss and S. Ezekiel, Phys. Rev. A **35**, 922 (1987).
[24]B. R. Mollow, Phys. Rev. A **5**; 2217 (1972).
[25]F. Y. Wu, S. Ezekiel, M. Ducloy, and B. R. Mollow, Phys. Rev. Lett. **38**, 1077 (1977).
[26]D. A. Holm, M. Sargent III, and S. Stenholm, J. Opt. Soc. Am. B **2**, 1456 (1985).

PHYSICAL REVIEW A VOLUME 39, NUMBER 4 FEBRUARY 15, 1989

Effect of optical gain on the fluorescence of two-level atoms into the modes of an optical cavity

Yifu Zhu, A. Lezama, and T. W. Mossberg
Department of Physics, University of Oregon, Eugene, Oregon 97403
(Received 31 October 1988)

The emission of strongly driven two-level-like Ba atoms into the modes of an optical cavity has been studied as a function of cavity tuning and Ba density. At low densities, the cavity-mode emission viewed as a function of cavity tuning is identical in form to the three-peaked Mollow emission spectrum. At high densities, however, the cavity-mode emission is strongly amplified (attenuated) when the cavity is tuned to the frequency of one (the other) Mollow sideband. It is predicted that modest increases in Ba density will cause lasing to occur in this system.

It has been predicted[1] and experimentally demonstrated[2,3] that strongly driven homogeneous assemblages of two-level atoms can exhibit optical amplification as well as absorption. The existence of gain in such systems can be expected to lead to novel new effects, especially when its influence is accentuated through the use of a high-finesse optical cavity. It has been predicted, for example, that the emission of strongly driven two-level atoms into the modes of a confining optical cavity can be strongly enhanced for certain cavity tunings. In fact, in the case of a suitable atomic density, gain is expected to exceed losses and steady-state lasing with two-level atoms as the amplifying medium is expected to occur.

In the present paper, we report on an experimental study of the effects of atomic gain and loss on atomic emission into the modes of a confining optical cavity as a function of cavity resonance frequency and atomic density. At low atomic densities, the intensity of cavity-mode emission versus cavity resonance frequency, hereafter loosely referred as the emission spectrum, is proportional to the three-peaked Mollow fluorescence spectrum[4-6] and is, therefore, symmetric around the driving-field frequency. In contrast, at high atomic densities the cavity-mode emission is found to be amplified when the cavity is resonant with one of the Mollow sidebands and attenuated when the cavity is resonant with the other sideband. The resulting cavity-mode emission spectrum is asymmetric about the driving-field frequency.

The problem that we have experimentally investigated has been explored theoretically by Holm, Sargent, and Stenholm.[7] Their system consists of an ensemble of identical two-level atoms confined within a single-mode optical cavity. The atomic (cavity) resonance frequency is ν_a (ν_c). The atoms are driven by a strong laser field of frequency ν_l that propagates normal to the cavity axis. The observable of interest $I_f(\nu_c)$ is the fluorescence intensity transmitted out of either end of the optical cavity as a function of ν_c. I_f depends on the laser-atom detuning $\Delta \equiv \nu_l - \nu_a$, on the driving-field Rabi frequency Ω, on the atomic-number density N, and on the cavity quality factor. Following Holm *et al.*,[7] the fluorescence intensity can be written as

$$I_f(\nu_c) = I_0 \frac{A'(\nu_c)}{\beta(N) - [A'(\nu_c) - B'(\nu_c)]}, \quad (1)$$

where I_0 is a proportionality constant. The coefficient β, which is inversely proportional to N, is given by the cavity-loss rate divided by the weak-signal $\Delta = 0$ atomic absorption rate. In the very low atomic-density limit (β large) $I_f(\nu_c)$ is simply proportional to $A'(\nu_c)$, which is identical to the standard free-space Mollow resonance fluorescence spectrum with ν_c interpreted as the fluorescence emission frequency.[7] The term $A' - B'$ in the denominator represents the atomic-gain coefficient;[7-9] it can be positive indicating gain or negative indicating loss. In simple two-level systems, the gain coefficient is symmetric about ν_l when $\Delta = 0$, but becomes asymmetric for Δ and Ω suitably large. As the atomic density increases, the role of the gain term in the denominator becomes significant, distorting the cavity-mode emission spectrum relative to the usual Mollow triplet. Eventually, the gain may exceed the losses and laser action may be expected. If we define $\beta_T(\Omega,\Delta)$ as the maximum value of $A'(\nu_c) - B'(\nu_c)$ for fixed Ω and Δ, we can then rewrite Eq. (1) as

$$I_f(\nu_c) = \frac{I_0}{\beta_T} \frac{A'}{\beta' - (A' - B')/\beta_T}, \quad (2)$$

with $\beta' = \beta/\beta_T$. The lasing threshold condition ($\beta' = 1$) will first be reached at the value of ν_c for which $A'(\nu_c) - B'(\nu_c) = \beta_T$.

In our experiments, a 1-mm-diam beam of Ba atoms is passed through the center of a 1-cm-long symmetric confocal optical cavity. The cavity mirrors are spherical and have a 1-cm radius of curvature. They are 5-mm in diameter, but one of them has been limited to a 2.2-mm clear aperture. The cavity finesse is measured to be approximately 200. The cavity mirror spacing and hence the cavity resonance frequency is tuned using a piezoelectric pusher attached to one of the mirrors. A single-mode cw-ring dye laser transversely illuminates the Ba beam from a direction normal to the cavity axis. The laser is tuned on or near to resonance with the 553.5-nm $6s^2(^1S_0) - 6s6p(^1P_1)$ ^{138}Ba transition, and is collimated with a diameter of 2 mm as it traverses the interaction region. The light emitted out one side of the cavity was collected and recorded to provide a relative measure N' of the number of atoms present in the interaction region as the temperature of the atomic-beam source was varied. The light em-

itted out one end of the cavity $I_f(\nu_c)$ was spatially filtered and detected. The weak signal absorption of the Ba beam at the center of the ^{138}Ba resonance line was found to be approximately 12% at the highest attainable Ba densities (see Fig. 1). The Ba employed in the beam was of natural isotopic composition. The laser beam was linearly polarized with its electric field vector perpendicular to the cavity axis, and the ambient magnetic field in the interaction region was < 1 G.

Our experimental system deviates from the theoretical model[7] in two important ways. First, our optical cavity possesses strong mode degeneracy. As a result, light collected in our experiment is actually emitted into a number of nearly degenerate modes. Second, the Ba beam contained a number of isotopes having nondegenerate resonance frequencies. As will be apparent below, only the second factor led to obvious deviations from predicted behavior.

We note that an experimental system similar to ours was employed some time ago in the measurement of what was assumed to be the free-space low-atomic-density Mollow spectrum.[10] The observed spectra displayed asymmetries, but no attempt was made to analyze these asymmetries in terms of atomic-gain effects.

In Fig. 2(a), we show $I_f(\nu_c)$ recorded for three different laser-^{138}Ba-atom detunings Δ at each of three Ba beam densities. Throughout these measurements, a fixed Rabi frequency of $\simeq 160$ MHz was employed. From bottom to top, the atomic-beam density has the approximate relative values of 1, 30, and 90. At the lowest atomic densities, the spectrum observed is symmetric for all detunings. At higher densities, however, the cavity-mode emission spectrum becomes increasingly asymmetric. One sideband is suppressed while the other is enhanced. Changing the sign of the detuning reverses the asymmetry, i.e., the enhanced sideband becomes the suppressed one and vice versa. Note that the reversal is not perfect, and that the $\Delta = 0$ spectrum is not symmetric at high densities. Note also that the suppression effect, fractionally speaking, is the larger effect. A number of factors contribute to the observed spectral width of the peaks. These factors include the 35–40 MHz single-mode resonance width of the cavity, the collection of Doppler-shifted light emitted into slightly nondegenerate cavity modes, the 19-MHz natural width, and in the case of the sidebands the inhomogeneity of the laser excitation field.

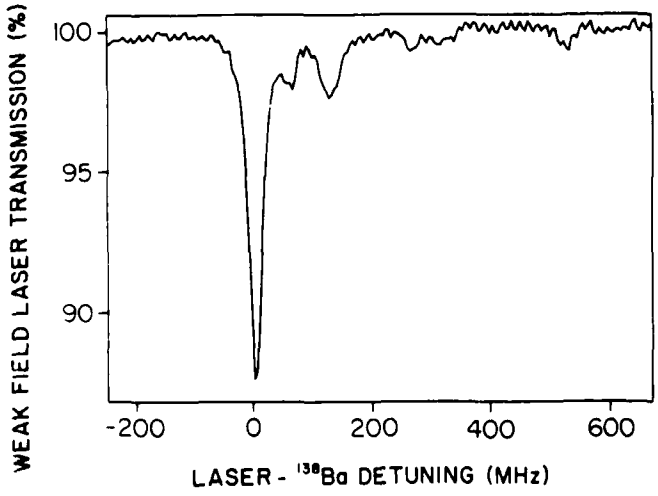

FIG. 1. Single-pass transmission of a weak laser beam through the atomic beam at the maximum attainable density. The deepest absorption corresponds to ^{138}Ba. Absorption corresponding to other Ba isotopes is seen at positive detunings.

In Fig. 2(b), we present spectra calculated using Eq. (2) under conditions appropriate to the experimental spectra of Fig. 2(a) and and convolved with a 45-MHz-width (FWHM) Lorentzian curve to simulate the instrumental resolution. The calculated spectra include the contributions from both elastic and inelastic processes. The A' and B' in Eq. (1) are calculated by summing over the contributions from six Ba-isotope transitions weighted according to their contribution to the weak-field absorption spectrum of Fig. 1. Complications associated with level degeneracy in the case of isotopes with nonzero nuclear spin were ignored. The asymmetry of the $\Delta = 0$ spectrum, the imperfect reversal of the spectral asymmetry on changing the sign of Δ, and an excess height of the central peak as compared to the sidebands at low atomic density are attributable to the presence of several Ba isotopes. The value of β used in calculating the top row of Fig. 2(b) was chosen freely to optimize the agreement with the corresponding spectra of Fig. 2(a). To produce the second and third rows in Fig. 2(b), the top-row β was scaled inversely with the measured relative atomic density—no additional fitting was done. Figure 2(c) gives the calculated atomic gain for the Δ and Ω values appropriate to Fig. 2(b). Note that the dominant feature in these figures is absorption. It is apparent from Figs. 2(a)–2(c) that increases (decreases) in the magnitude of the Mollow sidebands correlate with atomic gain (absorption).

Note that the value of β' required to simulate our high-atomic-density data for $\Delta = -100$ MHz is very close to the $\beta' = 1$ lasing threshold. No evidence of lasing was observed, and, unfortunately, it was not possible to achieve higher Ba densities using the available apparatus. We note that the fit-deduced value of β' is reasonably consistent with measured atomic absorption, measured cavity properties, and the calculated value of $\beta_T(\Omega,\Delta)$.

In Fig. 3, we show measurements of $I_f(\nu_c)$ as a function of N' for values of ν_c that correspond to the three peaks of the Mollow spectrum. For these measurements, $\Delta = -50$ MHz and $\Omega = 230$ MHz. Each experimental curve was fit to a function of the form

$$I(N') = I_i \frac{1}{\eta_i/N' \pm 1} \quad (i = e,c,a), \tag{3}$$

where the minus sign was used for enhanced sideband (e), which experienced gain, and the plus sign for the attenuated sideband (a) and the central peak (c), both of which experienced absorption. The quantities I_i and η_i were determined for each peak by a least-squares-fitting procedure. With the relative atomic density N' specified as on the horizontal axis of Fig. 3 ($N' = 1$ at the lowest density employed); best-fit values of η_i are 307, 38, and 622 for $i = e$, a, and c, respectively. The η_e value determined for the enhanced sideband corresponds to the atomic density, in the same relative units as employed in Fig. 3, needed to achieve the lasing threshold. The best-fit value

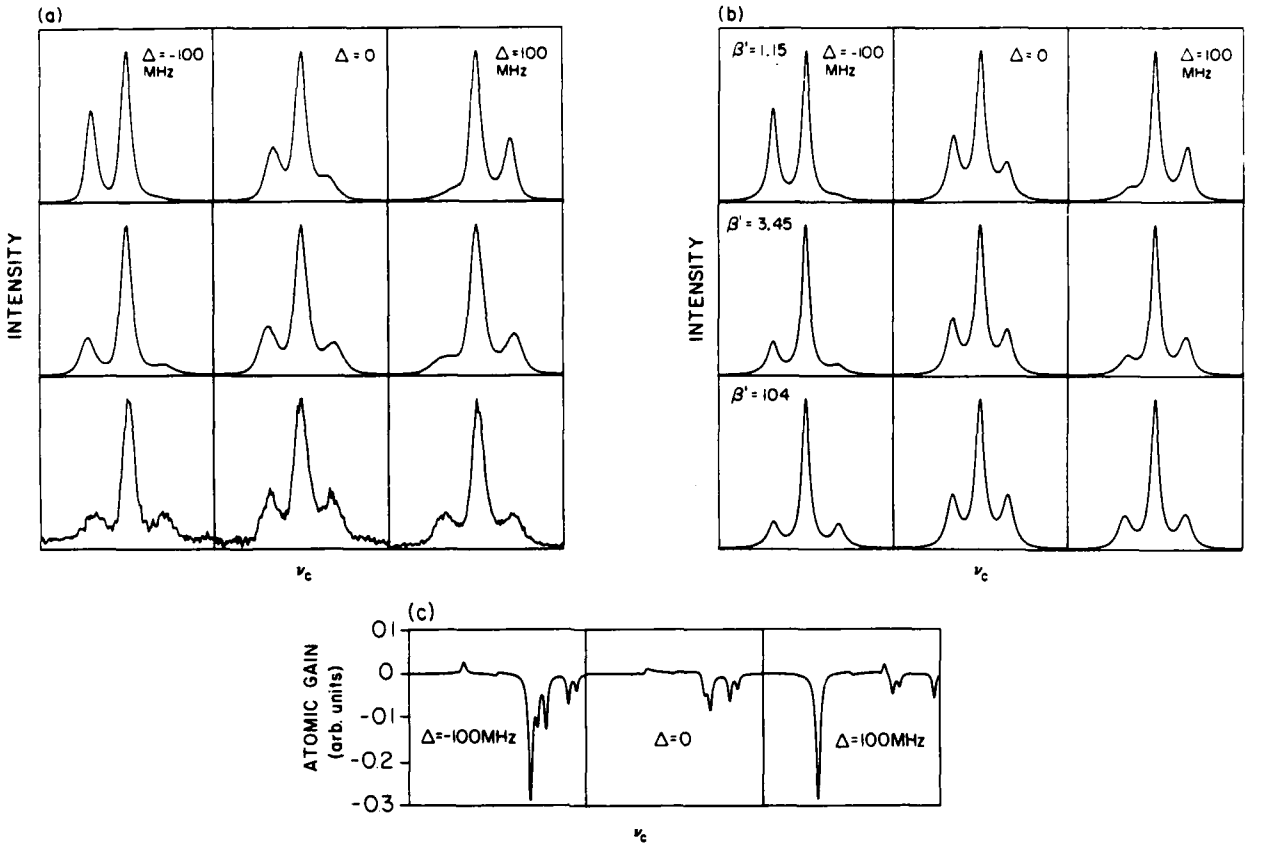

FIG. 2. (a) Measured cavity-mode fluorescence intensity vs cavity resonance frequency ν_c for different values of the laser-^{138}Ba detuning Δ and for different values of the atomic density. The vertical scale is arbitrary and varies in proportion to the density. The horizontal scale of each spectrum is centered at ν_l and has a full range of 1 GHz. Within each row the atomic density is approximately constant. Moving from the bottom up, the relative atomic densities are 1:30:90. The top-row density corresponds to that of Fig. 1. (b) Same as (a) except that the spectra are calculated as described in the text using $\Omega = 160$ MHz. The atomic density is constant within a row, however, due to the variation of β_T with Δ, the value of β' varies. The values of β' corresponding to the second and third columns are 2.60 and 1.33 times larger, respectively, than those of the first column. (c) Calculated atomic gain $(A'-B')$ vs ν_c for $\Omega = 160$ MHz and different values of Δ. In the units used here, the weak-field absorption of ^{138}Ba corresponds to -0.788. The horizontal scale is the same as in (a).

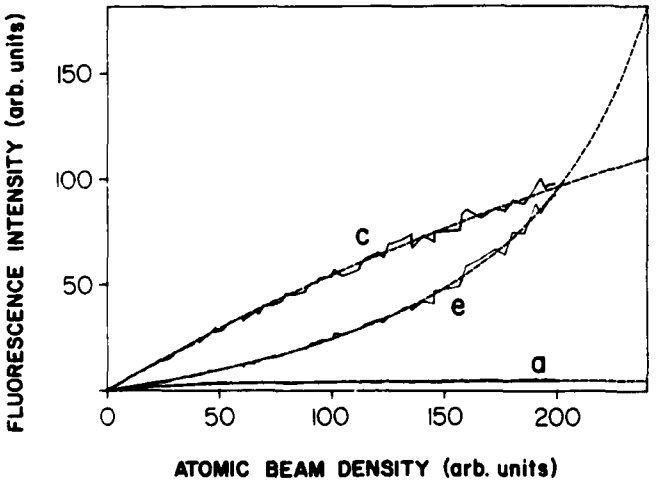

FIG. 3. Measured intensity of cavity-mode emission vs relative atomic density for $\Delta = -50$ MHz and $\Omega \simeq 230$ MHz with the cavity tuned to the three peaks of the fluorescence spectrum. *e*, enhanced sideband; *c*, central peak; *a*, attenuated sideband. The dashed lines represent fits of the data to Eq. (3) (see text).

of η_e indicates that the lasing threshold was at an atomic density only 50% higher than we were able to produce.

The existence of absorption at the frequency of the central peak is interesting. Calculations indicate that it arises only in the limit of a relatively weak driving field. In our experiment, the absorption apparently arises because of excitation field inhomogeneity and the concommitant existence of regions in which the driving field is weak. It should be noted that the presence of weak-field regions will tend, at high atomic densities, to reduce the magnitude of the central peak relative to the enhanced sideband. This, in turn, will tend to reduce the value of β' that in Fig. 2(b) gives the best fit to the measured spectrum. This conclusion is consistent with the fact that the analysis of Fig. 3 results in a somewhat larger difference between the achieved atomic density and the density needed for lasing.

In summary, we find that atomic gain plays a major role in determining the rate of atomic emission into the modes of an optical cavity. Experimental results in our mode-degenerate optical cavity are in excellent agreement with the single-mode calculations of Holm *et al.*,[7] and it appears that a very modest increase in atomic-beam densi-

ty will lead to laser action in a stationary ensemble of two-level atoms. From the context of the dressed-atom model,[11] the sideband lasing action can be viewed as arising from an inversion between levels of the dressed atom, and therefore a laser based on sideband gain might be termed a *dressed-atom* laser. Because the emission of successive photons is correlated in the dressed-atom picture, dressed-atom lasers may display interesting statistical properties.

We gratefully acknowledge the financial support of the Air Force Office of Scientific Research under Contract No. AFOSR-88-0086, and the National Science Foundation under Grant No. PHY-8718518. One of us (A.L.) acknowledges the support of Conselho Nacional de Desenvolvimento Científico e Tecnológico (Brazil). We thank D. A. Holm, M. Sargent III, and M. Ducloy for interesting comments.

[1]B. R. Mollow, Phys. Rev. A **5**, 2217 (1972).
[2]F. Y. Wu and S. Ezekiel, M. Ducloy, and B. R. Mollow, Phys. Rev. Lett. **38**, 1077 (1977).
[3]D. J. Harter, P. Narum, M. G. Raymer, and R. B. Boyd, Phys. Rev. Lett. **46**, 1192 (1981); R. B. Boyd, M. G. Raymer, P. Narum, and D. J. Harter, Phys. Rev. A **24**, 411 (1981).
[4]B. R. Mollow, Phys. Rev. **188**, 1969 (1969).
[5]F. Schuda, C. R. Stroud, Jr., and M. Hercher, J. Phys. B **7**, L198 (1974).
[6]R. E. Grove, F. Y. Wu, and S. Ezekiel, Phys. Rev. A **15**, 227 (1977).
[7]D. A. Holm, M. Sargent III, and S. Stenholm, J. Opt. Soc. Am. B **2**, 1456 (1985).
[8]S. Stenholm, D. A. Holm, and M. Sargent III, Phys. Rev. A **31**, 3124 (1985).
[9]M. Sargent III and D. A. Holm, Phys. Rev. A **31**, 3112 (1985).
[10]W. Hartig, W. Rasmussen, R. Schieder, and H. Walther, Z. Phys. A **278**, 205 (1976).
[11]C. Cohen-Tannoudji and S. Reynaud, J. Phys. B **10**, 345 (1977).

Radiative emission of driven two-level atoms into the modes of an enclosing optical cavity: The transition from fluorescence to lasing

A. Lezama,* Yifu Zhu, Manoj Kanskar, and T. W. Mossberg
Department of Physics, University of Oregon, Eugene, Oregon 97403
(Received 17 July 1989)

The radiative emission of strongly driven, two-level-like barium atoms into the modes of a confocal optical cavity is studied as a function of barium density. As the barium density is increased, the spatial profile, intensity, and spectrum of light emitted out the ends of the confocal cavity display dramatic changes indicative of a transition from fluorescence to lasing. In this novel two-level system, laser action can be explained in terms of an inversion between the dressed atom-field states or in terms of a type of stimulated hyper-Raman scattering in which atoms lase from the ground to the excited atomic state. A simple dressed-atom rate-equation analysis of this two-level-atom laser is presented. It is pointed out that this same system may provide a means of realizing two-photon-like laser action.

INTRODUCTION

Some time ago,[1-3] it was pointed out that population inversion (at least in the traditional sense) is not a prerequisite for optical gain in media consisting of strongly driven two-level atoms. Numerous theoretical works have subsequently elaborated on various aspects of this interesting result,[4-8] and experimental studies of the absorption spectrum of a weak probe beam interacting with an ensemble of strongly driven two-level atoms have indeed revealed regions of negative absorption or gain.[9,10] Just recently, Khitrova, Valley, and Gibbs,[11] working in a Doppler broadened sodium vapor, have demonstrated laser action based on this gain, and they point out that this gain relates to certain instabilities observed in driven systems. We note that a number of closely related effects involving amplification and gain via parametric interactions[12-16] and collisional effects[17,18] have also been found to occur in systems of driven two-level atoms, providing some additional measure of the richness of this fundamental system.

We present here the results of a study of driven two-level-atom gain performed in a simple Doppler-free system using nearly ideal two-level atoms. Specifically, we have studied the effect of gain on the radiative emission of driven two-level-like barium atoms into the degenerate modes of an enclosing confocal optical cavity.[8,19] In contrast to the case of Khitrova, Valley, and Gibbs,[11] our results are largely free of the complications associated with Doppler broadening, and they span regimes wherein the atomic emission is dominated by spontaneous as well as stimulated processes. In the former case, the cavity emission has the properties of strong-field resonance fluorescence,[20-23] while in the latter case, the atoms lase into the cavity modes. We attempt to characterize the transition from fluorescence to lasing in this elemental system by studying the spatial properties, spectral structure, and intensity of the cavity emission as a function of barium density.

It is interesting to note that the Mollow sideband gain observed in an ensemble of strongly driven two-level atoms can be explained from two very different perspectives. In one perspective, the presence of gain in this system can be portrayed as a result of the positive inversion that exists between certain pairs of dressed atom-field states when the driving-field frequency is detuned from the atomic transition frequency[4,24] (see Fig. 1). From another perspective, the gain arises from a two-photon Raman process (see Fig. 2), and the laser action can be viewed as a form of stimulated hyper-Raman scattering in which two pump photons are absorbed and the emission of one sideband photon is stimulated.[2] We will primarly adopt the former perspective, returning to the latter briefly when we discuss higher-order gain processes.

THEORY

We consider an ensemble of N_a two-level atoms of transition frequency ν_a located at the center of an open confocal optical cavity. The free-spectral range of the cavity is considered to be so large that only one cavity resonance interacts with the atoms. The atoms have a ground (excited) state $|g\rangle$ ($|e\rangle$) [see Fig. 1(a)]. The atoms are driven by a strong, coherent-state, pump field of frequency ν_l, detuning $\Delta \equiv \nu_l - \nu_a$, and resonance Rabi frequency Ω_0. The pump propagates transverse to the cavity axis. The pump-field energy spectrum consists of a ladder of number states $|n\rangle$, as shown in Fig. 1(b). On coupling the atoms and the pump field, we obtain the well-known dressed states $|i,n\rangle$ ($i=1,2$) of the pump plus atom system.[4,25] The dressed energy spectrum consists of a ladder of doublets separated by ν_l and split by $\nu_s \equiv (\Delta^2+\Omega_0^2)^{1/2}$ [see Fig. 1(c)]. The asymptotic decomposition of the dressed states in terms of atom-pump product states for large positive and negative Δ is also shown. Let Π_i be the population of the dressed-state component i ($i=1,2$) summed over n. We assume that A_{ij} is the total spontaneous-emission rate from the ith to the jth dressed-state components in adjacent doublets,

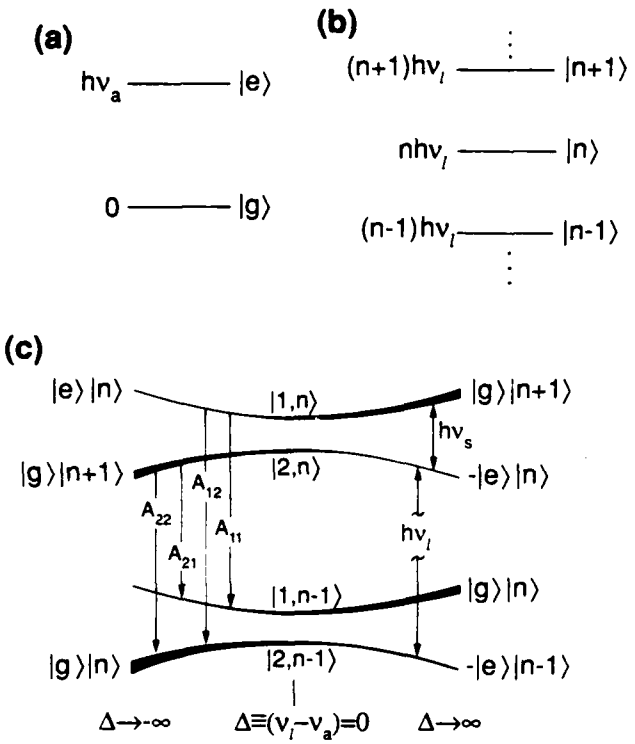

FIG. 1. Schematic energy diagram of (a) the two-level atom, (b) the quantized pump field, and (c) the dressed atom, i.e., the coupled atom-field system. In (c), the atom-field product states at the right (left) represent the asymptotic dressed-state composition for large positive (negative) detuning Δ. The thickness of the lines representing the energy levels in (c) provides a qualitative indication of the relative population of the corresponding level.

and that a_{ij} is the corresponding spontaneous-emission rate into the cavity modes. Let n_c be the mean number of photons in the cavity having the cavity resonance frequency, and let $B_{ij}n_c$ be the rate of stimulated transitions from the ith to the jth dressed-state component of adjacent doublets induced by the cavity-mode field. In the case of a simple single-mode cavity, a_{ij} and B_{ij} have the same magnitude. In a highly degenerate cavity, like the one we consider, the situation is more complex, and we retain these two quantities distinct throughout our calculation.

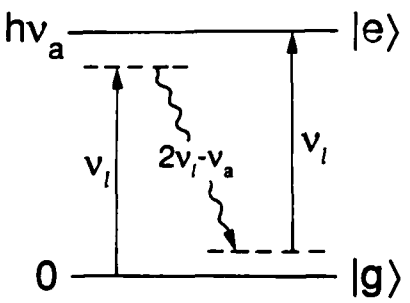

FIG. 2. Stimulated Raman process to which the driven two-level-atom gain of interest here can be attributed (Ref. 2). Note that this process transfers population from the ground to the excited state.

Considering, for example, the case of $\Delta<0$, the $|2,n\rangle$ dressed-state components take on more of the character of the atomic ground state, and can thus be expected to be more heavily populated under steady-state conditions than the $|1,n\rangle$ dressed-state components. Consequently, an inversion on dressed-state transitions of the form $|2,n\rangle\to|1,n-1\rangle$ will exist and provide for gain at the corresponding transition frequency. By similar arguments, one can predict the existence of absorption at the frequency of the $|2,n-1\rangle\to|1,n\rangle$ transitions.

One can immediately write down rate equations governing the populations of the dressed states, the mean number of photons in the cavity, and therefore of the intensity of light emitted out the ends of the cavity. For $\Delta<0$ and with the cavity resonant with the inverted transition, we have

$$\dot{\Pi}_2=\Pi_1(A_{12}+B_{21}n_c)-\Pi_2(A_{21}+B_{21}n_c)\ , \tag{1a}$$

$$\dot{n}_c=-kn_c+B_{21}n_c(\Pi_2-\Pi_1)+a_{21}\Pi_2\ , \tag{1b}$$

and

$$\Pi_1+\Pi_2=N_a\ , \tag{1c}$$

where k is the cavity loss rate. Setting the derivatives to zero and solving for n_c, one obtains

$$n_c=\frac{q\pm(q^2+8kB_{21}a_{21}A_{12}N_a)^{1/2}}{-4kB_{21}}\ , \tag{2a}$$

where

$$q=k(A_{21}+A_{12})-B_{21}N_a[A_{12}-(A_{21}-a_{21})]\ . \tag{2b}$$

In the limits of small and large N_a, n_c has a simple linear dependence on the number of atoms present, i.e., for N_a small

$$n_c=\frac{A_{12}a_{21}N_a}{k(A_{21}+A_{12})}\ , \tag{3a}$$

and for N_a large

$$n_c=\frac{[A_{12}-(A_{21}-a_{21})]N_a}{2k}\ . \tag{3b}$$

For small N_a, the growth in n_c is determined by spontaneous emission into the cavity mode. For higher N_a, stimulated processes dominate and n_c becomes limited by the pumping rate. In the present system, pumping can be viewed as spontaneous emission on transitions of the form $|1,n\rangle\to|2,n-1\rangle$, and it proceeds at the rate A_{12}. The laser threshold corresponds to the slope change observed on passing from Eq. (3a) to Eq. (3b).

In distinction to more standard laser systems in which the spontaneous-emission rates are constants, in the two-level-atom laser A_{21} and A_{12} are functions of Δ and the resonant pump-field Rabi frequency Ω_0. We have

$$A_{12}=\alpha_{12}\rho_{12}\cos^4(\theta) \tag{4a}$$

and

$$A_{21}=\alpha_{21}\rho_{21}\sin^4(\theta)\ , \tag{4b}$$

where $\alpha_{ij}=(\pi\nu_{ij}/3\epsilon_0\hbar)\,p^2$, ν_{ij} is the relevant dressed-state transition frequency, p is the appropriate transition matrix element connecting the atomic ground and excited states, and ρ_{ij} is the density of electromagnetic modes per unit volume and frequency at the frequency of the corresponding dressed-state transition. Also

$$2\theta=\tan^{-1}(-\Omega_0/\Delta)\ . \tag{4c}$$

In the high-N_a limit, Eqs. (1) can be analyzed to show that the populations of the dressed-state components become equalized (i.e., $\Pi_1=\Pi_2$), implying the same for the bare-state ($|g\rangle$, $|e\rangle$) populations. In the limit of small N_a, on the other hand, the dressed-state component with the largest admixture of the atomic ground state is preferentially populated. This result indicates that the onset of lasing results in a net transfer of population from the ground to the excited atomic state. In other words, the atoms lase upwards in energy. This rather novel result is consistent with the perspective that the lasing observed in the driven two-level-atom system can be viewed as a form of stimulated hyper-Raman scattering.[2] Note, however, that in the present case, the population transfer does not involve a virtual transition through a third level.

APPARATUS

In our experiments, a thermal, 1-mm-diam atomic beam of natural Ba was made to pass through the center of a 1-cm-long symmetric confocal cavity. Cavity mirrors were 5 mm in diameter, but one of them was limited to a 300-μm clear aperture. Measured cavity finesse was about 200. The cavity spacing and hence its resonance frequency was tuned by using a piezoelectric transducer attached to one of the mirrors. A collimated, 2-mm-diam beam from a single-mode cw ring laser intercepted the atomic beam at the geometrical center of the cavity. The atomic beam, pump beam, and cavity axis were made mutually orthogonal to provide for nearly Doppler-free observations and to suppress nonlinear effects dependent on phase matching. The laser was linearly polarized with its electric field vector perpendicular to the cavity axis, and was tuned near to resonance with the 553.5-nm $6s^2\,{}^1S_0\rightarrow 6s6p\,{}^1P_1$ ^{138}Ba transition. The compensated ambient magnetic field in the interaction region was <1 G. The laser frequency was actively locked to a magnetically tunable saturation resonance in an auxiliary Ba vapor cell. The fluorescent light emitted out one side of the cavity was recorded to provide a relative measure N of the total number of atoms present in the interaction region as the temperature of the atomic source was varied. The light emitted out one end of the cavity (axial emission) was spatially filtered and detected. We refer to measurements of the axial emission as a function of cavity resonance frequency as the axial emission spectrum.

In a previous publication,[19] we reported measurements of the axial emission spectrum for Ba beam densities below those required for lasing. At very low Ba densities, the axial emission spectrum duplicates the well-known symmetric Mollow triplet familar from strong-field resonance fluorescence work.[20–23] At higher densities, the spectrum was found to become asymmetric, one sideband was strongly enhanced while the other was suppressed. The enhanced sideband corresponds to the inverted dressed-state transition. In the present experiment, modifications to the atomic beam source have enabled us to reach Ba densities high enough to support lasing. At the maximum Ba beam density employed, the weak signal absorption at the center of the ^{138}Ba resonance line was measured to be approximately 30%. We used an on-resonance pump Rabi frequency of $\Omega_0\sim 230$ MHz, and fixed the laser-atom detuning at $\Delta=-100$ MHz. Here $\Delta<0$ was chosen to minimize the influence of the other Ba isotopes, all of which have transition frequencies above that of ^{138}Ba.

EXPERIMENTAL OBSERVATIONS

In Fig. 3, we present measurements of the axial emission intensity as a function of barium beam density with the cavity tuned to the frequency of the degenerate $1\rightarrow 1$ and $2\rightarrow 2$ dressed-state transitions (trace *a*) and to the frequency of the inverted $2\rightarrow 1$ dressed-state transition (trace *b*). The variation in emitted intensity versus density observed in the two cases is strikingly different. With the cavity tuned to the central Mollow peak ($1\rightarrow 1$ and $2\rightarrow 2$ transitions), the output intensity exhibits a slightly sublinear variation with Ba density, which, as discussed in Ref. 19, is attributable to absorption arising from weakly driven atoms located near the edges of the pump laser beam. The steplike structure seen in trace *b* of Fig. 3, corresponds to the slope change expected to occur [see Eq. (3)] with the onset of lasing on the inverted $2\rightarrow 1$ dressed-state transition.

In Fig. 4, the axial output intensity as a function of cavity tuning is shown for two different Ba beam densities. In each part of the figure, the relative atomic density is given in the same units as employed in Fig. 3. Fig-

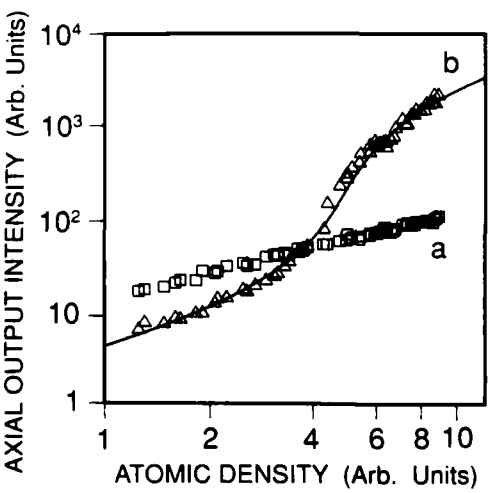

FIG. 3. Measured intensity of axial emission vs relative atomic density for $\Delta=-100$ MHz and $\Omega_0=230$ MHz with the cavity tuned to (a) the central Mollow peak and (b) the sideband exhibiting gain. The solid line is a fit of the data to Eq. (2a) (see text).

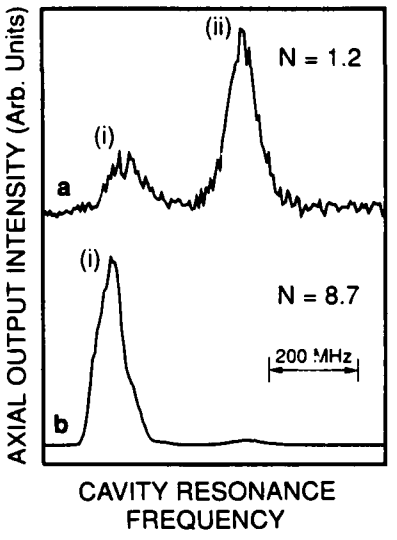

FIG. 4. Measured axial emission intensity vs cavity resonance frequency (horizontal) for two different relative Ba densities. (i) corresponds to the inverted $|2,n\rangle$-$|1,n-1\rangle$ type transitions, while peak (ii) corresponds to the central Mollow peak. The high-frequency sideband is totally suppressed due to absorption. The relative atomic density in the units of Fig. 3 is indicated for each case. The horizontal scale has a full range of 0.8 GHz.

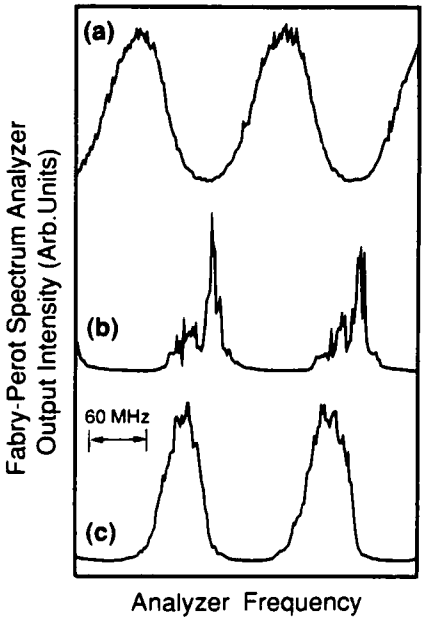

FIG. 5. Frequency spectrum of the axial light output for different cavity tunings. (a) Cavity tuned to the central Mollow peak, (b) cavity slightly detuned from the inverted dressed-state transition frequency ($\nu_l-\nu_s$) (see Fig. 1), (c) cavity tuned to the maximum of the gain profile for the enhanced sideband. In obtaining the spectra shown here, the Fabry-Pérot analyzer was scanned over slightly more than two 150-MHz free-spectral ranges.

ure 4(a) was recorded below the laser threshold, but the spectrum is significantly altered from the classic Mollow form,[20] which consists of a central peak at frequency ν_l and two sidebands at the frequencies $\nu_l\pm\nu_s$. In the present case, the peak (i), corresponding to the inverted $2\rightarrow1$ dressed-state transition at frequency $\nu_l-\nu_s$, is amplified while the opposite sideband, corresponding to the uninverted and hence absorptive $1\rightarrow2$ dressed-state transition at frequency $\nu_l+\nu_s$, is so highly attenuated that it cannot be seen. Peak (ii) at frequency ν_l corresponds to the central component of the Mollow triplet. Figure 4(b) was recorded at a barium density above the laser threshold. Notice that the amplified sideband now dwarfs the central peak.

Finally, with the cavity tuning fixed, we have measured the spectrum (Fig. 5) and the spatial profile (Fig. 6) of the light emitted axially out of the cavity for various cavity resonance frequencies ν_c and a constant large barium density. Output spectra were measured using an external 50-cm, 5-MHz resolution, 150-MHz free-spectral range, confocal Fabry-Pérot spectrum analyzer. In recording

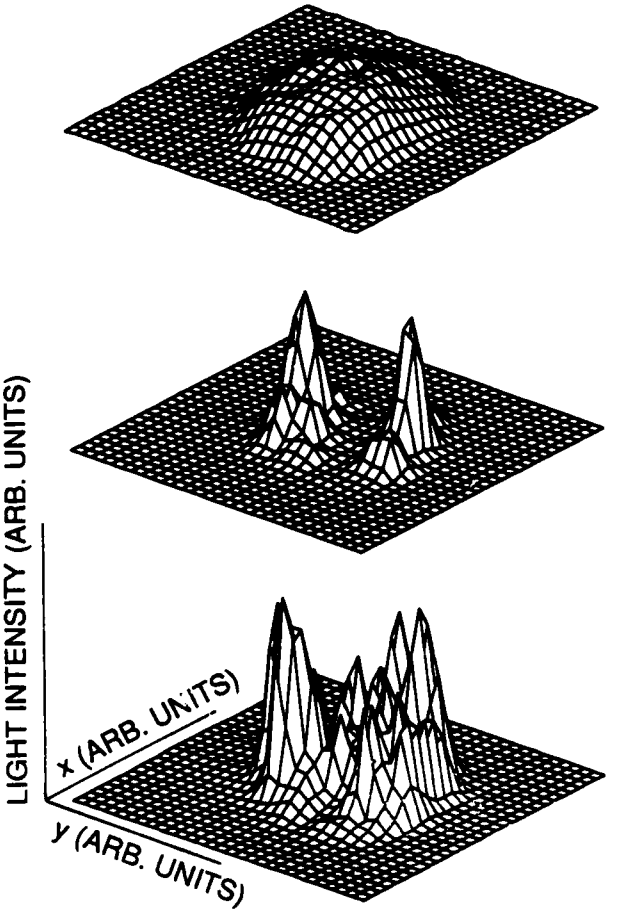

FIG. 6. Spatial light intensity profile at the optical image of the center of the cavity. The vertical axis is proportional to the intensity of the light and the transverse axes to spatial position. Each part of this figure was recorded under the same conditions as the corresponding part of Fig. 5.

the spectra of Fig. 5, the 50-cm Fabry-Pérot analyzer was scanned through approximately two free-spectral ranges producing two recordings of each spectrum separated horizontally by the 150-MHz free-spectral range of the Fabry-Pérot analyzer. For these measurements, the Ba beam density was $\simeq 9$ in the relative density units of Fig. 3. In Fig. 5(a), the cavity is tuned to the central peak of the resonance fluorescence spectrum at frequency ν_l. In Fig. 5(b), the cavity is tuned near the $2 \rightarrow 1$ transition frequency ($\nu_l - \nu_s$) slightly off from the maximum gain position. In Fig. 5(c), the cavity is tuned near the $2 \rightarrow 1$ dressed-state transition frequency so as to optimize the cavity output intensity. The spatial axial-output-intensity distributions shown in Fig. 6 were recorded by imaging the center of the cavity onto a CCD array detector. The corresponding parts of Figs. 5 and 6 were recorded simultaneously.

ANALYSIS

The results presented above characterize and are consistent with a transition from spontaneous to stimulated atomic emission into the cavity modes. The magnitude of the step shown in Fig. 3 is determined [see Eq. (3)] by the ratio of A_{21}/a_{21}. In the present case, the observed step size is small, but this is entirely consistent with the small value of the ratio A_{21}/a_{21} characteristic of our small mode-degenerate optical cavity. Using the measured values of Ω_0, Δ (to determine A_{21} and A_{12}), and k, we have adjusted the value of the ratio a_{21}/A_{21} in Eq. (2) to fit the step size (slope change) experimentally observed (Fig. 3, trace *b*). The best fit is obtained for $a_{21}/A_{21} \simeq 2 \times 10^{-2}$. The corresponding calculated variation of n_c with N_a is shown in Fig. 3 as the solid line. The value obtained for a_{21}/A_{21} is in good agreement with the experimentally measured value of 0.05 obtained under similar experimental conditions in the same cavity.[24] We note that the ratio B_{ij}/a_{ij} determines the horizontal location of the step (laser transition) in Fig. 3, but does not affect the step size. This ratio was adjusted to achieve horizontal overlap of the experimental and theoretical curves.

The results shown in Figs. 5 and 6 demonstrate the dramatic changes in the spectral and spatial structure of the axial cavity emission that coincides with the onset of lasing. In Fig. 5(a), which shows the spectrum of the cavity output when the cavity is tuned to the central peak of the Mollow triplet, the observed linewidth (60 MHz) is due to the natural linewidth of the transition and to residual Doppler width. No structure is observed in the line. Similar results were obtained with the cavity tuned to either of the Mollow sidebands at very low atomic density, where the atomic radiation is due to spontaneous emission. The spatial profile of the cavity output obtained under the conditions just discussed [Fig. 6(a)] is smooth and featureless. This observation is entirely in agreement with the spatial profile expected in the case of fluorescence from an extended atomic sample. Under lasing conditions (large N and the cavity tuned to the enhanced Mollow sideband) a very different behavior is observed. With the cavity slightly detuned from the inverted dressed-state transition (corresponding to reduced gain), very sharp structures appear both in the spectral [Fig. 5(b)] and in the spatial [Fig. 6(b)] profile of the cavity field. The individual peaks in the output spectrum have widths determined by the resolution of the Fabry-Pérot analyzer (5 MHz). These peaks are substantially narrower than the free-space natural atomic linewidth (19 MHz). At the same time the spatial profile of the field becomes nonuniform. Both results can be understood by assuming that the gain in the medium is just enough to bring a few of the cavity modes above the lasing threshold. These modes would be the ones most efficiently coupled to the atomic medium. The peaks observed in the spectrum correspond to the small number of modes above threshold. The spectral narrowness of the peaks [Fig. 5(b)] results from an increase in the field correlation time associated with the laser oscillation. The spatial intensity pattern observed corresponds to the field distribution of the lasing modes. It is important to point out that the results shown in Figs. 5(b) and 6(b) correspond to a particular observation. Minor changes in the experimental parameters result in a large variety of spectral and spatial patterns with similar qualitative characteristics. As the cavity is tuned to the maximum gain frequency [Figs. 5(c) and 6(c)], the number of lasing modes is increased. It is no longer possible to resolve the frequencies of the individual modes and the spatial pattern becomes increasingly complicated.

TWO-PHOTON TWO-LEVEL-ATOM LASER

As mentioned earlier, the gain discussed in this paper can be attributed to the Raman-type process shown in Fig. 2. In Fig. 7, we show a higher-order Raman process in which three pump photons are absorbed, two photons are emitted, and the atoms are promoted to the excited state. In a cavity, the frequencies of the emitted photons can be constrained to be equal, and we have what amounts to a two-photon gain process. Since the process is nearly resonant at every step, the associated two-photon gain, which in the weak-field limit arises at the frequency $\nu_l + (\nu_l - \nu_a)/2$, should be relatively strong and provide a means of realizing an optical two-photon laser. A dressed-state analysis of this possibility will be published elsewhere.

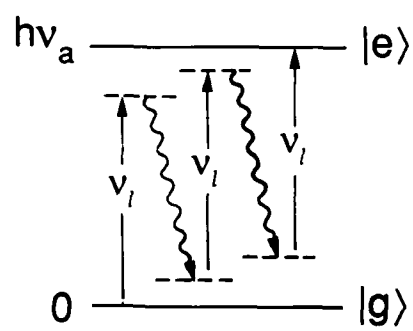

FIG. 7. Possible mechanism for two-photon gain in systems of driven two-level atoms.

CONCLUSIONS

We have experimentally demonstrated that laser action can take place in very simple system, i.e., a nearly homogeneous ensemble of strongly driven two-level atoms. The dynamics of this novel laser is entirely determined by radiative processes with dressed-atom spontaneous emission serving as both a pumping and a damping mechanism. Interestingly, in this system, the lasing takes place in the absence of atomic inversion and results in the increase of the excited-state population. The two-level-atom laser constitutes the realization of a new regime of driven-atom dynamics where the usual relaxation through spontaneous emission is replaced by an alternate sequence of spontaneous and stimulated emission processes. Although the simple rate-equation treatment of the system accounts for the features studied here, a more detailed theoretical analysis of this new dynamical regime is necessary. Finally, we point out that the driven two-level-atom system may provide a means of achieving steady-state optical two-photon gain.

ACKNOWLEDGMENTS

It is a pleasure to thank Professor M. G. Raymer for lending us a Video Frame Grabber and many useful discussions. We thank expert assistance of S. J. Kuo and S. E. Hodges. This work is supported by the National Science Foundation (Grant No. PHY-8718518) and Air Force Office of Scientific Research (Grant No. AFOSR-88-0086). One of us (A.L.) acknowledges support from the Conselho Nacional de Desenvolvimento Cientifico e Tecnologico (Brazil).

---

*Present address: Departamento de Fisica, Pontificia Universidade Catolica de Rio de Janeiro, Caixa Postal 38071, 22452 Rio de Janeiro, Brazil.

[1]B. R. Mollow, Phys. Rev. A **5**, 2217 (1972).
[2]S. Haroche and F. Hartmann, Phys. Rev. A **6**, 1280 (1972).
[3]S. L. McCall, Phys. Rev. A **9**, 1515 (1974).
[4]C. Cohen-Tannoudji and S. Reynaud, J. Phys. B **10**, 345 (1977).
[5]G. Khitrova, P. R. Berman, and M. Sargent III, J. Opt. Soc. Am. B **5**, 160 (1988).
[6]G. S. Agarwal, Phys. Rev. A **19**, 923 (1979).
[7]R. W. Boyd and M. Sargent III, J. Opt Soc. Am. B **5**, 99 (1988).
[8]D. A. Holm, M. Sargent III, and S. Stenholm, J. Opt. Soc. Am. B **2**, 1457 (1985).
[9]F. Y. Wu, S. Ezekiel, M. Ducloy, and B. R. Mollow, Phys. Rev. Lett. **38**, 1077 (1977).
[10]M. T. Gruneisen, K. R. MacDonald, and R. W. Boyd, J. Opt. Soc. Am. **5**, 123 (1988).
[11]G. Khitrova, J. F. Valley, and H. M. Gibbs, Phys. Rev. Lett. **60**, 1126 (1988).
[12]A. C. Tam, Phys. Rev. **19**, 1971 (1979).
[13]D. J. Harter, P. Narum, M. G. Raymer, and R. W. Boyd, Phys. Rev. Lett. **46**, 1192 (1981).
[14]R. W. Boyd, M. G. Raymer, P. Narum, and D. J. Harter, Phys. Rev. A **24**, 411 (1981).
[15]D. J. Harter and R. W. Boyd, Phys. Rev. A **29**, 739 (1984).
[16]D. Grandclement, G. Grynberg, and M. Pinard, Phys. Rev. Lett. **59**, 44 (1987).
[17]G. Grynberg, E. LeBihan, and M. Pinard, J. Phys. (Paris) **47**, 1321 (1986).
[18]D. Grandclement, G. Grynberg, and M. Pinard, Phys. Rev. Lett. **59**, 40 (1989).
[19]Y. Zhu, A. Lezama, and T. W. Mossberg, Phys. Rev. A **39**, 2268 (1989).
[20]B. R. Mollow, Phys. Rev. **188**, 1969 (1969).
[21]W. Hartig, W. Rasmussen, R. Schieder, and H. Walther, Z. Phys. A **278**, 205 (1976).
[22]F. Schuda, C. R. Stroud, Jr., and M. Hercher, J. Phys. B **7** L198 (1974).
[23]R. E. Grove, F. Y. Wu, and S. Ezekiel, Phys. Rev. A **15**, 227 (1977).
[24]As recently demonstrated, dressed-state inversions can be controlled by introducing spectral structure into the electromagnetic vacuum and dressed-state inversions can be created even when the atom and driving field are exactly resonant. See Y. Zhu, A. Lezama, T. W. Mossberg, and M. Lewenstein, Phys. Rev. Lett. **61**, 1946 (1988); A. Lezama, Y. Zhu, S. Morin, and T. W. Mossberg, Phys. Rev. A **39**, 2754 (1989). For related results see M. Lindberg and C. M. Savage, Phys. Rev. A **38**, 5182 (1988). In the present experiment, the mode-degenerate cavity employed introduces a small ($\simeq 5\%$) variation in the electromagnetic mode density across the Mollow triplet. This variation is not expected to play a major role in our experiments and is ignored in the analysis.
[25]C. Cohen-Tannoudji, in *Frontiers in Laser Spectroscopy*, Proceedings of the Les Houches Lectures, Session XXVII, 1975, edited by R. Balian, S. Haroche, and S. Liberman (North-Holland, New York, 1977).

Two-Photon Gain and Lasing in Strongly Driven Two-Level Atoms

M. Lewenstein
Institute for Theoretical Physics, Polish Academy of Sciences, 02-668 Warsaw, Poland

Y. Zhu and T. W. Mossberg
Department of Physics, University of Oregon, Eugene, Oregon 97403
(Received 7 July 1989)

Driven two-level atoms are shown to exhibit strong, resonantly enhanced, two-photon gain. This gain, unlike that observed in nonlinear mixing processes, is not constrained by a phase-matching condition involving the pump beam. Physically, the gain can be associated with inverted two-photon transitions between dressed states or multiphoton stimulated Raman scattering, and it may be useful in the realization of a two-photon laser. Comparison with the well-known single-photon gain found in the same system is made.

PACS numbers: 42.50.Hz, 42.55.Bi

Two-photon gain, which is based on the stimulated emission of photon pairs, was discussed early on in the laser era.[1,2] Lasers based on two-photon gain have been analyzed in numerous theoretical works[3-10] and predictions of intriguing characteristics have been made. Two-photon lasers have been predicted to have special noise properties,[3,6,10] to display bistable behavior,[7] and to turn on only with the help of an injected signal.[2] The novel properties expected of two-photon-gain–based lasers make the construction and study of such lasers an interesting scientific objective. As it turns out, this objective is made challenging by a general dearth of suitable two-photon-gain media. In fact, in the optical and infrared regimes, where effects involving photon statistics can be studied most easily, transient two-photon gain has been reported,[11,12] but steady-state two-photon gain has not yet been demonstrated. In the microwave regime, on the other hand, a Rydberg-atom gain medium has recently been shown capable of supporting steady-state two-photon maser action.[13]

In this paper, we examine the behavior of strongly driven two-level atoms and show that they can exhibit two-photon gain and support two-photon lasing. The gain observed in this system contrasts with the gain observed in wave-mixing processes in that it is not subject to a momentum-conservation (phase-matching) condition involving the pump field. It can be seen to arise as a result of population inversion on two-photon transitions between dressed atom-field states[14] or as a form of multiphoton-stimulated Raman scattering. In either picture, the internal state of the atom or atom and field system changes in the course of the two-photon stimulated emission process. The change in the internal state is associated with normal laser-type gain rather than a wave-mixing-type gain. In the following analysis, we work in the dressed-state picture.

In Fig. 1(a) [1(b)], we show the bare states [standard dressed states[14]] of a driven two-level atom. For nonvanishing atom-pump detuning, it is well known that certain single-photon transitions between the dressed levels display a positive inversion [see Fig. 1(b)]. The resulting single-photon gain has been thoroughly investigated both theoretically[15-17] and experimentally.[18,19] In fact, single-photon laser action has very recently been reported in cell[20] and atomic-beam-type[21] samples of two-level atoms. Of interest in the present context, one notes in Fig. 1(b) that the dressed-level spectrum also contains inverted two-photon transitions, and, owing to the periodic spacing of the dressed levels, near-resonant intermediate states. One is led to expect that a sample of driven two-level atoms will display two-photon gain and,

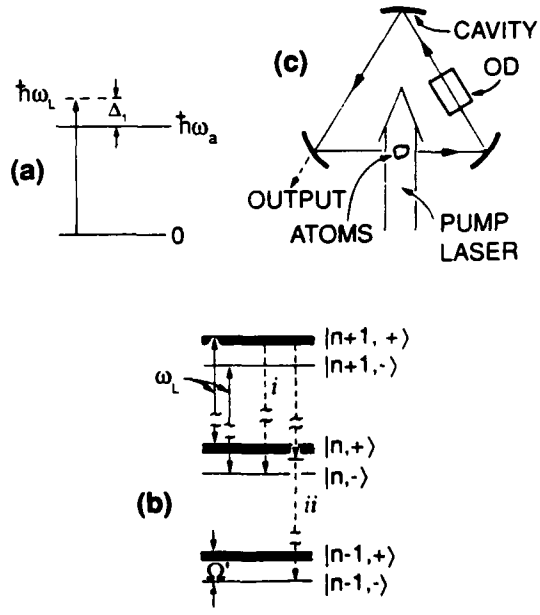

FIG. 1. (a) Two-level atom driven at frequency ω_L. (b) Standard dressed states (Ref. 14) describing the driven atom of (a). The lines representing the dressed levels have thicknesses indicating their relative populations. Transition *i* (*ii*) is an inverted one- (two-) photon transition. (c) Two-photon-laser system consisting of N two-level atoms coupled to a unidirectional ring cavity and transversely driven by a pump laser of frequency ω_L. OD denotes an optical diode.

in particular, that it will display degenerate two-photon gain useful in a two-photon laser. This expectation will be confirmed below and is also borne out in calculations of susceptibilities describing[22] the response of two-level atoms to two strong fields.

The dressed-state energy diagram in Fig. 1(b) provides a strong motivation to think that useful two-photon gain will exist in the driven two-level-atom system. We quantitatively analyze this gain through investigating the possibility of using it to realize two-photon-laser action. Consider a system of N two-level atoms located in a unidirectional, ring-type cavity and pumped by a field $\Omega\exp(-i\omega_L t)$ [see Fig. 1(c)]. The traveling-wave character and orthogonal orientation of the pump and cavity fields serve to discriminate against nonlinear gain processes requiring phase matching. In the rotating frame, the density matrix of the system obeys the following equation:

$$\dot{\rho} = -i[\mathcal{H},\rho] + \mathcal{L}_A\rho + \mathcal{L}_F\rho , \tag{1}$$

where the Hamiltonian is

$$\mathcal{H} = \tfrac{1}{2}\sum_{\mu}^{N}[\Delta_1\sigma_{3\mu} + \Omega(\sigma_\mu + \sigma_\mu^+) + g_\mu\sigma_\mu^+ a + g_\mu^* a^\dagger\sigma_\mu] + \Delta_2 a^\dagger a , \tag{2}$$

$\sigma_{3\mu}$, σ_μ, and σ_μ^+ are the standard Pauli matrices describing atom μ, a and $a^\dagger$ are cavity-mode operators, $\Delta_1 = \omega_a - \omega_L$, $\Delta_2 = \omega_c - \omega_L$, ω_a (ω_c) is the atomic (cavity) resonance frequency, and g_μ denotes the coupling of atom μ to the cavity mode. We assume that the atoms are localized to a small region of the cavity-mode volume within which we can let $|g_\mu| = g$, where g is a constant. We choose the phases of the individual atomic dipoles to be fixed relative to the pump field, and thereby introduce, in the absence of correlated pump and cavity fields, a spatially varying phase into the g_μ's. The last two terms in Eq. (1) describe cavity and spontaneous emission damping, i.e.,

$$\mathcal{L}_F\rho = 2\Gamma(a\rho a^\dagger - \tfrac{1}{2}a^\dagger a\rho - \tfrac{1}{2}\rho a^\dagger a) \tag{3}$$

and

$$\mathcal{L}_A\rho = 2\gamma\sum_{\mu}(\sigma_\mu\rho\sigma_\mu^+ - \tfrac{1}{2}\sigma_\mu^+\sigma_\mu\rho - \tfrac{1}{2}\rho\sigma_\mu^+\sigma_\mu) , \tag{4}$$

where Γ is the cavity half width at half maximum and 2γ denotes a spontaneous emission rate.

The system described by Eq. (1) is quite similar to the one describing optical bistability.[23] The only difference is that in Eq. (1), the pump field does not occupy a cavity mode. Quite recently, de Oliveira and Knight[24] observed a unitary equivalence between transverse and cavity-mode pumping provided that one assumes a correlation between the phases of the pump and cavity fields. Such a correlation does not exist in our model system [Fig. 1(c)].

We first transform Eqs. (1)–(4) to the dressed-state basis[14,25] using the unitary operator

$$\mathcal{U} = \prod_{\mu}\exp(i\alpha\sigma_{2\mu}) , \tag{5}$$

where $\sigma_{2\mu} = (\sigma_\mu^+ - \sigma_\mu)/i$, $\Omega' = (\Omega^2 + \Delta_1^2)^{1/2}$, and α is defined through $\Omega = \Omega'\sin2\alpha$ and $\Delta_1 = \Omega'\cos2\alpha$. Obviously, $\mathcal{U}$ diagonalizes the sum of the free-atom and pump Hamiltonians.

After transforming to the dressed basis,

$$\mathcal{H} = \sum_{\mu}\frac{\Omega'}{2}\sigma_{3\mu} + \Delta_2 a^\dagger a + \sum_{\mu}\frac{g_\mu^*}{4}[(1+\cos2\alpha)\sigma_\mu - (1-\cos2\alpha)\sigma_\mu^+ + \sin2\alpha\,\sigma_{3\mu}]a^\dagger + \sum_{\mu}\frac{g_\mu}{4}[(1+\cos2\alpha)\sigma_\mu^+ - (1-\cos2\alpha)\sigma_\mu + \sin2\alpha\,\sigma_{3\mu}]a , \tag{6}$$

where

$$\mathcal{L}_A = \frac{\gamma}{2}\sum_{\mu}\{[\sin2\alpha\,\sigma_{3\mu} + (1+\cos2\alpha)\sigma_\mu - (1-\cos2\alpha)\sigma_\mu^+]\rho[\sin2\alpha\,\sigma_{3\mu} + (1+\cos2\alpha)\sigma_\mu^+ - (1-\cos2\alpha)\sigma_\mu] - [1+\sigma_{3\mu}\cos2\alpha - (\sigma_\mu+\sigma_\mu^+)\sin2\alpha]\rho - \rho[1+\sigma_{3\mu}\cos2\alpha - (\sigma_\mu+\sigma_\mu^+)\sin2\alpha]\} , \tag{7}$$

whereas $\mathcal{L}_F$ remains the same. In Eqs. (6) and (7), $\sigma_{3\mu}$ (σ_μ and σ_μ^+) now refer to the dressed-state inversion (polarization) operators for atom μ.

We first use the above results to analyze the case of lasing mediated by one-photon gain.[15–21] The frequencies at which the driven atoms display large one- and two-photon gain differ [see Fig. 1(b)] so that one can select one-photon gain by appropriate tuning of the cavity, i.e., by making $\Delta_2 \approx \Omega'$. Antiresonant terms in Eqs. (6) and (7) can be dropped by invoking (1) standard rotating-wave approximation arguments based on the assumption that Δ_2 and Ω' are both much larger than g, γ, and Γ; and (2) the fact that in our system these terms contain atom-specific phase factors which tend to zero on summing over μ. The latter justification does not depend on the largeness of Δ_2 and Ω' compared to the other relevant frequencies.

Neglecting antiresonant terms in Eqs. (6) and (7) and assuming $\Delta_2 > 0$, one can derive the semiclassical equations associated with the standard laser model, i.e.,

$$\dot{S} = -(\gamma_1 + i\Omega')S + i\frac{g_1}{2}S_3 a ,$$
$$\dot{S}_3 = -\gamma_2(S_3 - \bar{S}_3) + ig_1(a^*S - S^*a) , \tag{8}$$
$$\dot{a} = -(\Gamma + i\Delta_2)a - i\frac{g_1}{2}S ,$$

where

$$S = \sum_{\mu}\sigma_\mu\exp(-i\phi_\mu)$$

denotes the macroscopic dressed-state polarization, $\mathbf{S}^*$ its conjugate,

$$S_3=\sum_\mu \sigma_{3\mu}$$

is the macroscopic inversion, and ϕ_μ is the phase of g_μ, $\gamma_1=\gamma(2+\sin^2 2\alpha)/2$, $\gamma_2=\gamma(1+\cos^2 2\alpha)$, and $g_1=g(1+\cos 2\alpha)/2$. The stationary value of $\bar{S}_3$, which describes the inversion of the dressed states, is given by

$$\bar{S}_3=\frac{-2N\cos 2\alpha}{1+\cos^2 2\alpha}. \tag{9}$$

For any $\Delta_1\neq 0$, the levels within each dressed-state doublet have unequal populations and, consequently, some dressed-state transitions are inverted and lasing can occur. For negative Δ_1, $\alpha>\pi/4$ and $\bar{S}_3>0$, corresponding to the situation shown in Fig. 1(b). The frequency of the single-photon lasing, $\omega_L^{(1\gamma)}=\omega_L+\Delta_L^{(1\gamma)}$, can be determined from

$$\Delta_L^{(1\gamma)}=\frac{\gamma_1\Delta_2+\Gamma\Omega'}{\Gamma+\gamma_1}, \tag{10}$$

and the laser threshold condition is

$$-\frac{Ng^2\cos 2\alpha(1+\cos 2\alpha)^2}{4\gamma\Gamma(2+\sin^2 2\alpha)(1+\cos^2 2\alpha)}\left[1+\frac{(\Delta_2-\Omega')^2}{(\gamma_1+\Gamma)^2}\right]^{-1}\geq 1. \tag{11}$$

It is interesting to note that relation (11) correctly predicts the single-photon dressed-state lasing observed in the experiment of Ref. 21, where $\cos 2\alpha\approx -\frac{1}{2}$, $\Delta_2\approx\Omega'\approx 20\gamma$, and $\Gamma\approx 2\gamma$. Using these values, we can write the threshold condition as

$$\frac{Ng^2}{\gamma^2}\geq 200,$$

or with $g\approx 0.04\gamma$, as in Ref. 21, one expects one-photon lasing to occur for $N\approx 10^5$, in agreement with observations.

Let us now turn to the discussion of two-photon gain and lasing. We assume that the cavity is tuned so that $2\Delta_2\approx\Omega'$. The Hamiltonian, Eq. (6), contains various nonresonant terms which do not conserve the excitation number. For $\epsilon=O(g/\Omega',\gamma/\Omega',\Gamma/\Omega')$ small, we wish to approximate Eq. (6) with an effective Hamiltonian describing resonant two-photon processes. Such an effective Hamiltonian will conserve a generalized number of excitations,

$$N_{\rm eff}=a^\dagger a+2\sum_\mu \sigma_\mu^+\sigma_\mu.$$

In order to derive the effective Hamiltonian, we work along the lines of Ref. 26; i.e., first, we write down the Schrödinger equation, which follows from Eq. (6). Vectors which correspond to a definite value of $N_{\rm eff}$ couple to those with $N_{\rm eff}\pm 1,\pm 3$. Eliminating the latter ones in the lowest order of the coupling g, we obtain an equation containing couplings within the subspace of the fixed $N_{\rm eff}$ only. This equation determines $H_{\rm eff}$ completely. After introducing a new macroscopic polarization operator

$$S=\sum_\mu \sigma_\mu\exp(-2i\phi),$$

and its conjugate $\mathbf{S}^*$, we again utilize the fact that terms summed over randomly distributed phases can be neglected. The effective Hamiltonian then takes the simplified form

$$\mathcal{H}_{\rm eff}=\Delta_2 a^\dagger a+\frac{\Omega'}{2}S_3-\frac{g^2}{8\Delta_2}\sin 2\alpha(1+\cos 2\alpha)[S^+a^2+(a^\dagger)^2S]$$
$$+\frac{g^2}{16\Delta_2}[(1+\cos 2\alpha)^2+\tfrac{1}{3}(1-\cos 2\alpha)^2](a^\dagger aS_3+\tfrac{1}{2}S_3). \tag{12}$$

Note that $\mathcal{H}_{\rm eff}$ does not have the form of a standard two-photon-laser Hamiltonian in that it contains a dynamical Stark-shift term which causes the laser frequency to be intensity dependent. Nevertheless, after dropping antiresonant terms in $\mathcal{L}_A$, a semiclassical theory of two-photon lasing governed by Eq. (12) may be easily formulated.[27]

The frequency of the two-photon laser, $\omega^{(2\gamma)}=\omega_L+\Delta_L^{(2\gamma)}$, which is dependent on the laser output intensity, can be determined from

$$\Delta_L^{(2\gamma)}=\frac{\gamma_1(\Delta_2+\delta S_3)+\Gamma(\Omega'+\delta+2\delta|a|^2)}{2\Gamma+\gamma_1}, \tag{13}$$

where

$$\delta=\frac{g^2}{16\Delta_2}[(1+\cos 2\alpha)^2+\tfrac{1}{3}(1-\cos 2\alpha)].$$

Note that the self-consistency of our theory (i.e., validity of the resonant approximation used for derivation of $\mathcal{H}_{\rm eff}$) requires that $\Delta_L^{(2\gamma)}\approx\Delta_2$. The Stark-shift effects tend to destroy the resonant condition making the stability of the two-photon laser quite complicated. We assume here that the cavity is tuned to compensate for the dynamical Stark shift. In this case, the laser threshold condition is simply

$$\frac{g^2\bar{S}_3}{8}\frac{\sin 2\alpha(1+\cos 2\alpha)}{\Delta_2\Gamma}\left[\frac{\gamma_2}{\gamma_1}\right]^{1/2}\geq 1. \tag{14}$$

Slightly above threshold, the laser intensity is approximately given by

$$|a|^2\approx\frac{\bar{S}_3\gamma_2}{2\Gamma}. \tag{15}$$

In our analysis, we have assumed that the two lasing processes of Fig. 1(b) (based on one- and two-photon gain)

can be spectrally distinguished. This implies that

$$\frac{2\Delta_L^{(2\gamma)}-\Omega'}{\Omega'}=\frac{2\delta|a|^2}{\Omega'}\approx\frac{g^2\gamma_2\bar{S}_3}{16\Delta_2\Omega'\Gamma}[(1+\cos 2\alpha)^2+\tfrac{1}{3}(1-\cos 2\alpha)^2]\ll 1. \tag{16}$$

It is easy to check that for $\Omega'\approx 50\gamma$, and other parameters chosen as in the single-photon, dressed-state-laser experiment discussed above, condition (14) implies

$$\left[\frac{g}{\gamma}\right]^2 N\geq 1\times 10^3,$$

whereas condition (16) implies

$$\left[\frac{g}{\gamma}\right]^2 N\ll 4\times 10^4,$$

so that one has roughly 1.5 decades of parameter range, in which the present analysis is valid and two-photon-laser action is expected to occur. Note also that under the experimental conditions employed to observe single-photon lasing,[21] the two-photon-lasing threshold is only about 5 times higher than the single-photon-lasing threshold.

One should stress that two-photon lasing will, in principle, compete with strongly detuned single-photon lasing. For the same choice of parameters as in the preceding paragraph, Eq. (11) indicates that detuned single-photon lasing is possible for

$$\left[\frac{g}{\gamma}\right]^2 N\geq 10^4.$$

Note, however, that the phases of the individual dipoles required for single-photon lasing and two-photon lasing are different. Therefore, we expect that the two processes will have a strong anticorrelation. As soon as the macroscopic polarization required for the buildup of the two-photon laser is created, it will automatically destroy the coherence needed for single-photon lasing and vice versa. Consequently, when two-photon lasing is turned on by the requisite injection signal a strong bias is set up against competing processes.

In conclusion, we have shown that driven two-level atoms display two-photon gain and that this gain may be useful in the realization of two-photon-laser action. In fact, generalization of the analysis presented here indicates that three- or more-photon amplification and lasing may be possible in the same system.

We acknowledge stimulating discussions with A. Lezama, H. Carmichael, and J. Wynne. We thank the National Science Foundation (Grant No. PHY8718518) and the Air Force Office of Scientific Research (Contract No. AFOSR-88-0086) for financial support.

[1]P. P. Sorokin and N. Braslau, IBM J. Res. Dev. **8**, 177 (1964).
[2]A. M. Prokhorov, Science **149**, 828 (1965).
[3]N. Nayak and B. K. Mohanty, Phys. Rev. A **19**, 1204 (1979).
[4]H. P. Yuen, Appl. Phys. Lett. **26**, 505 (1975).
[5]L. M. Narducci, W. W. Eidson, P. Furcinitti, and D. C. Eteson, Phys. Rev. A **16**, 1665 (1977).
[6]H. P. Yuen, Phys. Rev. A **13**, 2226 (1976).
[7]Z. C. Wang and H. Haken, Z. Phys. B **55**, 361 (1984); **56**, 77 (1984); **56**, 83 (1984).
[8]M. Brune, J. M. Raimond, and S. Haroche, Phys. Rev. A **35**, 154 (1987).
[9]L. Davidovich, J. M. Raimond, M. Brune, and S. Haroche, Phys. Rev. A **36**, 3771 (1987).
[10]M. O. Scully, K. Wodkiewicz, M. S. Zubairy, J. Bergou, N. Lu, and J. Meyer ter Vehn, Phys. Rev. Lett. **60**, 1832 (1988).
[11]B. Nikolaus, D. Z. Zhang, and P. E. Toschek, Phys. Rev. Lett. **47**, 171 (1981).
[12]M. M. T. Loy, Phys. Rev. Lett. **41**, 473 (1978).
[13]M. Brune, J. M. Raimond, P. Goy, L. Davidovich, and S. Haroche, Phys. Rev. Lett. **59**, 1899 (1987); IEEE J. Quantum Electron. **24**, 1323 (1988).
[14]C. Cohen-Tannoudji, in *Frontiers in Laser Spectroscopy*, Proceedings of the Les Houches Summer School, Session XXVII, edited by R. Balian, S. Haroche, and S. Liberman (North-Holland, Amsterdam, 1977).
[15]B. R. Mollow, Phys. Rev. A **5**, 2217 (1972).
[16]S. Haroche and F. Hartmann, Phys. Rev. A **6**, 1280 (1972).
[17]S. L. McCall, Phys. Rev. A **9**, 1515 (1974).
[18]F. Y. Wu, S. Ezekiel, M. Ducloy, and B. R. Mollow, Phys. Rev. Lett. **38**, 1077 (1977).
[19]M. T. Gruneisen, K. R. MacDonald, and R. W. Boyd, J. Opt. Soc. Am. B **5**, 123 (1988).
[20]G. Khitrova, J. F. Valley, and H. M. Gibbs, Phys. Rev. Lett. **60**, 1126 (1988).
[21]A. Lezama, Y. Zhu, M. Kanskar, and T. W. Mossberg, Phys. Rev. A **41**, 1576 (1990).
[22]G. S. Agarwal and N. Nayak, J. Opt. Soc. Am. B **1**, 164 (1984); Phys. Rev. A **33**, 391 (1986); see also M. T. Gruneisen, K. R. MacDonald, A. L. Gaeta, R. W. Boyd, and D. J. Harter, Phys. Rev. A **40**, 3464 (1989).
[23]L. A. Lugiato, Prog. Opt. **21**, 69 (1984).
[24]F. A. M. de Oliveira and P. L. Knight, Phys. Rev. Lett. **61**, 830 (1988); Phys. Rev. A **39**, 3417 (1989).
[25]C. Cohen-Tannoudji and S. Reynaud, J. Phys. B **10**, 365 (1977).
[26]S. Stenholm, Phys. Rep. **6**, 1 (1973).
[27]H. Haken, *Laser Light Dynamics* (North-Holland, Amsterdam, 1981).

PHYSICAL REVIEW A VOLUME 41, NUMBER 11 1 JUNE 1990

Resonance fluorescence of two-level atoms under strong bichromatic excitation

Yifu Zhu, Qilin Wu, A. Lezama, Daniel J. Gauthier, and T. W. Mossberg
Department of Physics and Chemical Physics Institute, University of Oregon, Eugene, Oregon 97403
(Received 18 December 1989)

We have measured the emission spectrum of two-level-like Ba atoms driven by two, strong, equal-amplitude fields with frequency separation 2δ. The spectrum consists of a series of peaks with an essentially constant spacing δ and alternating linewidths. These features differ qualitatively from the characteristic triplet spectrum observed in the case of strong monochromatic excitation. Certain features of the observed spectrum such as its comblike structure can be motivated in terms of the energy spectrum of atom–bichromatic-field product states. Other features, such as the alternating linewidths, require more subtle analysis.

The fluorescence spectrum of two-level atoms (TLA's) driven by strong monochromatic excitation has been the subject of considerable theoretical and experimental study over the years.[1,2] This spectrum, initially predicted by Mollow[3] and subsequently observed by various groups,[4–6] possesses a characteristic symmetric triplet structure that can be inferred from the dressed-atom model.[7] The detailed understanding of the spectrum is an important achievement of quantum optics. An obvious and intriguing generalization of the Mollow problem is to determine the nature of the atomic fluorescence spectrum under conditions of bichromatic or multichromatic excitation. TLA dynamics in the presence of multichromatic excitation has been explored from a number of contexts,[8–22] but the question of resonance fluorescence has received only limited attention.[19–22] In fact, to our knowledge, no experimental work in this area has yet appeared.

We report here an experimental study of the resonance fluorescence spectrum characteristic of two-level atoms driven by a strong bichromatic excitation field. Specifically, we have studied the fluorescence spectrum of two-level-like barium atoms driven by two equal-amplitude fields that have frequencies $\nu_a-\delta$ and $\nu_a+\delta$ and are tuned near the ^{138}Ba 553.5-nm $^1S_0\rightarrow{}^1P_1$ transition frequency, ν_0. The experimental apparatus is depicted in Fig. 1. Light from a frequency-stabilized ring dye laser (Coherent 699-21) is passed through an acousto-optic modulator (AOM). The deflected and undeflected portions of the AOM output, differing in frequency by the AOM drive frequency 2δ provide the two components of the bichromatic excitation field. On emerging from the AOM, the two beams were collimated, spatially superimposed, intensity matched, and angularly aligned to maximize the depth of the 2δ intensity beat signal observed on a large-area photodiode. An 80% modulation depth was obtained. The combined, linearly polarized, beams intersected an atomic beam of natural Ba at a position coinciding with the center of a 5-cm-long confocal Fabry-Perot cavity. The Fabry-Perot is piezoelectrically scannable, has a free-spectral range of 1.5 GHz, and has an empty-cavity finesse of approximately 200. The bichromatic laser beam, Ba atomic beam, and cavity axis were mutually orthogonal. Fluorescent light transmitted out one end of the cavity was spatially filtered and imaged onto the cathode of a photomultiplier tube (PMT). The PMT output was sent to computer-controlled photon-counting electronics. In the limit of low atomic-beam densities where gain effects[23,24] can be ignored, recordings of the Fabry-Perot output intensity as a function of ν_c, where ν_c is the cavity resonance frequency, correspond to the single-atom resonance fluorescence spectrum. In our experiments, Doppler broadening and finite Fabry-Perot finesse contribute to an overall instrumental resolution of 25 MHz. The natural width of the $^1S_0\rightarrow{}^1P_1$ Ba transition is $\simeq$19 MHz.[25]

Figure 2 shows the spectra recorded for $\Delta\equiv\nu_a-\nu_0=0$, $2\delta=200$ MHz, and for various values of Ω, where Ω is the single-excitation-field-component resonant Rabi frequency. The observed spectra consist of a series of peaks symmetrically located about a central peak coinciding with the atomic transition frequency ν_0. From Fig. 2, one sees that neighboring peaks are separated in frequency by δ, and that the number of peaks increases with increasing Ω. Interestingly, the peak spacing is independent of Ω. At very low values of Ω (not shown in Fig. 2), the spectrum is observed to consist of only two peaks which correspond to elastic scattering at the excitation frequencies. These observations are consistent with the numerical cal-

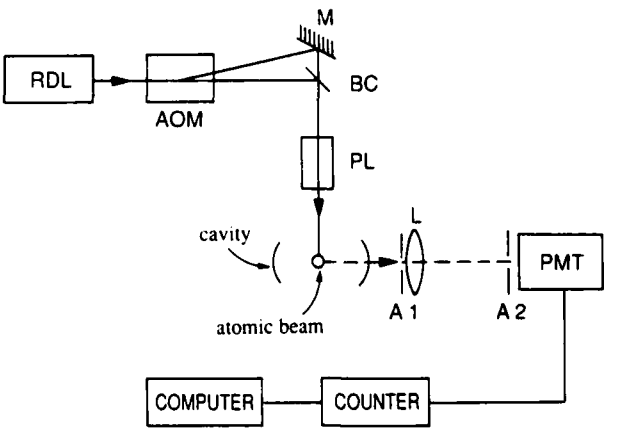

FIG. 1. Schematic of the experimental apparatus: RDL, cw ring dye laser; BC, beam combiner; AOM, acousto-optic modulator; M, mirror; PL, linear polarizer; A1 and A2, apertures; L, lens; PMT, photomultiplier tube.

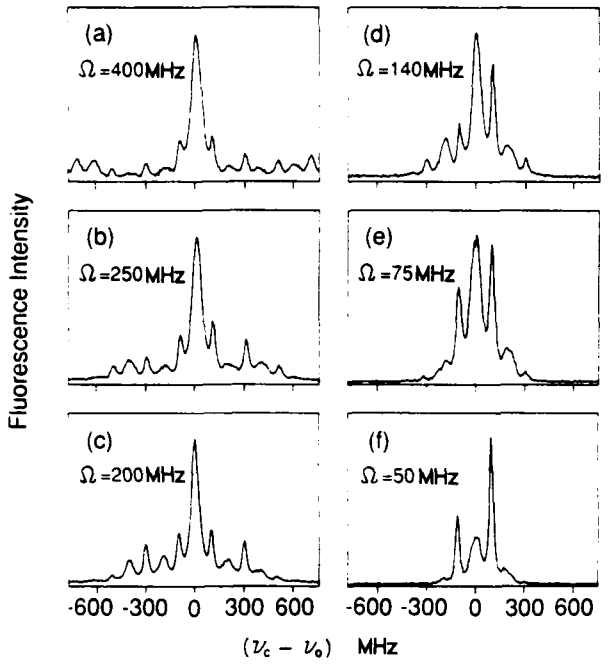

FIG. 2. Atomic fluorescence intensity vs cavity detuning from the atomic transition frequency $(\nu_c - \nu_0)$. Ba atoms are driven by a bichromatic excitation field whose components differ in frequency by 200 MHz and are located symmetrically about the atomic resonance frequency ν_0. The resonant Rabi frequency of each component of the driving field considered separately, Ω, is (a) 400 MHz; (b) 250 MHz; (c) 200 MHz; (d) 140 MHz; (e) 75 MHz; (f) 50 MHz. The small asymmetry in the spectra about ν_0 is attributed to the presence of Ba isotopes other than ^{138}Ba. Note that in (a) the 1.5-GHz free-spectral range of the Fabry-Perot cavity employed leads to distortions in the peak amplitudes observed in the portions of the spectrum most removed from ν_0.

culations of Newbold and Salamo.[20] Another interesting feature of these spectra is the alternation in linewidth as one moves from peak to peak in the spectrum. Peaks with frequencies given by $\nu_0 \pm m\delta$ with m even (m odd) have a relatively larger (smaller) linewidth. Newbold and Salamo predicted that the elastic scattering occurs only at frequencies $\nu_0 \pm m\delta$ (m odd), and for small Ω, the contributions from elastic scattering at these frequencies are larger than the contributions from inelastic scattering. Since the linewidth of the elastic scattering should be relatively narrow, its contribution to the odd-m peaks may explain the linewidth variation observed in our experiment. The observation that the number of peaks in the spectra is Rabi frequency dependent, that the peak spacings are Rabi frequency independent, and that the peak linewidths alternate all constitute features qualitatively different from those found in the case of monochromatic excitation.

A motivation for the basic structure of the observed spectra can be found in the level structure of the product states representing the uncoupled atom–bichromatic-field system. These product states can be written as $|n_a\rangle|n_1\rangle|n_2\rangle$, where $n_a = 0$ (1) represents the atomic ground state (excited state), and n_1 and n_2 represent the photon occupation numbers of the field modes at frequency $\nu_a - \delta$ and $\nu_a + \delta$, respectively. It is straightforward to show that these product states group into manifolds each corresponding to a particular value of $N = n_a + n_1 + n_2$. The centers of the manifolds are split by $h\nu_0$ (with $\nu_a = \nu_0$). Within each manifold, individual states are separated in energy by $h\delta$ (see Fig. 3). In the limit of weak excitation ($\Omega \ll \delta$) the product states should provide a good description of the system, and peaks in the fluorescence spectrum must then correspond to transitions from individual states in one manifold to states in the next lower manifold. It is clear that the only possible transition frequencies are $\nu_a \pm m\delta$, where m is an integer. Inclusion of the atom-field coupling leads to dressed states,[26] which are linear combinations of the uncoupled atom-field product states. For $\Omega \geq \delta$ one must work with the actual dressed states to predict the spectra. Interestingly, the peak positions in the observed spectra imply that the level structure of the dressed states is essentially identical to that of the product states. On the other hand, the change in the number and the relative intensity of the peaks indicates that the composition of the dressed states (in terms of the product states) depends sensitively on the atom-field interaction strength. It is interesting that the atom-field interaction modifies the composition of the dressed states without significantly perturbing their energies. While the simple energy-level considerations mentioned here provide some motivation for the locations of the peaks shown in Fig. 2, they provide no reliable insight into the alternation of peak linewidths.

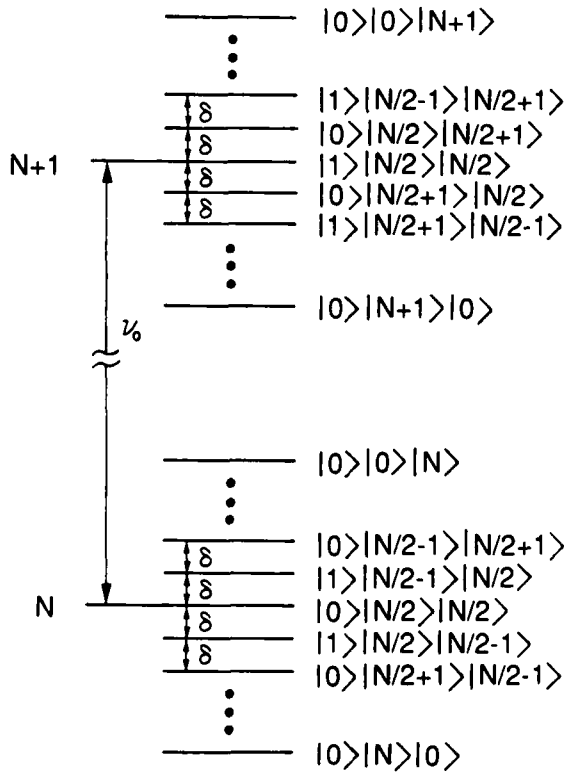

FIG. 3. Atom–bichromatic-field product states. The number $(N, N+1)$ to the left of each manifold represents the total number of excitations, i.e., $n_a + n_1 + n_2$. In the case of the lower manifold, N has been arbitrarily assumed to be even.

In conclusion, we have measured the resonance fluorescence spectrum of two-level atoms under strong bichromatic excitation. The observed spectra are qualitatively different from the Mollow spectrum. Further work involving a broader range of experimental parameters and careful comparison with the theoretical calculations is planned, and in view of the recent calculations of Wilkens and Rzazewski[22] indicating rich spectra associated with doubly amplitude modulated excitation fields, measurements are planned in this area as well.

It is a pleasure to thank M. Lewenstein for many useful discussions. We gratefully acknowledge financial support from National Science Foundation Grant No. PHY871-8518 and Air Force Office of Scientific Research Grant No. AFOSR-88-0086.

[1]P. L. Knight and P. W. Milonni, Phys. Rep. **66**, 21 (1980).
[2]J. D. Cresser, Phys. Rep. **94**, 47 (1983).
[3]B. R. Mollow, Phys. Rev. **188**, 1969 (1969).
[4]R. E. Grove, F. Y. Wu, and S. Ezekiel, Phys. Rev. A **15**, 227 (1977).
[5]F. Schuda, C. R. Stroud, Jr., and M. Hercher, J. Phys. B **7**, L198 (1974).
[6]W. Hartig, W. Rasmussen, R. Schieder, and H. Walther, Z. Phys. A **278**, 205 (1976).
[7]C. Cohen-Tannoudji and S. Reynaud, J. Phys. B **10**, 345 (1977).
[8]L. W. Hillman, J. Krasinski, K. Koch, and C. R. Stroud, Jr., J. Opt. Soc. Am. B **2**, 211 (1985), and references therein.
[9]P. Thomann, J. Phys. B **13**, 1111 (1980).
[10]A. M. Bonch-Bruevich, T. A. Vartanyan, and N. A. Chigir, Zh. Eksp. Teor. Fiz. **77**, 1899 (1979) [Sov. Phys. JETP **50**, 901 (1979)].
[11]A. M. Bonch-Bruevich, S. G. Przhibelskii, and N. A. Chigir, Zh. Eksp. Teor. Fiz. **80**, 565 (1981) [Sov. Phys. JETP **53**, 285 (1981)].
[12]G. I. Toptygina and E. E. Fradkin, Zh. Eksp. Teor. Fiz. **82**, 429 (1982) [Sov. Phys. JETP **55**, 246 (1982)].
[13]G. S. Agarwal and N. Nayak, J. Opt. Soc. Am. B **1**, 164 (1984).
[14]G. S. Agarwal and N. Nayak, Phys. Rev. A **33**, 391 (1986).
[15]S. Chakmakjian, K. Koch, and C. R. Stroud, Jr., J. Opt. Soc. Am. B **5**, 2015 (1988), and references therein.
[16]J. H. Eberly and V. D. Popov, Phys. Rev. A **37**, 2012 (1989).
[17]T. W. Mossberg and M. Lewenstein, Phys. Rev. A **39**, 163 (1989).
[18]R. Guccione-Gush and H. P. Gush, Phys. Rev. A **10**, 1474 (1974).
[19]B. Blind, P. R. Fontana, and P. Thomann, J. Phys. B **13**, 2717 (1980).
[20]M. A. Newbold and G. J. Salamo, Phys. Rev. A **22**, 2098 (1980).
[21]V. Hizhnyakov and M. Rozman, Opt. Commun. **52**, 183 (1984).
[22]M. Wilkens and K. Rzazewski, Phys. Rev. A **40**, 3164 (1989).
[23]Y. Zhu, A. Lezama, and T. W. Mossberg, Phys. Rev. A **39**, 2268 (1989).
[24]D. A. Holm, M. Sargent III, and S. Stenholm, J. Opt. Soc. Am. B **2**, 1456 (1985).
[25]A. Lurio, Phys. Rev. **136**, A376 (1964).
[26]Bichromatic-field dressed states have been considered in other contexts. See, for example, S. Haroche, Ann. Phys. **6**, 189 (1971); **6**, 327 (1971); G. Grynberg and P. R. Berman, Phys. Rev. A **39**, 4016 (1989).

Vacuum Rabi Splitting as a Feature of Linear-Dispersion Theory: Analysis and Experimental Observations

Yifu Zhu, Daniel J. Gauthier, S. E. Morin, Qilin Wu, H. J. Carmichael, and T. W. Mossberg
Department of Physics and Chemical Physics Institute, University of Oregon, Eugene, Oregon 97403
(Received 7 February 1990)

The spectral and temporal response of an optical cavity resonantly coupled to an ensemble of barium atoms has been investigated experimentally. The empty-cavity transmission resonances are found to split in the presence of the atoms and, under these conditions, the cavity's temporal response is found to be oscillatory. These effects may be viewed as a manifestation of a vacuum-field Rabi splitting, or as a simple consequence of the linear absorption and dispersion of the intracavity atoms.

PACS numbers: 42.50.−p, 42.60.Da, 42.65.Pc

A composite atom-cavity system can be created by placing atoms inside an optical cavity. The behavior of such a coupled system can often be more complex and hence richer than that of either the atoms or the cavity considered separately. Elucidation of the properties of such atom-cavity systems is important since they play a vital role in the analysis of effects such as optical bistability, laser operation, and quantum fluctuations. Recently, it has been predicted that the insertion of a single atom into a cavity can lead to a splitting in the atomic fluorescence spectrum[1] and the empty-cavity transmission resonances[2,3] when the atom is strongly coupled to the cavity. This splitting, termed the vacuum Rabi splitting, has attracted the attention of the quantum-optics community because it is considered to be an important manifestation of the quantum nature of the electromagnetic field.

In the optical regime, the experimental confirmation of the single-atom vacuum Rabi splitting has been precluded by the smallish size of the coupling between the atom and the cavity.[4] Fortunately, it has been shown that cavity resonance splitting also occurs when many atoms are inserted into a cavity, and that the magnitude of the splitting increases with the square root of the number of atoms inserted.[2,3] Recently, multiatom enhancement has been employed successfully in an effort to observe vacuum Rabi splittings.[5-7]

In this paper, we describe an experimental investigation of resonant, multiatom, vacuum Rabi splitting. Cavity throughput as a function of both frequency (continuous-wave input) and time (pulsed input) has been measured in the same system. We find that our experimental results are in excellent agreement with a *completely classical* model in which the cavity transmission function is derived using the standard concepts of multibeam interference[8] applied to a cavity containing atoms displaying *linear* absorption and dispersion.[9] This approach to calculating the cavity's transmission function is dramatically different from the one employed in QED descriptions of the problem. The success of a totally classical model indicates, contrary to popular belief, that the vacuum Rabi splitting is not an inherently quantum phenomenon. In addition, our experimental results demonstrate that the multiatom vacuum Rabi splitting can be observed in cavities having an active volume (finesse) more than an order of magnitude larger (smaller) than previously demonstrated.

In our model of the coupled atom-cavity system, the cavity is taken to be a confocal cavity with length $\mathcal{L}_c$, and the atoms are taken to be classical Lorentz oscillators whose resonance frequency ν_0 is near a cavity resonance (transmission maxima) at frequency ν_m. The cavity mirrors have an intensity reflection (transmission) coefficient of R (T). The Lorentz oscillators have a full width at half maximum (FWHM) δ_H, an oscillator strength f_0, a number density N, and are contained in a slab of length $L < \mathcal{L}_c$.

Using a standard multibeam interference analysis, it can be shown that the intensity transmission function of the coupled atom-cavity system is given by

$$T_c(\nu) = |t_c(\nu)|^2 = \frac{T^2 e^{-aL}}{(1-Re^{-aL})^2 + 4Re^{-aL}\sin^2(\epsilon/2)} \tag{1}$$

for a plane wave propagating along the cavity axis where

$$\epsilon(\nu) = 2\pi(\Delta - \Delta_m)/\Delta_{FSR} + 4\pi(n-1)L\nu/c$$

is the phase shift experienced by the field upon completion of a round-trip through the cavity, aL is the single-pass absorption, and $t_c(\nu)$ is the amplitude transmission function. Here, $\Delta = \nu - \nu_0$, $\Delta_m = \nu_m - \nu_0$, and $\Delta_{FSR} = c/2\mathcal{L}_c$ is the free spectral range of the empty cavity where c is the speed of light in vacuum. For an empty cavity with a large finesse $F = \pi\sqrt{R}/(1-R)$, the empty-cavity resonance width is given by $\delta_c = \Delta_{FSR}/F$. The frequency-dependent intensity-absorption coefficient and refractive index of the collection of Lorentz oscillators are given by

$$a = a_0 \frac{\delta_H}{4\Delta^2 + \delta_H^2}, \quad n = 1 - a_0 \frac{c}{2\pi\nu} \frac{\Delta\delta_H}{4\Delta^2 + \delta_H^2}, \tag{2}$$

respectively, where $a_0 = 2f_0 Ne^2/mc\delta_H$ is the line-center absorption coefficient, and e (m) is the electron charge (mass). It should be noted that only *linear*-absorption and refractive-index terms are included in Eq. (2). The inclusion of nonlinear, i.e., intensity-dependent, terms leads to effects such as optical bistability.[10]

We find that linear absorption and dispersion introduced by the intracavity atoms alter the transmission function in that $T_c(\nu)$ may exhibit a structure which is completely different from that found in the empty-cavity case. The location and even the number of cavity resonances [maxima in $T_c(\nu)$] may change. In the analysis of these changes, we limit our attention to the case of low single-pass absorption ($a_0 L \ll 1$), high-cavity finesse ($R \simeq 1$), atom-cavity resonance ($\Delta_m = 0$), small-frequency differences ($\Delta \ll \Delta_{FSR}$), and comparable atomic and cavity resonance widths ($\delta_c \simeq \delta_H$).

Neglecting the effects of absorption, the zeros of $\epsilon(\nu)$ determine the peaks in the cavity transmission function $T_c(\nu)$, and the slope of $\epsilon(\nu)$ at the zeros provides a measure of the resonance widths. In Fig. 1(a), we plot $\epsilon(\nu)$ for several different atomic number densities. In Fig. 1(b), the atomic absorption and dispersion functions of Eq. (2) are plotted. At zero density, the expression for $\epsilon(\nu)$ contains a single nonzero term corresponding to a straight line with a slope of $2\pi/\Delta_{FSR}$ [dashed line in Fig. 1(a)] indicating that the cavity has a single peak at $\Delta = 0$. For nonzero atomic densities, a second term, proportional to the atomic dispersion function, contributes to $\epsilon(\nu)$ as well. At low densities, the dispersion reduces the slope of $\epsilon(\nu)$ at $\Delta = 0$ thereby broadening the cavity transmission resonance. (Absorption also contributes to this broadening.) At higher atomic densities, $\epsilon(\nu)$ is so distorted by the dispersive term that it actually passes through zero three times. One zero, as in the empty-cavity case, occurs at $\Delta = 0$, and two new zeros, located symmetrically about $\Delta = 0$, appear [see Fig. 1(a)]. For atomic densities high enough to produce a three-zero structure in $\epsilon(\nu)$, the absorptive part of the atomic response destroys the central transmission peak and slightly shifts the remaining two peaks away from the zeros of the function $\epsilon(\nu)$ [see Fig. 1(c)].

A more detailed analysis reveals that the two peaks in the cavity transmission are approximately Lorentzian in shape,[2] occur at the frequencies $\Delta = \pm \Omega/2$, where

$$\Omega = \left[\frac{Fa_0 L}{\pi} \delta_H \delta_c - \frac{(\delta_H - \delta_c)^2}{4} \right]^{1/2}, \tag{3}$$

and have a height

$$h = \left[\frac{T^2}{(1-R)^2} \right] \left[\frac{\delta_c^2}{(\delta_H + \delta_c)^2} \right] \tag{4}$$

and a width (FWHM) of

$$\delta_c' = (\delta_H + \delta_c)/2. \tag{5}$$

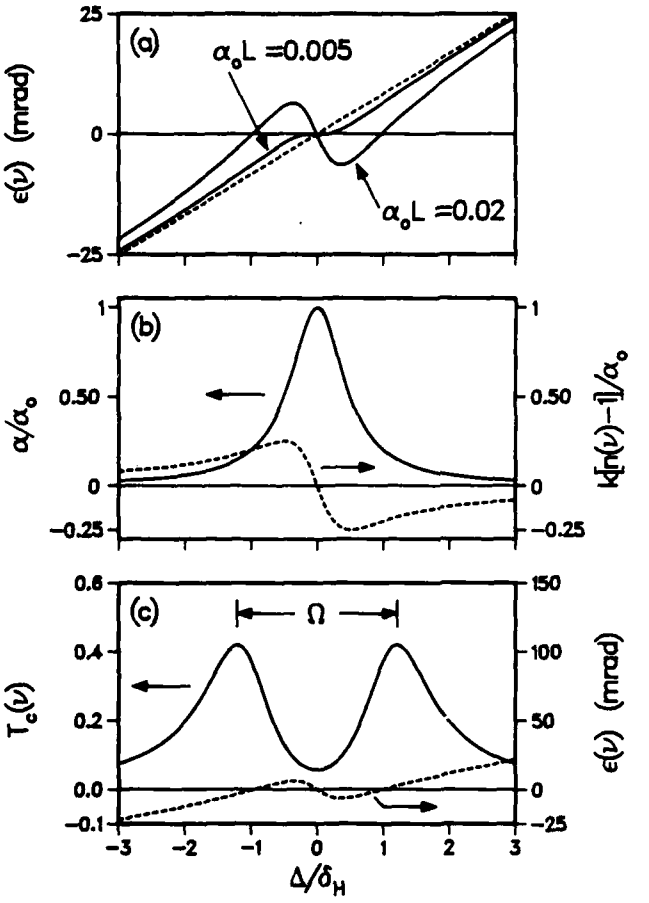

FIG. 1. (a) Phase shift experienced by the field upon completion of a round trip through the cavity for various values of the line-center, single-pass absorption as a function of the detuning of the probe-laser frequency from the atomic resonance frequency normalized to the atomic resonance width. The cavity resonance is tuned to the atomic resonance ($\Delta_m = 0$), $\Delta_{FSR}/\delta_H = 750$, $\delta_c/\delta_H = 1.5$, and $F = 500$. The dashed line is the empty-cavity phase shift. (b) Normalized absorption (solid line) and change in refractive index (dashed line) produced by the collection of Lorentz oscillators. The magnitude of the probe wave vector is denoted by k. (c) Cavity transmission function and phase shift as functions of the normalized frequency. The values of the parameters used to generate this plot are the same as in (a) with $a_0 L = 0.02$.

Note that the width of the peaks is the average of the uncoupled atom and cavity widths.[7] The splitting will be resolved when $\Omega \gg (\delta_H + \delta_c)/2$; that is, when

$$a_0 L \gg \pi/F. \tag{6}$$

The high-atomic-density resonance splitting Ω and width δ_c' predicted above with our totally classical model are identical to the corresponding vacuum-field Rabi-splitting results obtained by Carmichael *et al.*[11] We may thus conclude that the multiatom vacuum Rabi splitting may also be regarded as a feature of linear-dispersion theory. While this same point can be inferred from the

demonstrated success of mean-field, Maxwell-Bloch-type calculations in the treatment of vacuum Rabi splittings,[11,12] the completely classical nature of vacuum Rabi splittings has not been emphasized.

In all our experiments we measured the transmission of a weak continuous-wave (cw) or pulsed-probe laser through a 1-cm confocal optical cavity. The probe beam had a cw linewidth of $\simeq 2$ MHz, was carefully aligned to propagate along the cavity axis, and was focused to a 90-μm spot at the center of the cavity where it intersected at normal incidence a collimated beam of natural barium (72% ^{138}Ba), having a 20-MHz residual Doppler width and $a \simeq 1$ mm diameter. The cavity was adjusted to be nearly resonant with the 554-nm ^{138}Ba $6s^2\,{}^1S_0$-$6s6p\,{}^1P_1$ transition (19-MHz natural width). Approximately 2 pW of the probe power was coupled into the cavity, resulting in a maximum intracavity intensity of $\simeq 15\ \mu\mathrm{W\,cm^{-2}}$ which is far below the $15\text{-mW\,cm}^{-2}$ saturation intensity of the barium transition. Absolute single-pass absorption of the atomic beam was determined by direct measurements at high atomic number densities. Absorption at lower atomic densities was assumed to scale linearly with the atomic fluorescence signal produced by an auxiliary laser beam. The atomic-beam density was varied by adjusting the temperature of the beam source oven, and was as high as 1.5×10^9 $\mathrm{atoms\,cm^{-3}}$, corresponding to a maximum line-center single-pass absorption equal to $2.2\ \mathrm{cm^{-1}}$.

Measured and calculated cavity transmission functions are shown in Fig. 2. In the calculations of Figs. 2(b)–2(d), we have accounted for the residual atomic-beam Doppler width and the lower abundance, blueshifted barium isotopes. The empty-cavity transmission function [Fig. 2(a)] displays a linewidth of $\simeq 30$ MHz (FWHM) corresponding to a cavity finesse of $\simeq 500$. Therefore, a splitting should appear [see Eq. (6)] when $a_0L > 0.006$. For $a_0L = 0.0013$ [Fig. 2(b)], only a broadening of the transmission peak is found. With $a_0L = 0.008$ [corresponding to $\simeq 300$ atoms in the cavity, Fig. 2(c)], a well-resolved mode splitting is observed. For $a_0L = 0.055$ [Fig. 2(d)], an even larger splitting is observed. The asymmetry in the peak heights is attributable to barium isotopes other than ^{138}Ba. Predicted and observed transmission functions are in excellent agreement.

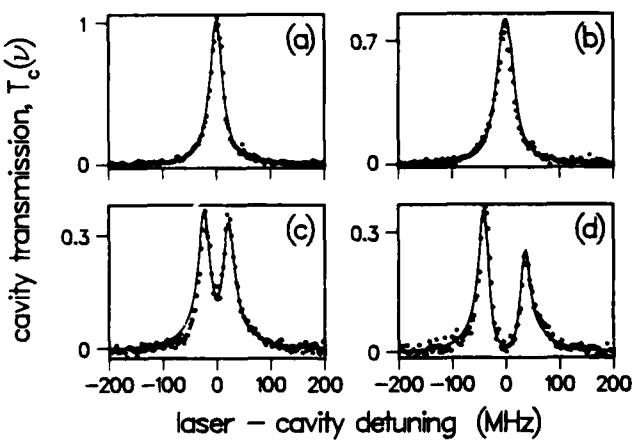

FIG. 2. Experimentally measured (solid circles) and theoretically predicted (solid line) cavity transmission functions. The values of the parameters for the cavity are $\Delta_{FSR} = 15$ GHz, $\delta_c = 30$ MHz, and $F = 500$. The cavity resonance is precisely set to the ^{138}Ba $6s^2\,{}^1S_0$-$6s6p\,{}^1P_1$ transition ($\delta_H = 19$ MHz). The value of the line-center, single-pass absorption a_0L was set to (a) 0, (b) 0.0013, (c) 0.008, and (d) 0.055. The measured cavity transmission functions have been scaled in the vertical direction so that the measured empty-cavity transmission is equal to 1.

From the perspective of quantum optics, the vacuum Rabi splitting may be seen to follow from the exchange of excitation back and forth between the atoms and the cavity field. In the transient regime, this exchange is manifest as a temporal oscillation on the light transmitted through the cavity. From the classical perspective, the atom-cavity system is a simple linear system, and the time- and frequency-domain responses of the system are connected via Fourier transform. If we denote the Fourier transform of a pulse incident in one end of (after transmission through) the cavity by $E_{inc}(\nu)$ [$E_{out}(\nu)$], we can immediately write

$$E_{out}(\nu) = t_c(\nu)E_{inc}(\nu)\,. \tag{7}$$

If the atomic density is large enough to make $t_c(\nu)$ double peaked and if the input pulse is sufficiently short, inverse Fourier transformation of $E_{out}(\nu)$ reveals that the output pulse will contain an oscillation with a period of $1/\Omega$ and have a duration on the order of $1/\pi(\delta_H + \delta_c)$. This behavior is in agreement with that expected from the perspective of quantum optics.

The transient response of our atom-cavity system was investigated by injecting a pulse (acousto-optically sliced from the cw probe laser) in one end of the cavity and measuring the temporal evolution of the light emitted out through the other end. The temporal evolution of the input [output] pulse intensity is shown in Fig. 3(a) [3(b)]. The data shown in Fig. 3(b) were recorded with the single-pass atomic absorption a_0L set to 0.22 and with a small atom-cavity detuning Δ_m equal to 25 MHz introduced in order to minimize the effect of the less abundant Ba isotopes on the measurement. Under these conditions, a 150-MHz frequency-domain cavity-resonance splitting was observed. To fit the data with our model, we used Eq. (7) and assumed that the spectrum of the incident pulse was given by the transform of the square root of the measured intensity profile. The predicted output pulse is shown as the solid line in Fig. 3(b). The data are somewhat noisy; however, the expected oscillations are clearly evident.

In summary, we have shown that the steady-state and

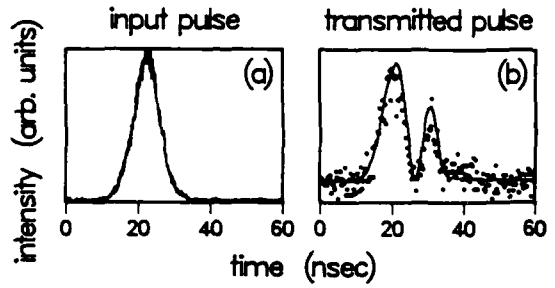

FIG. 3. Temporal behavior of the coupled atom-cavity system. (a) Experimentally measured intensity of the pulse input to the cavity as a function of time. (b) Experimentally measured (solid circles) and theoretically predicted (solid line) evolution of the pulse transmitted from the cavity. The cavity resonance was tuned 25 MHz to the high-frequency side of the ^{138}Ba $6s^2\,{}^1S_0$-$6s6p\,{}^1P_1$ transition and $\alpha_0 L = 0.22$.

transient transmission characteristics of a cavity coupled to a collection of atoms can be understood using an entirely classical, steady-state multibeam interference analysis of an optical cavity. In particular, it is found that the empty-cavity resonances can be split due to the effects of linear absorption and dispersion and that this mode splitting is identical to the vacuum-field Rabi splitting predicted by a fully quantum electrodynamical formalism. This of course implies that the mere observation of oscillatory transmission and/or mode splitting is no more intrinsically quantum than the observation of linear absorption and dispersion.

We gratefully acknowledge support from the National Science Foundation, Grant No. PHY 87-18518, the Air Force Office of Scientific Research, Grant No. AFOSR-88-0086, and one of us (H.J.C.) gratefully acknowledges support from the National Science Foundation, Grant No. PHY-8810502.

[1]J. J. Sanchez-Mondragon, N. B. Narozhny, and J. H. Eberly, Phys. Rev. Lett. **51**, 550 (1983).

[2]G. S. Agarwal, Phys. Rev. Lett. **53**, 1732 (1984).

[3]G. S. Agarwal, J. Opt. Soc. Am. B **2**, 480 (1985).

[4]The resonances of a single atom strongly coupled to a cavity have been measured under detuned conditions by J. J. Childs, J. T. Hutton, D. J. Heinzen, M. S. Feld, and F. W. Dalby, contribution to the Conference on Quantum Electronics and Laser Science, Baltimore, MD, 1989 (unpublished).

[5]Y. Kaluzny, P. Goy, M. Gross, J. M. Raimond, and S. Haroche, Phys. Rev. Lett. **51**, 1175 (1983).

[6]R. J. Brecha, L. A. Orozco, M. G. Raizen, M. Xiao, and H. J. Kimble, J. Opt. Soc. Am. B **3**, 238 (1986).

[7]M. G. Raizen, R. J. Thompson, R. J. Brecha, H. J. Kimble, and H. J. Carmichael, Phys. Rev. Lett. **63**, 240 (1989).

[8]M. Born and E. Wolf, *Principles of Optics* (Pergamon, New York, 1980), 6th ed., pp. 323–329.

[9]M. Born and E. Wolf, *Principles of Optics* (Ref. 8), pp. 90–98.

[10]L. A. Lugiato, in *Progress in Optics XXI*, edited by E. Wolf (Elsevier, Amsterdam, 1984), Chap II.

[11]H. J. Carmichael, R. J. Brecha, M. G. Raizen, H. J. Kimble, and P. R. Rice, Phys. Rev. A **40**, 5516 (1989). The comparison can be made through use of the relations $\delta_c = 2\kappa/\pi$, $\delta_H = \gamma/\pi$, and $F\alpha_0 L/\pi = N_a g^2/\pi^2 \delta_H \delta_c$, where N_a is the number of atoms interacting with the cavity.

[12]M. G. Raizen, R. J. Thompson, R. J. Brecha, H. J. Kimble, and H. J. Carmichael, in *Quantum Optics V*, edited by J. Harvey and D. F. Walls (Springer-Verlag, Berlin, 1989), pp. 176–180.

Observation of a Two-Photon Gain Feature in the Strong-Probe Absorption Spectrum of Driven Two-Level Atoms

Yifu Zhu, Qilin Wu, S. Morin, and T. W. Mossberg

Department of Physics and Chemical Physics Institute, University of Oregon, Eugene, Oregon 97403

(Received 9 April 1990)

A feature associated with continuous-wave two-photon optical gain has been observed in the absorption spectrum of an ensemble of barium atoms driven by a strong near-resonant optical field. In the dressed-atom picture, the observed gain is attributable to inverted two-photon transitions with nearly resonant intermediate states. A cw optical two-photon laser utilizing this gain appears feasible.

PACS numbers: 42.50.Hz, 42.55.Hq, 42.65.Dr, 42.65.Pc

The interaction of two-level atoms (TLA's) with strong resonant or nearly resonant optical radiation has been analyzed from a number of perspectives.[1,2] Of interest here, it has been shown that TLA's driven by a near-resonant driving field (pump) can act to amplify a weak-probe laser appropriately tuned relative to the atomic and pump frequencies.[3-8] In fact, single-photon lasers based on driven TLA gain have been constructed.[9-12] Driven TLA gain occurs in the absence of inversion between the ground and excited states. The largest weak-probe gain feature, which has been referred to as Raman gain,[4] can be understood in terms of a stimulated hyper-Raman-scattering process or in terms of population inversions on transitions between dressed atom-field states. Raman gain can be viewed as a single-photon gain process. At higher probe intensities, additional gain features, corresponding to multiphoton analogs of the Raman gain process and involving two- or more-photon gain,[13,14] become important. In this paper, we describe an experimental study of the interaction of a strong probe with a driven TLA and provide the first demonstration of cw two-photon gain in the optical regime.

Consider an ensemble of stationary TLA's having a transition frequency ν_a, an upper-state radiative lifetime T_1, and a homogeneous dephasing time $T_2=2T_1$. The atoms are driven by a monochromatic pump field of frequency ν_0, atom-pump detuning $\Delta\equiv\nu_a-\nu_0$, and resonant Rabi frequency Ω_0. We study the gain and absorption spectrum of a probe field interacting with the pump-driven TLA's. The probe is assumed to have a frequency ν_1, probe-pump detuning $\delta=\nu_1-\nu_0$, and resonant Rabi frequency Ω_1. This spectrum can be evaluated using the expressions for nonlinear susceptibility derived by Agarwal and Nayak[15] using a continued-fractions method. This approach has also recently been employed by Gruneisen *et al.*[16] in calculations related to the energy transfer between propagating beams using stimulated Rayleigh scattering.

Using the method of Agarwal and Nayak, we have calculated the probe gain and absorption as a function of probe-pump detuning for various probe intensities. The results are presented in Fig. 1. Throughout Fig. 1 we have set $\Omega_0/\Delta=3$ and $2\pi\Delta T_2=10$. In the weak-probe limit ($\Omega_1/\Delta=0.1$), the probe gain and absorption spectrum reduces [see Fig. 1(a)] as expected to the probe spectrum studied by Mollow and co-workers.[3,6] The dominant features in this spectrum correspond to single-photon gain (positive peak at $\delta\simeq-\Omega'$) and single-photon absorption (negative peak at $\delta\simeq\Omega'$), where $\Omega'\equiv(\Omega_0^2+\Delta^2)^{1/2}$. For $\Omega_1/\Delta=0.6$ [Fig. 1(b)], new features appear in the probe gain and absorption spectrum. The peak at $\delta\simeq-\Omega'/2$ ($\delta=\Omega'/2$) corresponds to

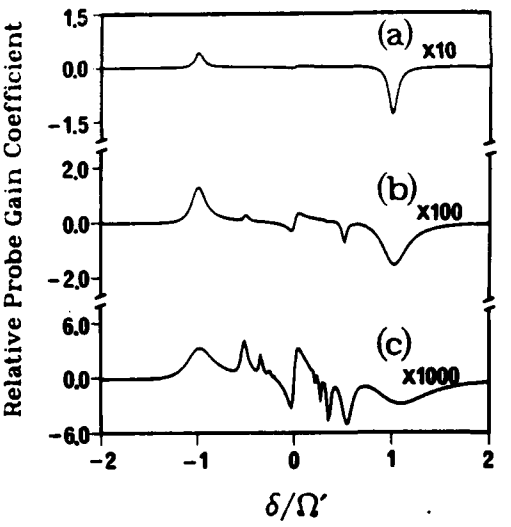

FIG. 1. Calculated probe gain coefficient as a function of probe-pump detuning δ/Ω' for $\Omega_0/\Delta=3$, $2\pi\Delta T_2=10$, and $\Omega'\equiv(\Omega_0^2+\Delta^2)^{1/2}=\sqrt{10}\Delta$. The vertical scale corresponds to the probe gain coefficient normalized so as to be -1 at the center of the weak-probe absorption profile measured in the absence of a pump laser. In the figure, the calculated values have been multiplied by (a) 10 times, (b) 100 times, and (c) 1000 times. (a) Weak-probe laser, $\Omega_1/\Delta=0.1$. One-photon gain (absorption) features exist at $\delta\simeq-\Omega'$ ($\delta\simeq\Omega'$), a Rayleigh-scattering feature at $\delta=0$. (b) For $\Omega_1/\Delta=0.6$, two-photon gain (absorption) appears at $\delta\simeq-\Omega'/2$ ($\delta=\Omega'/2$). (c) For $\Omega_1/\Delta=1.4$, two-photon gain is the largest gain feature. Generally, n-photon gain occurs at $\delta\simeq-\Omega'/n$, while n-photon absorption occurs at $\delta\simeq\Omega'/n$.

two-photon gain (absorption). For $\Omega_1/\Delta = 1.4$ [Fig. 1(c)], still more features appear with n-photon gain (absorption) occurring at $\delta \simeq -\Omega'/n$ ($\delta \simeq \Omega'/n$). In Fig. 1(c), the two-photon gain feature is actually larger than the one-photon gain feature. Reversing the sign of Δ simply reverses all the gain and absorption features in the spectra about $\delta = 0$. The existence of probe gain and absorption features at probe-pump detunings given by subharmonics of the pump Rabi frequency has been discussed in several contexts[17-21] including cases involving nonzero Δ,[16] but the connection of these features with multiphoton gain has apparently been overlooked. As in the case of the single-photon Raman gain, the n-photon gain can be understood in terms of a high-order stimulated hyper-Raman effect or in terms of n-photon transitions between dressed states in nonadjacent doublets (see Fig. 2).

To avoid unessential complexity, the spectra of Fig. 1 were calculated assuming Doppler-free conditions. To realize this condition experimentally, we have employed a collimated atomic beam of natural barium. The use of an atomic beam limited the achievable atomic densities, interaction lengths, and hence single-pass gain and absorption to relatively small values. To compensate, the probe gain and absorption was measured in an intracavity mode; i.e., the probe power was measured after transmission through a confocal optical cavity whose mirrors were positioned symmetrically about the atomic beam. The cavity performed two functions. First, it increased the effective optical thickness of the atomic beam. Second, it increased the achievable probe intensity for a given probe input power. High probe intensity is essential to bring the nonlinear gain into operation, but low probe power is essential to avoid saturation of the gain medium. The atomic beam was chopped at 191 Hz. Probe gain and absorption spectra represent measurements of probe power transmitted through the cavity during atomic-beam-on cycles normalized by measurements of probe power transmitted during atomic-beam-off cycles. Standard frequency-modulation techniques, active while the atomic beam was blocked, were employed to keep the empty-cavity resonance frequency locked to the probe frequency. Probe gain and absorption measurements, obtained as described above using an enhancement cavity, are complicated by the fact that atomic dispersion can cause shifts in the cavity resonance frequency and thereby affect probe transmission through the cavity. With our scheme of locking the empty-cavity resonance frequency to the probe frequency, dispersive effects always act to decrease atomic-beam-on probe transmission and therefore mimic absorption rather than gain.

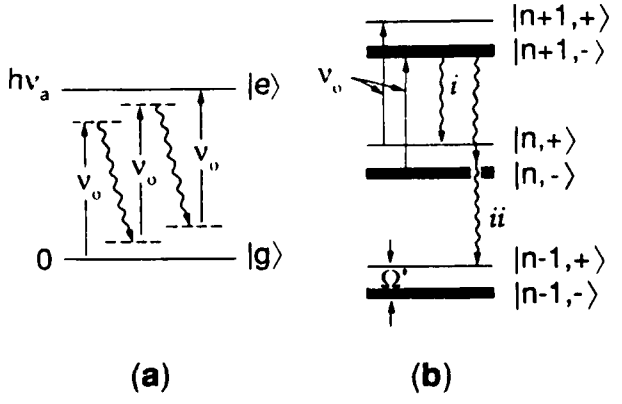

FIG. 2. Alternative pictures of the two-photon gain process. (a) Stimulated hyper-Raman scattering. Three photons from the pump laser are scattered, leading to the emission of two photons (wavy lines). (b) Dressed-state picture. Two-photon gain results from the two-photon transition (indicated by *ii*) between the inverted dressed levels $|n+1,-\rangle$ and $|n-1,+\rangle$. Here *i* indicates the well-known single-photon gain process (thick lines represent the more heavily populated states). Analogous pictures can be drawn for n-photon gain processes.

Our experimental apparatus is depicted in Fig. 3. The atomic beam was 800 μm in diameter as it passed through the center of a 1-cm-long, 200 finesse, confocal enhancement cavity. The linearly polarized pump and probe lasers were tuned near the ^{138}Ba 553.5-nm $^1S_0 \rightarrow {}^1P_1$ transition which has a natural linewidth of 19 MHz. Since ^{138}Ba has zero nuclear spin, the $^1S_0$-$^1P_0$ transition closely approximates a two-level quantum system. The experiment is complicated, however, by the presence of other barium isotopes (about 22% total abundance) some of which have nonzero nuclear spin. The axis of the enhancement cavity, the Ba atomic beam, and the propagation direction of the traveling-wave pump laser were mutually orthogonal. The probe laser propagated along the cavity axis. In our experimental configuration, nonlinear-wave-mixing-type gain processes are not phase matched. The Rabi frequency Ω_0 of the pump laser was determined by measuring the

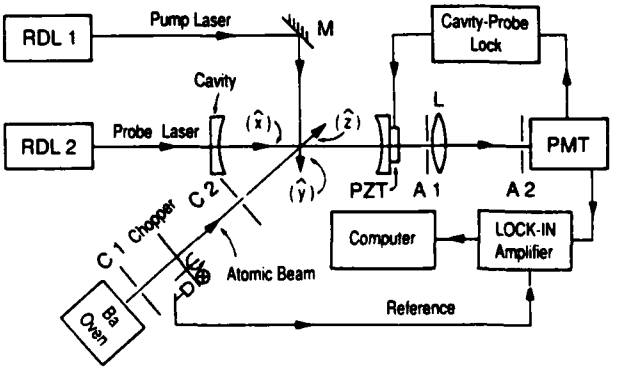

FIG. 3. Experimental schematic. RDL1, pump laser; RDL2, probe laser. Both are single-mode cw ring dye lasers. PZT, piezoelectric transducer; M, mirror; PMT, photomultiplier tube; A1 and A2, apertures; L, lens; C1 and C2, atomic-beam collimators; x, y, and z, three perpendicular spatial axes.

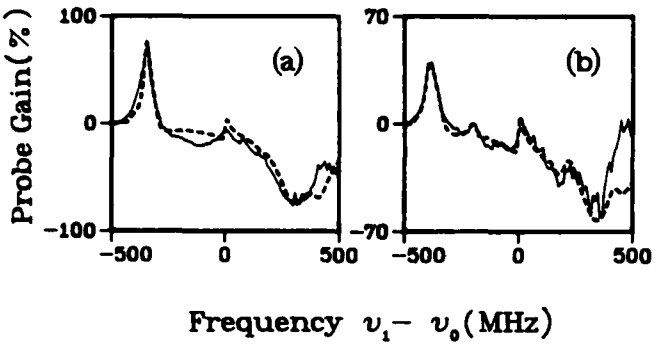

FIG. 4. Measured gain in probe power transmitted through the cavity as a function of probe-pump detuning ($\delta = \nu_l - \nu_0$). Solid curves represent experimental data. Dashed curves represent numerical calculations including effects of the dispersion (pseudoabsorption), pump-field inhomogeneity, the standing-wave character of the probe field, and Ba isotopes. The vertical scales represent 100×[(atomic-beam-on probe power transmission) − (atomic-beam-off probe power transmission)]/(atomic-beam-off probe power transmission). This quantity is positive for gain. (a) $\Omega_0 \simeq 340$ MHz, $\Omega_1 \simeq 44$ MHz, and $\Delta \simeq 100$ MHz; features observed are one-photon gain (absorption) at $\delta \simeq -\Omega_0$ ($\delta \simeq \Omega_0$), and Rayleigh scattering at $\delta \simeq 0$. (b) $\Omega_0 \simeq 390$ MHz, $\Omega_1 \simeq 140$ MHz, and $\Delta \simeq 100$ MHz; the peak at $\delta = -\Omega'/2$ is the two-photon gain feature.

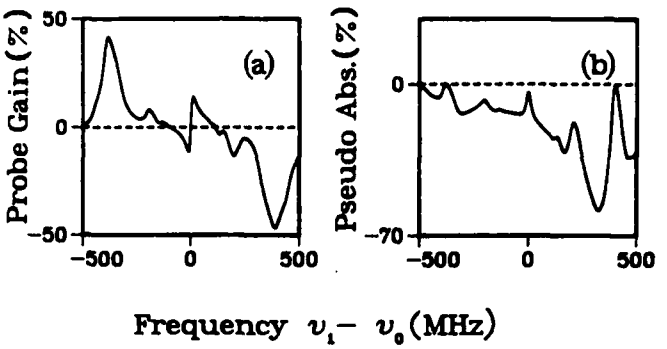

FIG. 5. (a) Calculated probe gain (positive) of Fig. 4(b) excluding pseudoabsorption effects. (b) Calculated probe absorption resulting exclusively from pseudoabsorption (dispersive) effects. The vertical scale in both parts of the figure represents 100×[(transmitted probe power) − (incident probe power)]/(incident probe power). Parameters are the same as those in Fig. 4(b). Dashed lines are zero-gain (-absorption) base lines.

splitting of the Mollow triplet resonance fluorescence spectrum produced by the pump with no probe. This spectrum was observed by using the enhancement cavity as a Fabry-Pérot interferometer. The Rabi frequency Ω_1 of the probe laser was deduced by measuring the power-broadened width of the probe absorption spectrum while the pump laser was shut off.

A weak-probe gain and absorption spectrum is shown in Fig. 4(a) for the case where $\Omega_0 \simeq 340$ MHz, $\Omega_1 \simeq 44$ MHz, and $\Delta \simeq 100$ MHz. It is seen that there are only single-photon gain (absorption) features at $\delta = -\Omega'$ ($\delta = \Omega'$), and a Rayleigh-scattering feature at $\delta \simeq 0$. The absorption feature is complicated primarily because of the effects of the other Ba isotopes which are all distributed to the blue-frequency side of the ^{138}Ba resonance. As the probe-laser Rabi frequency was increased to $\Omega_1 \simeq 140$ MHz (with $\Omega_0 \simeq 390$ MHz, $\Delta \simeq 100$ MHz), a two-photon gain (absorption) feature appeared [see Fig. 4(b)] as a small peak at $\delta \simeq -\Omega'/2$ ($\delta \simeq \Omega'/2$). While these peaks are small and comparable to the experimental noise level, they are observed to appear consistently in many separate measurements of the probe spectrum. It will be noticed that the peak of the two-photon gain feature is near zero, and hence the peak constitutes a decrease in absorption rather than an actual gain. This occurs, as discussed above, because of dispersion-mediated shifts in the cavity resonance frequency and concomitant decreases in the atomic-beam-on probe transmission. Since our detection scheme compares the transmitted probe-laser power with and without the Ba atomic beam, and since the empty cavity was actively locked to the probe-laser frequency, dispersion-mediated cavity frequency shifts look like absorption. We refer to this effect as pseudoabsorption. The dashed lines shown in Fig. 4 are calculated probe gain and absorption spectra. Except for the extreme blue end, the calculated and observed spectra are in excellent agreement, indicating that we have indeed observed cw two-photon gain. The discrepancies between the experiment and theory at the blue end of the spectra are due to a persistent partial loss of the cavity-probe lock at the end of the locking range. In Fig. 5(a), we plot the probe gain calculated as in Fig. 4(b) except that the effect of pseudoabsorption has not been included. Note that in this case the two-photon gain peak is positive and represents what our observations would have shown if we had been able to eliminate dispersive (pseudoabsorption) effects. In Fig. 5(b), probe pseudoabsorption calculated using the same parameters as in Fig. 5(a) is plotted. This spectrum shows how much the transmitted probe power was reduced due exclusively to the effect of pseudoabsorption. In the absence of pseudoabsorption, we conclude that the experimentally observed probe transmission would actually have increased by 8% at the center of the measured two-photon gain peak.

In conclusion, we have experimentally demonstrated that strongly driven two-level atoms can be utilized as a two-photon gain medium and may therefore be useful in the realization of a two-photon laser.[22] We point out that this simple system is also a potential gain medium for three- or more-photon amplification.

It is a pleasure to thank D. J. Gauthier, M. Lewenstein, and A. Lezama for useful discussions. We gratefully acknowledge the financial support of the National Science Foundation (PHY8718518) and the Air Force Office of Scientific Research (AFOSR-88-0086).

[1]C. Cohen-Tannoudji, in *Frontiers in Laser Spectroscopy*, Proceedings of the Les Houches Summer School Session XXVII, edited by R. Balian, S. Haroche, and S. Liberman (North-Holland, Amsterdam, 1977).

[2]P. L. Knight and P. W. Milonni, Phys. Rep. **66**, 21 (1980).

[3]B. R. Mollow, Phys. Rev. A **5**, 2217 (1972).

[4]S. Haroche and F. Hartmann, Phys. Rev. A **6**, 1280 (1972).

[5]S. L. McCall, Phys. Rev. A **9**, 1515 (1974).

[6]F. Y. Wu, S. Ezekiel, M. Ducloy, and B. R. Mollow, Phys. Rev. Lett. **38**, 1077 (1977).

[7]M. T. Gruneisen, K. R. MacDonald, and R. W. Boyd, J. Opt. Soc. Am. B **5**, 123 (1988).

[8]G. Khitrova, P. R. Berman, and M. Sargent, III, J. Opt. Soc. Am. B **5**, 160 (1988).

[9]G. Grynberg, E. LeBihan, and M. Pinard, J. Phys. (Paris) **47**, 1321 (1986).

[10]D. Grandclement, G. Grynberg, and M. Pinard, Phys. Rev. Lett. **59**, 40 (1987).

[11]G. Khitrova, J. F. Valley, and H. M. Gibbs, Phys. Rev. Lett. **60**, 1126 (1988).

[12]A. Lezama, Y. Zhu, M. Kanskar, and T. W. Mossberg, Phys. Rev. A **41**, 1576 (1990).

[13]M. M. T. Loy, Phys. Rev. Lett. **41**, 473 (1978).

[14]M. Brune, J. M. Raimond, and S. Haroche, Phys. Rev. A **35**, 154 (1987); L. Davidovich, J. M. Raimond, M. Brune, and S. Haroche, *ibid.* **36**, 3771 (1987).

[15]G. S. Agarwal and N. Nayak, Phys. Rev. A **33**, 391 (1986); J. Opt. Soc. Am. B **1**, 164 (1984).

[16]M. T. Gruneisen, K. R. MacDonald, A. L. Gaeta, R. W. Boyd, and D. J. Harter, Phys. Rev. A **40**, 3464 (1989).

[17]A. M. Bonch-Bruevich, T. A. Vartanyan, and N. A. Chigir, Zh. Eksp. Teor. Fiz. **77**, 1899 (1979) [Sov. Phys. JETP **50**, 901 (1979)].

[18]G. I. Toptygina and E. E. Fradkin, Zh. Eksp. Teor. Fiz. **82**, 429 (1982) [Sov. Phys. JETP **55**, 246 (1982)].

[19]Y. Zur, M. H. Levitt, and S. Vega, J. Chem. Phys. **78**, 5293 (1983).

[20]H. Friedmann and A. D. Wilson-Gordon, Phys. Rev. A **36**, 1333 (1987).

[21]S. Chakmakjian, K. Koch, and C. R. Stroud, Jr., J. Opt. Soc. Am. B **5**, 2015 (1988).

[22]P. P. Sorokin and N. Braslau, IBM J. Res. Dev. **8**, 177 (1964); A. M. Prokhorov, Science **149**, 828 (1965); H. P. Yuen, Appl. Phys. Lett. **26**, 505 (1975); L. M. Narducci, W. W. Eidson, P. Furcinitti, and D. C. Eteson, Phys. Rev. A **16**, 1665 (1977); N. Nayak and B. K. Mohanty, Phys. Rev. A **19**, 1204 (1979); B. Nikolaus, D. Z. Zhang, and P. E. Toschek, Phys. Rev. Lett. **47**, 171 (1981); Z. C. Wang and H. Haken, Z. Phys. B **55**, 361 (1984); **56**, 77 (1984); **56**, 83 (1984); M. Brune, J. M. Raimond, P. Goy, L. Davidovich, and S. Haroche, Phys. Rev. Lett. **59**, 1899 (1987); IEEE J. Quantum. Electron. **24**, 1323 (1988); M. O. Scully, K. Wodkiewicz, M. S. Zubairy, J. Bergou, N. Lu, and J. Meyer ter Vehn, Phys. Rev. Lett. **60**, 1832 (1988); G. S. Agarwal and F. Rattay, Phys. Rev. A **37**, 3351 (1988).

FINAL 12-26-90 Tom

Observation of Linewidth Narrowing due to Coherent Stabilization of Quantum Fluctuations

Daniel J. Gauthier, Yifu Zhu, and T. W. Mossberg

Department of Physics, University of Oregon

Eugene, OR 97403

Abstract

Quantum fluctuations of an optical transition moment are observed to be suppressed by strong coherent excitation of a weak auxiliary transition. The stabilization is manifest through the appearance of subnatural linewidths in the resonance fluorescence spectrum and is due to coherent mixing of atomic states. Our results are in quantitative agreement with the predictions of Narducci et al. [Phys. Rev. A, **42** 1630 (1990)].

PACS numbers: 42.50.-p, 42.60.Da, 42.65.Pc, 32.30.Jc, 32.70.Jz, 32.80.Wr

It has been shown that the quantum fluctuations exhibited by atoms contained within optical or microwave cavities can be dramatically different from those exhibited by atoms in free-space.[1] Recently, Narducci et al.[2] predicted that certain quantum fluctuations associated with three-level atoms can be significantly modified *without* the use of a cavity by exposing the atoms to a strong coherent-state driving field.[3] This prediction is intriguing because it opens up to researchers a new class of systems in which quantum fluctuations can be manipulated and the effects directly observed. In the present experimental work, a stabilization of quantum fluctuations, manifest in a narrowing of resonance fluorescence linewidths to subnatural values, is reported. Agreement with theory is excellent.

The atomic system considered by Narducci et al.[2] consists of a v-configuration, three-level atom (see Fig. 1a) with ground-state $|g\rangle$, and excited states $|s\rangle$ and $|w\rangle$. The excited states, $|s\rangle$ and $|w\rangle$, decay back to the ground-state at the rates γ_s and γ_w, respectively. The $|g\rangle \rightarrow |s\rangle$ ($|g\rangle \rightarrow |w\rangle$) transition is driven by a resonant, coherent-state, driving-field of frequency ω_s (ω_w) and Rabi frequency Ω_s (Ω_w). It is assumed that the $|g\rangle \rightarrow |w\rangle$ transition is much weaker than the $|g\rangle \rightarrow |s\rangle$ transition (i.e. $\gamma_w << \gamma_s$). In Ref. 2, it is shown that the light inelastically scattered by the atom in the spectral vicinity of the strong transition frequency ω_s displays a spectral narrowing (i.e., stabilization of the quantum fluctuations) when the weak transition is driven more and more strongly. For $\Omega_w >> \Omega_s >> \gamma_s$, the strong-transition inelastic fluorescence spectrum consists of a central component with a spectral full-width-at-half-maximum (FWHM) of γ_w and two symmetric sidebands of width $3\gamma_w/2$. This result is surprising because the inelastic spectrum scattered by the atom for $\Omega_w = 0$ and $\Omega_s >> \gamma_s$ (the Mollow spectrum[5]) has features with FWHM widths of γ_s (central peak) and

$3\gamma_s/2$ (sidebands).

Our experiment involved measuring the resonance fluorescence spectrum emitted on the stronger of two transitions within v-configuration, three-level-like, barium atoms as depicted in Fig. 1a. The strong (weak intercombination line) $6s^2\ ^1S_0 \rightarrow 6s6p\ ^1P_1$ ($6s^2\ ^1S_0 \rightarrow 6s6p\ ^3P_1$) transition has a frequency denoted by ω_{sg} (ω_{wg}), a spontaneous lifetime of 8.37 ± 0.08 nsec[6] (3.35 ± 0.5 μsec[7]), a resonance wavelength of 553.5 nm (791.1 nm) and is hereafter called the strong (weak) transition. The coherent-state driving fields were derived from the outputs of two actively stabilized ring dye lasers (Coherent 699-21, linewidth ≈1 MHz) and were collimated, superimposed, and made incident on a Ba atomic beam which passed through the center of a 50-cm confocal Fabry-Perot interferometer. The finesse of the Fabry-Perot was ≈100 based on the measured ≈1.5 MHz transmission linewidth. The atomic beam had a residual Doppler width of ≈3 MHz. In the interaction region, the atomic, weak-transition laser, and strong-transition laser beams had diameters (FWHM) of 200 μm, 750 μm, and 2 mm, respectively. The weak- and strong-transition laser beams had nearly Gaussian profiles and had maximum powers of 200 mW and 20 mW, respectively. The laser beams, the atomic beam, and the cavity axis were mutually orthogonal (see Fig. 1b).

The fluorescence spectrum of the atoms was obtained by recording the fluorescence intensity emitted out the ends of the confocal Fabry-Perot interferometer as a function of the Fabry-Perot mirror spacing (i.e. transmission frequency). At the low atomic number densities used in the present experiment, the measured spectrum corresponds to the single-atom resonance fluorescence spectrum with contributions from both elastic and inelastic

scattering.[8] Imaging and spatial filtering techniques were employed to select only that light which was emitted nearly orthogonal to the atomic beam and which originated from a source volume of approximately 850 μm in diameter. Spectral filtering was employed to block light scattered at the weak-transition frequency. We stress that placing the atomic beam inside the confocal Fabry-Perot cavity merely serves to facilitate measurement of the fluorescence spectrum and, in the configuration employed, does not significantly affect atomic relaxation. The instrumental resolution, which is limited by the combined effects of cavity linewidth, laser linewidth, and Doppler broadening, was equal to 8.5 ± 0.5 MHz. This value was determined from measurements of the apparent linewidth of elastically scattered resonance fluorescence[9] generated via weak excitation of the strong transition (i.e. $\Omega_w = 0$, $\Omega_s << \gamma_s$).

When only the strong transition of the atoms is driven, a classic Mollow-type, three-peaked resonance fluorescence spectrum is expected. This spectrum has contributions from both elastically and inelastically scattered light. The elastic contribution decreases in importance as the driving-field strength is increased, has negligible spectral width, and contributes only to the central component of the Mollow triplet. Inelastic scattering contributes to all three peaks and is responsible for the ultimate strong-field widths that were given above. In Ref. 2, it is predicted that excitation of the weak transition will modify the spectrum emitted on the strong transition by changing the fractional contributions of elastic and inelastic scattering (generally decreasing the importance of the former), and by narrowing the spectral width of features arising from inelastic scattering. Our primary objective is to measure the latter effect. Ideally, measurements involving the Mollow

sidebands would reveal this effect uncomplicated by elastic scattering. Unfortunately, the widths of these peaks are strongly affected by difficult-to-avoid spatial variations in the excitation-field intensities and we therefore concentrate our analysis on the behavior of the central-peak linewidth.

Shown in Fig. 2 are measured strong-transition fluorescence spectra (dashed lines) obtained for one value of the strong-transition Rabi frequency ($\Omega_s \approx 35$ MHz) without (Fig. 2a) and with (Fig. 2b) simultaneous excitation of the weak transition. The dot-dashed curve in Fig. 2a was generated using a theoretical expression for the Mollow spectrum convolved with the measured instrumental response function. The strong-transition Rabi frequency and the vertical scale factor were taken as free parameters. The solid line in Fig. 2a was calculated in the same manner as the dot-dashed line except that the adjacent transmission peaks of the 150-MHz free-spectral-range analyzer Fabry-Perot were included in the instrumental response function. Excellent agreement between the calculated and observed spectra is obtained when the free-space linewidth used in the theoretical expression for the Mollow spectrum is taken to be 19 MHz. This value is equal to the best independently measured values of the quantity.[6]

In Fig. 2b, both transitions are driven ($\Omega_w \approx 43$ MHz). It is clear that excitation of the weak transition dramatically modifies the spectrum of fluorescence emitted on the strong transition. The sideband peaks are spread further apart, and most interestingly, the measured FWHM of the central peak drops to 16 MHz. The dot-dashed curve in Fig. 2b was calculated following Ref. 2 using the same values for the strong-transition natural linewidth and Rabi frequency that were employed in the corresponding calculation in Fig.

2a. The weak-transition natural linewidth employed in the calculation was deduced from the upper-state lifetime given above. Variations in the weak-transition excitation-field intensity (important because of the small diameter of that beam) were accounted for by averaging the calculated spectrum across the weak-excitation-field cross section. The resulting spectrum was convolved with the instrumental response function. In the simulations, the average value of the weak-transition Rabi frequency and the vertical scale factor were allowed to vary so as to maximize the fidelity. The best-fit value of the former was consistent with experimental measurements. In addition, the best-fit vertical scale was within 5% of that used to generate Fig. 2a.

The data shown in Fig. 2b clearly demonstrates that the linewidth narrowing is a pronounced effect since the 16-MHz FWHM of the central peak in Fig. 2b is less than the 19 MHz free-space natural linewidth of the strong transition even before deconvolving the instrumental response function. Our best estimate of the actual width of the inelastic contribution to the central peak is 7 MHz. This width corresponds to the width of the calculated spectrum (dot-dashed line) prior to convolution with the instrumental response function. We note that our simulations explicitly account for elastic scattering, and indicate that it cannot account for the narrowness of the central peak observed in Fig. 2b. We thus conclude that the quantum fluctuations of the strong-transition moment are dramatically stabilized by the application of the weak-transition driving field. The solid line in Fig. 2b was calculated in the same manner as the solid line in Fig. 2a.

In Fig. 3, strong-transition fluorescence spectra obtained with a higher strong-transition Rabi frequency are shown. In Fig. 3a ($\Omega_s \approx 55$ MHz, $\Omega_w = 0$), we see that at this

larger value of Ω_s the classic triplet structure of the Mollow spectrum begins to be apparent. In Fig. 3b, a strong-transition spectrum obtained with excitation on both the weak and strong transitions ($\Omega_s \approx 55$ MHz, $\Omega_w \approx 43$ MHz) is presented. It is seen that the application of the weak-transition driving field increases the sideband spacing in the strong-transition fluorescence spectrum and causes a narrowing of the central peak. The dot-dashed and solid lines represent simulations calculated according to the procedure described in the case of Fig. 2. The simulations provide a good description of the observed spectra. From the best-fit simulations, we deduce that the widths of the inelastic components of the central peaks shown in Fig. 3a and 3b are 21 MHz and 12 MHz, respectively. The 21-MHz width found in the former case is slightly larger than the 19-MHz natural width of the strong transition and results from the close proximity of the still not-fully-resolved Mollow sidebands. In the case of Fig. 3b, the 12-MHz deduced width of the central peak's inelastic component is significantly narrower than the strong-transition natural width.

In limiting cases, the stabilization effect observed here can be calculated in a rather straightforward manner (see Ref. 2 for the general case). We first derive the semiclassical equations-of-motion for the expectation values of the density operator in a transformed basis. The eigenstates in the transformed basis are given in terms of the energy eigenstates of the undriven atom through the relation

$$\begin{bmatrix} |g(t)\rangle \\ |c(t)\rangle \\ |d(t)\rangle \end{bmatrix} = \frac{1}{\Omega} \begin{bmatrix} \Omega & 0 & 0 \\ 0 & \Omega_s e^{i\omega_s t} & \Omega_w e^{i\omega_w t} \\ 0 & \Omega_w e^{i\omega_s t} & -\Omega_s e^{i\omega_w t} \end{bmatrix} \begin{bmatrix} |g\rangle \\ |s\rangle \\ |w\rangle \end{bmatrix} \tag{1}$$

where the generalized Rabi frequency is given by $\Omega = (\Omega_s^2+\Omega_w^2)^{1/2}$. We have assumed, for simplicity, that Ω_s and Ω_w are real quantities. The equations-of-motion in the transformed basis take on a particularly simple form for the case of intense, resonant excitation of the strong and weak transitions ($\Omega_w >> \Omega_s >> \gamma_s, \gamma_w$) and are approximately given by

$$\frac{d}{dt}\sigma_{cg} = -\frac{\gamma}{2}\sigma_{cg} - i\frac{\Omega w_{cg}}{2} \tag{2a}$$

and

$$\frac{d}{dt}w_{cg} = -\gamma(w_{cg}+1) - i\,\Omega(\sigma_{cg} - \sigma_{gc}), \tag{2b}$$

where the slowly varying coherence and the inversion between the states are denoted by σ_{cg} and w_{cg}, respectively and $\sigma_{gc}=\sigma_{cg}^*$. The effective, coherently modified decay rate is defined as

$$\gamma = \frac{\Omega_s^2}{\Omega^2}\gamma_s + \frac{\Omega_w^2}{\Omega^2}\gamma_w . \tag{3}$$

Physically, the state $|d(t)\rangle$ is decoupled from the other states[11] and any population initially in the state $|d(t)\rangle$ is rapidly pumped into the other states. Hence, the one set of equations (2) completely describes the interaction of the two, intense coherent fields with the three-level atom. Note that Eqs. 2 are *identical* to the equations-of-motion for a two-level atom characterized by a population decay rate γ, driven by a resonant, monochromatic field of Rabi frequency Ω.[12] These equations are valid to order $(\Omega_s\gamma_s/\Omega_w^2)$ and are consistent with the approximate results derived in Ref. 2.

The inelastic spectra for the strong and weak transition can be derived from the transformed equations-of-motion (2) through use of the quantum regression theorem.[2,10] Alternatively, the spectra could be derived using the dressed-state formalism.[13] It is found that the functional dependence of the spectra for the two different transitions are the same and that only the scaling is different. As could be inferred from Eq. (2), the spectrum is that of a two-level atom, where the width of the central component of the triplet is equal to γ and the sideband spacing is equal to Ω. Hence, the widths of the spectral features for the strong (weak) transition are narrower (broader) than they would be in comparison to the case when either of the transitions is excited individually (since $\gamma_s \geq \gamma \geq \gamma_w$). Therefore, the coherent coupling between the atomic levels suppresses the quantum fluctuations of the strong transition at the expense of increasing the fluctuations of the weak transition. We have verified that our experimentally measured spectra showing dramatic spectral narrowing are in good agreement with the approximate model just presented.

We would like to thank L.M. Narducci for transmitting his results prior to publication. In addition, we thank H.J. Carmichael, M.G. Raymer, S.E. Morin and Q. Wu

for useful discussions and we gratefully acknowledge financial support from the National Science Foundation (PHY-8718518) and the Air Force Office of Scientific Research (AFOSR-88-0086).

REFERENCES

1. S. Haroche and D. Kleppner, Physics Today **42**, 24 (1989); D.F. Walls, Nature, **306**, 141 (1983); M.C. Teich and B.E.A. Saleh, Physics Today **43**, 26 (1990); L.A. Lugiato, Theory of Optical Bistability, in Progress in Optics, Vol. 21, Emil Wolf, ed. (North-Holland, Amsterdam, 1984); H.J. Carmichael, Phys. Rev. Lett. **55**, 2790 (1985); H.J. Carmichael, Phys. Rev. A **33**, 3262 (1986); L.A. Lugiato, Phys. Rev. A **33**, 4079 (1986); H.J. Carmichael, R.J. Brecha, M.G. Raizen, H.J. Kimble, P.R. Rice, Phys. Rev. A **40**, 5516 (1989); M.O Scully, S.-Y. Zhu, and A. Gavrielides, Phys. Rev. Lett. **62**, 2813 (1989); M. Lewenstein, J. Zakrzewski, and T. W. Mossberg, Phys. Rev. A **38**, 808 (1988); Y. Zhu, A. Lezama, T. W. Mossberg, and M. Lewenstein, Phys. Rev. Lett. **61**, 1946 (1988); and A. Lezama, Y. Zhu, S. Morin, and T. W. Mossberg, Phys. Rev. A **39**, 2754 (1989).

2. L.M. Narducci, G.-L. Oppo, and M.O. Scully, Opt. Commun. **75**, 111 (1990); and L.M Narducci, M.O. Scully, G.-L. Oppo, P. Ru and J.R. Tredicce, Phys. Rev. A **42**, 1630 (1990).

3. It has been predicted that changes in the resonance fluorescence linewidth occurs when the atom is driven by a squeezed field. See H.J. Carmichael, A.S. Lane, and D.F. Walls, Phys. Rev. Lett. **58**, 2539 (1987); P.R. Rice and H.J. Carmichael, J. Opt. Soc. Am. B **5**, 1661 (1988); A.S. Parkins and C.W. Gardiner, Phys. Rev. A **37**, 3867 (1988); and A. Joshi and S.V. Lawande, Phys. Rev. A **41**, 2822 (1990).

4. The statistics of resonance fluorescence scattered by three-level, v-configuration atoms for the case of weak excitation by at least one of the fields has been analyzed theoretically by numerous authors. See for example: H. Dehmelt, in Laser Spectroscopy V, A.R.W. McKellar, T. Oka, and B.P. Stoicheff, eds., p. 353 (Springer, Berlin, 1981); D.T. Pegg, R. Loudon, and P.L. Knight, Phys. Rev. A **33**, 4085 (1986); and H.J. Kimble, R.J. Cook, and A.L. Wells, Phys. Rev. A **34**, 3190 (1986). Experimental studies of this system have been performed by W. Nagourney, J. Sandberg, and H. Dehmelt, Phys. Rev. Lett. **56**, 2797 (1986); T. Santer, W. Neuhauser, R. Blatt and P.E. Toschek, Phys. Rev. Lett. **57**, 1696 (1986); and J.C. Bergquist, R.B. Hulet, W.M. Itano, and D.J. Wineland, Phys. Rev. Lett. **57**, 1699 (1986).

5. B.R. Mollow, Phys. Rev. **188**, 1969 (1969); F. Schuda, C.R. Stroud Jr., and M. Hercher, J. Phys. B: Atom. Mol. Phys. **9**, L19, (1974); G.S. Agarwal, Quantum Statistical Theories of Spontaneous Emission and Their Relation to Other Approaches, (Springer, Berlin, 1974); R.W. Grove, F.Y. Wu and S. Ezekial, Phys. Rev. A **15**, 227 (1977); C. Cohen-Tannoudji and S. Reynaud, J. Phys. B: Atom. Mol. Phys. **10**, 345 (1977); and P.L. Knight and P.W. Milloni, Phys. Rep. **66**, 21 (1980).

6. F.M. Kelly and M.S. Mathur, Can. J. Phys. **55**, 83 (1977).

7. W.H. Parkinson and F.S. Tomkins, J. Opt. Soc. Am. **68**, 535 (1978).

8. W. Hartig, W. Rasmussen, R. Schieder and H. Walter, Z. Physik A **278**, 205 (1976); and Y. Zhu, A. Lezama, and T.W. Mossberg, Phys. Rev. A **39**, 2268 (1989).

9. H.M. Gibbs and T.N.C. Venkatesan, Opt. Commun. **17**, 87 (1976).

10. R.M. Whitley and C.R. Stroud Jr., Phys. Rev. A **14**, 1498 (1976).

11. G. Orriolis, Nuvo Cimento B **53**, 1 (1979); and H.R. Gray, R.M. Whitley and C.R. Stroud Jr., Opt. Lett. **3**, 218 (1978).

12. L. Allen and J.H. Eberly, Optical Resonances and Two-Level Atoms, (Dover, Mineola, NY, 1987).

13. Y. Zhu, (accepted for publication in Phys. Rev. A).

Figure Captions

Figure 1 (a) Energy level structure of a ^{138}Ba atom. γ_s (γ_w) is the spontaneous decay rate of the $^1P_1$ ($^3P_1$) state. ω_{gs} (ω_{gs}) is the $^1S_0 \rightarrow {}^1P_1$ ($^1S_0 \rightarrow {}^3P_1$) transition frequency. (b) Experimental setup. The cavity is used to increase the fluorescence signal that reaches the detector and does not significantly modify the total spontaneous emission rate of the atom.

Figure 2 Measured (dashed line) and calculated (solid and dot-dashed lines) fluorescence spectra near the $^1S_0 \rightarrow {}^1P_1$ transition frequency. (a) $\Omega_s \approx 35$ MHz, $\Omega_w = 0$, the spectrum corresponds to the monochromatic excitation of two-level atoms. (b) $\Omega_s \approx 35$ MHz, $\Omega_w \approx 43$ MHz, the spectrum is significantly modified from that of (a). See the text for a discussion of the significance of the observed 16-MHz spectral width. The channel width used in the experiment was 0.8 MHz.

Figure 3 Measured (dashed line) and calculated (solid and dot-dashed lines) fluorescence spectra near the $^1S_0 \rightarrow {}^1P_1$ transition frequency. (a) $\Omega_s \approx 55$ MHz, $\Omega_w = 0$. (b) $\Omega_s \approx 55$ MHz, $\Omega_w \approx 43$ MHz, the spectrum is significantly modified from that of (a).

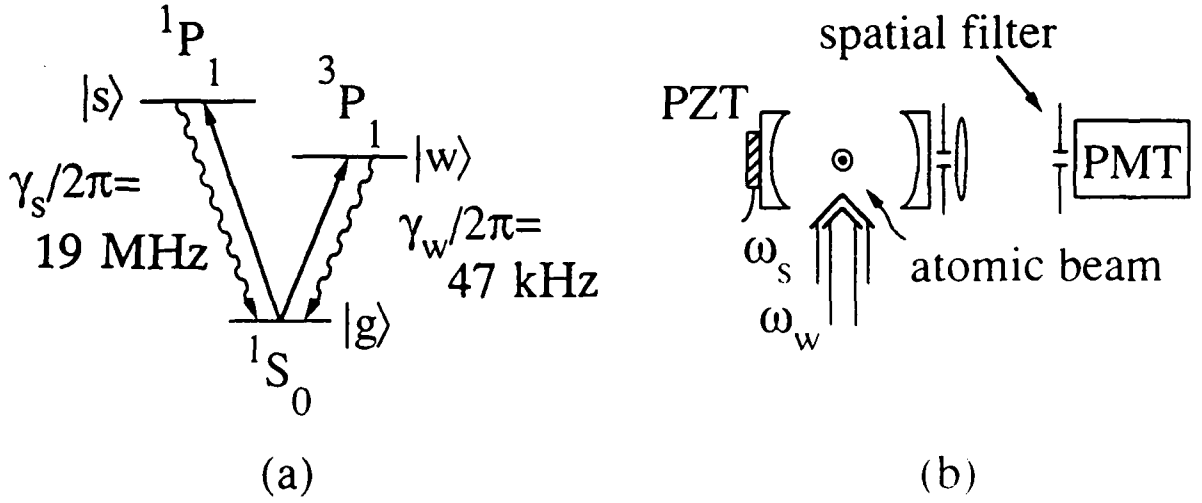

Figure 1 (a) Energy level structure of a ^{138}Ba atom. γ_s (γ_w) is the spontaneous decay rate of the $^1P_1$ ($^3P_1$) state. ω_{gs} (ω_{gs}) is the $^1S_0 \rightarrow {}^1P_1$ ($^1S_0 \rightarrow {}^3P_1$) transition frequency. (b) Experimental setup. The cavity is used to increase the fluorescence signal that reaches the detector and does not significantly modify the total spontaneous emission rate of the atom.

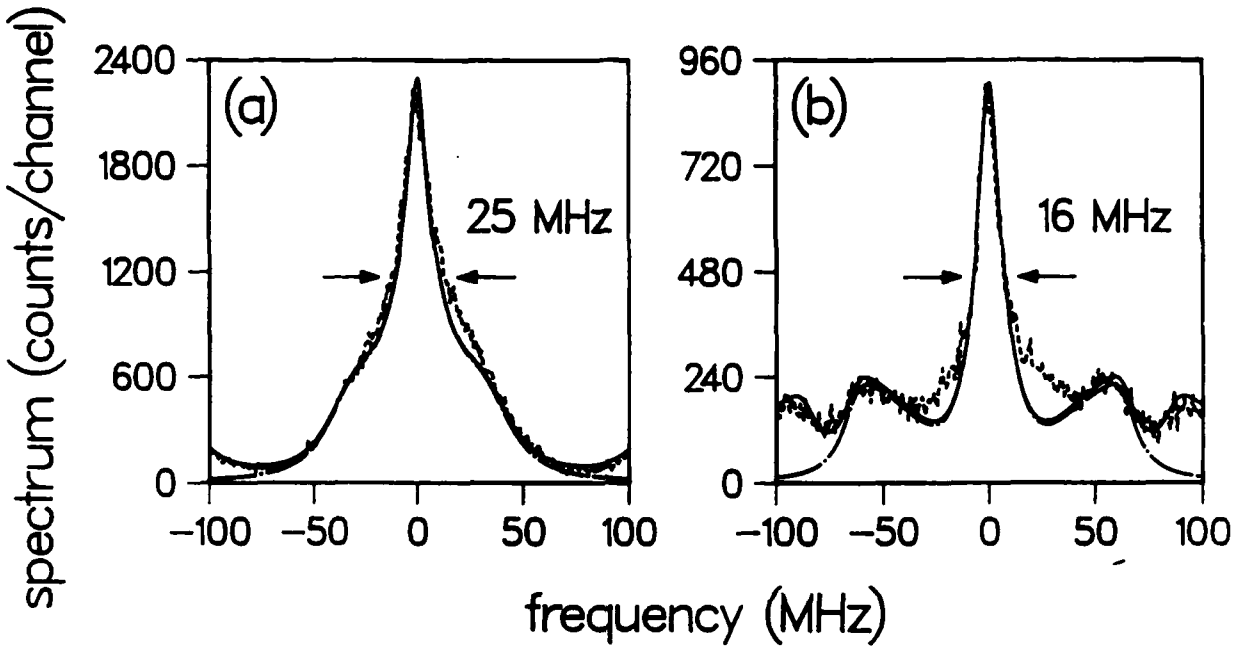

Figure 2 Measured (dashed line) and calculated (solid and dot-dashed lines) fluorescence spectra near the $^1S_0 \rightarrow {}^1P_1$ transition frequency. (a) $\Omega_s = 35$ MHz, $\Omega_w = 0$, the spectrum corresponds to the monochromatic excitation of two-level atoms. (b) $\Omega_s = 35$ MHz, $\Omega_w = 43$ MHz, the spectrum is significantly modified from that of (a). See the text for a discussion of the significance of the observed 16-MHz spectral width. The channel width used in the experiment was 0.8 MHz.

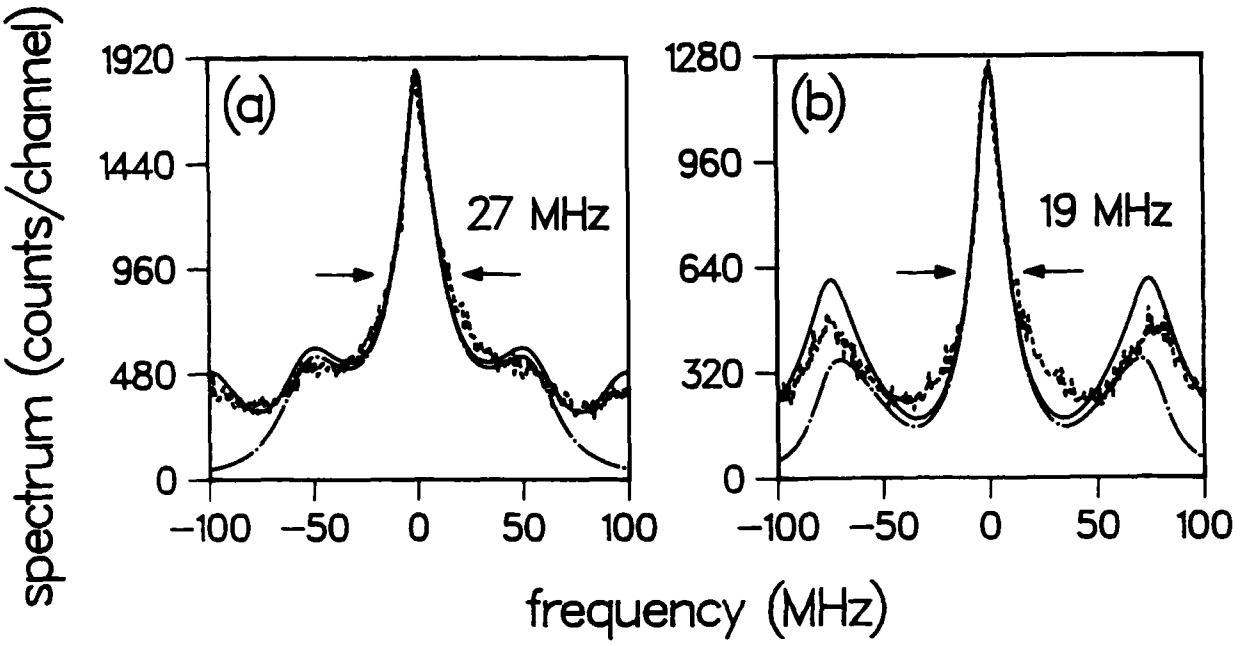

Figure 3 Measured (dashed line) and calculated (solid and dot-dashed lines) fluorescence spectra near the $^1S_0 \rightarrow {}^1P_1$ transition frequency. (a) $\Omega_s \approx 55$ MHz, $\Omega_w = 0$. (b) $\Omega_s \approx 55$ MHz, $\Omega_w \approx 43$ MHz, the spectrum is significantly modified from that of (a).

+149 OCS m Galley 25 ◆
EL 2-7-91 Cor EL 2-14-91

Prof. T.W. Mossberg
Phone: (503) 346-4779
FAX: (503) 346-4791

Spectrum of radiation from two-level atoms under intense bichromatic excitation

G. S. Agarwal

School of Physics, University of Hyderabad, Hyderabad 500 134, India

Yifu Zhu, Daniel J. Gauthier, and T. W. Mossberg

Department of Physics and Chemical Physics Institute, University of Oregon, Eugene, Oregon 97403

Received April 17, 1990; revised August 18, 1990; accepted January 15, 1991

We develop a theoretical framework for calculating the spectrum of resonance fluorescence emitted by two-level atoms that are excited by a strong bichromatic field. The dressed states for the two-level system that is interacting with a fully modulated field are identified, and the spectral features are interpreted in terms of transitions among these dressed states.

INTRODUCTION

Interpretation of the radiation emitted by an atom [redacted] interacting with an intense field is one of the key problems in quantum optics. In an early study Mollow[1] pointed out that the spectrum of the fluorescence is considerably different from the spectrum that is expected for weak monochromatic excitation.[2,3] It was later shown that the spectrum for a strong monochromatic field could easily be interpreted in terms of the dressed states[4] of the system.

AU: See manuscript p. 2

replace with: Determining the characteristics

More recently Zhu *et al.*[5] experimentally demonstrated that the fluorescence spectrum for the case of bichromatic excitation[6-12] differs qualitatively from the characteristic triplet spectrum that is observed for the case of strong monochromatic excitation. In this paper we present a theoretical approach to this problem and show that the fluorescence spectrum can be calculated by solving the coupled equations for the dipole–dipole correlation functions with continued-fraction methods. We find that the spectrum consists of multiple peaks whose spacing is independent of the Rabi frequency and that for on-resonance excitation the spacing is equal to half of the frequency difference of the two fields. These results are achieved by consideration of the dressed states of the system and the possible transitions among them. We also point out that a significant fraction of the total scattered power is contained in the elastic part of the spectrum even for large values of the Rabi frequency.

insert bichromatic-field-induced

replace with interpreted in terms

CALCULATION OF THE EMISSION SPECTRUM BY CONTINUED-FRACTION METHODS

Consider a two-level atom with transition frequency ω_0 and upper and lower states denoted by $|1\rangle$ and $|0\rangle$, respectively, that is driven by a bichromatic field with components ω_1 and ω_2. Let $S^{\pm}$ and S^z be the spin-1/2 angular-momentum operators for the dipole moment and for the inversion,[13] respectively. In a frame that is rotating at frequency ω_0 the optical Bloch equations, generalized for the case of bichromatic-field excitation, can be written as

0740-3224/91/050000-00$05.00

replace with n

where

$$\frac{\partial \phi}{\partial t} = \mathbf{M}\phi + [\mathbf{M}_- \exp(-i\Omega t) + \mathbf{M}_- \exp(i\Omega t)]\phi + \mathbf{I}, \quad (1)$$

when $\Omega = \omega_1 - \omega_2$ and ~~where~~ the column matrix ϕ has components $\phi_1 = \langle S^+(t)\rangle$, $\phi_2 = \langle S^-(t)\rangle$, and $\phi_3 = \langle S^3(t)\rangle$. The nonzero elements of the other matrices are

$$M_{11} = M_{22}^* = (i\Delta_2 - 1/T_2), \qquad M_{33} = -1/T_1,$$

$$M_{13} = M_{23}^* = -M_{31}^*/2 = -M_{32}/2 = ig_2^*/2,$$

$$(M_-)_{23} = -(M_-)_{31}/2 = -ig_1/2,$$

$$(M_-)_{13} = -(M_-)_{32}/2 = ig_1^*/2, \qquad I_3 = \eta/T_1,$$

where $\Delta_2 = \omega_0 - \omega_2$. The longitudinal and the transverse relaxation times are denoted by T_1 and T_2, respectively, and η is the population inversion in the absence of an applied field. The Rabi frequencies for the two components of the field are denoted by g_1 and g_2.

The resonance fluorescence spectrum is given in terms of the atomic dipole–dipole correlation function. Hence we introduce the correlation matrix $\Phi(t + \tau, t)$ with components

$$\Phi_1(t + \tau, t) = \langle S^+(t + \tau)S^-(t)\rangle - \langle S^+(t + \tau)\rangle\langle S^-(t)\rangle,$$

$$\Phi_2(t + \tau, t) = \langle S^-(t + \tau)S^-(t)\rangle - \langle S^-(t + \tau)\rangle\langle S^-(t)\rangle,$$

$$\Phi_3(t + \tau, t) = \langle S^3(t + \tau)S^-(t)\rangle - \langle S^3(t + \tau)\rangle\langle S^-(t)\rangle. \quad (2)$$

The inelastic spectrum is related to the correlation function Φ_1. It can be shown by means of the quantum regression theorem that the correlation matrix Φ satisfies Eq. (1) with $\mathbf{I} = 0$ and the substitutions $\partial/\partial t \to \partial/\partial\tau$ and $\exp(\pm i\Omega t) \to \exp[\pm i\Omega(t + \tau)]$. This new equation of motion can be simplified by decomposition of the correlation matrix into slowly varying amplitudes that oscillate at the modulation frequency and at its harmonics. This decomposition is given by the relation

$$\Phi = \sum_{l=-\infty}^{\infty} \Phi^{(l)} \exp[-il\Omega(t + \tau)]. \quad (3)$$

The evolution of these amplitudes is governed by

$$\frac{\partial \Phi^{(l)}}{\partial \tau} = (\mathbf{M} + il\Omega)\Phi^{(l)} + \mathbf{M}_-\Phi^{(l-1)} + \mathbf{M}_-\Phi^{(l+1)}. \quad (4)$$

$z = i(\omega - \omega_2)$.

We solve Eq. (4) by using Laplace transform techniques and denote the transformed correlation as $\hat{\Phi}^{(l)}(z)$, where $z = i(\omega - \omega_0)$. One can show that $\hat{\Phi}_1$ can be obtained from

$$\hat{\Phi}_1^{(l)}(z) = [\Phi_1^{(l)}(\tau = 0) + \tfrac{1}{2}ig_2^*\hat{\Phi}_3^{(l)} + \tfrac{1}{2}ig_1^*\hat{\Phi}_3^{(l+1)}]P_l. \quad (5)$$

The components $\hat{\Phi}_3^{(l)}$ and $\hat{\Phi}_3^{(l+1)}$ are determined from an inhomogeneous, three-term recursion relation given by

$$A_l\hat{\Phi}_3^{(l)} + B_l\hat{\Phi}_3^{(l-1)} + C_l\hat{\Phi}_3^{(l+1)} = D_l. \quad (6)$$

AU: See manuscript ✓ p. 4

The coefficients that appear in the recursion relation are given by

$$A_l = z + (1/T_1) - il\Omega + \tfrac{1}{2}|g_2|^2(P_l + Q_l) + \tfrac{1}{2}|g_1|^2(P_{l-1} + Q_{l+1}),$$

$$B_l = \tfrac{1}{2}g_1g_2^*(Q_l + P_{l-1}), \qquad C_l = \tfrac{1}{2}g_1^*g_2(P_l + Q_{l+1}),$$

$$D_l = ig_2P_l\Phi_1^{(l)}(\tau = 0) - ig_2^*Q_l\Phi_2^{(l)}(\tau = 0) + ig_1P_{l-1}\Phi_1^{(l+1)}(\tau = 0) - ig_1^*Q_{l+1}\Phi_2^{(l+1)}(\tau = 0) + \Phi_3^{(l)}(\tau = 0),$$

where

$$P_l = [z + (1/T_2) - il\Omega - i\Delta_2]^{-1},$$

$$Q_l = [z + (1/T_2) - il\Omega + i\Delta_2]^{-1}.$$

The physical quantity of interest is the stationary component of Φ_1 ~~with regard to its t dependence~~, which is given by $\Phi_1^{(0)}$ and can be obtained from Eq. (5) after substitution of Eq. (6). The solution of the recursion relation of Eq. (6) for the correlation amplitudes $\Phi_3^{(l)}$ is complex because of the inhomogeneities and is obtained with Green's-function techniques for recursion relations.[14]

The recursion relation of Eq. (6) requires the knowledge of the initial values of the correlations, which are given in terms of the single-time expectation values by

$$\Phi_1^{(l)}(\tau = 0) = \exp(il\Omega t)(\tfrac{1}{2} + \tfrac{1}{2}\phi_3 - \phi_1\phi_2),$$

$$\Phi_2^{(l)}(\tau = 0) = -\exp(il\Omega t)\phi_2\phi_2,$$

$$\Phi_3^{(l)}(\tau = 0) = -\exp(il\Omega t)\phi_2(1 + \phi_3). \tag{7}$$

We decompose the single-time expectation values into slowly varying amplitudes given by

$$\phi = \sum_{r=-\infty}^{\infty} \phi^{(r)} \exp(-ir\Omega t). \tag{8}$$

The slowly varying amplitude for the population inversion $\phi_3^{(r)}$ can be obtained from the recursion relation, Eq. (6), with $l = r$, $z = 0$, and with D_l replaced by $\eta\delta_{r,0}/T_1$, which can be solved with standard continued-fraction methods. The other slowly varying amplitudes are then obtained through the relations

$$\phi_1^{(r)} = \tfrac{1}{2}[ig_2^*\phi_3^{(r)} + ig_1^*\phi_3^{(r-1)}]p_r,$$

$$\phi_2^{(r)} = -\tfrac{1}{2}[ig_2\phi_3^{(r)} + ig_1\phi_3^{(r-1)}]q_r, \tag{9}$$

where $p_r = P_r(z = 0)$ and $q_r = Q_r(z = 0)$.

The inelastic spectrum $S_{in}(\omega)$ is obtained from $\hat{\Phi}_1$ according to

$$S_{in}(\omega) = \hat{\Phi}_1^{(0)}[i(\omega - \omega_2)] + \text{c.c.}, \tag{10}$$

The elastic part of the spectrum is obtained from $\langle S^+(t + \tau)\rangle\langle S^-(t)\rangle$, which is given by

$$S_{el}(\omega) = \sum_{j=-\infty}^{\infty} \delta(\omega - \omega_2 + j\Omega)|\phi_1^{(j)}|^2. \tag{11}$$

With the above formulation the elastic and inelastic contributions to the fluorescence spectrum can be calculated under a wide range of parameters of the bichromatic field.

We calculate fluorescence spectra by using values of the parameters that correspond to the situation studied experimentally by Zhu *et al.*,[5] i.e., $(\omega_1 - \omega_0)T_2 = -(\omega_2 - \omega_0)T_2 = 10$, $\Omega T_2 = 20$, $(\omega_1 + \omega_2)/2 = \omega_0$, $|g_1| = |g_2| \equiv |g|$, and $T_2 = 2T_1$. In the experiment the spectrum was measured for various values of the Rabi frequency $|g|$. The corresponding fluorescence spectra that are predicted by Eqs. (10) and (11) are shown in Fig. 1. We note that the spectra are symmetric. It is seen that the elastic peaks occur at frequencies $\omega_0 \pm (k + 1/2)\Omega$, $(k = 0, 1, 2, \ldots)$, as predicted by Eq. (11). The intensity of a given elastic peak depends on $|\phi_1^{(m)}|^2$, and it is seen that some elastic peaks are greatly enhanced for particular values of the Rabi frequency. The inelastic peaks occur at frequencies $\omega_0 \pm k\Omega/2$ $(k = 0, 1, 2, \ldots)$ ~~independently of the value of the Rabi frequency.~~ However, the number of peaks in the spectrum increases with as the Rabi frequency increases. We determine the width of the peaks directly from the plots and find that the linewidth (FWHM) of the central inelastic peak at ω_0 is approximately equal to $1/T_1$ and that the linewidth for the other inelastic peaks is approximately equal to $3/(2T_1)$. Our results are consistent with the numerical calculations of Newbold and Salamo,[15] who calculated the spectrum by direct integration of the equations of motion for the correlation functions.

insert
$\eta = -1$,

Fig. 1

insert
the g-independent

insert
Although the emission frequencies are g-independent,

AU: See manuscript
p. 7 Correct as typed

An interesting feature in the experimentally measured spectra[5] is that the spectral peaks at frequencies $\omega_0 \pm (k + 1/2)\Omega$ $(k = 0, 1, 2, \ldots)$ were narrower than the peaks at frequencies $\omega_0 \pm k\Omega$. We believe that the apparent narrowness of the peaks at frequencies $\omega_0 \pm (k + 1/2)\Omega$ results from the presence of both inelastic and narrow-linewidth elastic contributions to the fluorescence. Quantitative comparison of our theory and the experiment of Zhu *et al.*[5] requires detailed knowledge of experimental parameters that are not directly considered in our theory, such as the homogeneity of the driving field, the residual Doppler width, and the instrumental linewidth.

In Fig. 2 we plot the calculated spectra for the bichromatic excitation with the same parameters as those in Fig. 1 except $(\omega_1 + \omega_2)/2 - \omega_0 = 6/T_2$, corresponding to off-resonance excitation. The spectra are markedly asymmetric and apparently contain more peaks than in Fig. 1.

AU: See manuscript ✓
p. 8
Fig. 2

The calculated fluorescence spectra of Fig. 1 qualitatively demonstrate the importance of elastic scattering. We quantify these results by calculating the total fluorescence intensity $I_{\rm tot}$, the total elastic intensity $I_{\rm tot}^{\rm el}$, and the fluorescence intensity of some individual elastic peaks $I_n^{\rm el}$ as functions of the Rabi frequency. Results of these calculations are shown in Fig. 3, where for the purpose of comparison we plot the analogous quantities that are characteristic of resonant monochromatic excitation. In Fig. 3(a) we plot the total fluorescence intensity $I_{\rm tot} \propto (1 + \langle S^z \rangle)/2$ and find, in agreement with previous studies,[7-11] that it oscillates as a function of the Rabi frequency g. The peaks of $I_{\rm tot}$ have been referred to as Rabi subharmonic resonances.

AU: See manuscript ✓
p. 8

Fig. 3

Also plotted in Fig. 3(a) is the total elastic intensity, which is given by

$$I_{\rm tot}^{\rm el} \propto \sum_{m=-\infty}^{\infty} |\phi_1(m)|^2. \qquad (12)$$

superscript

$|\phi_1^{(m)}|^2$.

subscript

AB (5301r)
OCS Galley 25 05 ◆
2-8-91 Cor EL 2-14-91

One sees that in the bichromatic case elastic scattering remains significant for large values of the Rabi frequency and that the total elastic intensity also displays resonances. In Fig. 3(b) we plot the intensities of the first three elastic peaks, which occur at frequencies $\omega_0 \pm s\Omega/2$ ($s = 1, 3, 5$). Comparing Figs. 3(a) and 3(b), one sees that clearly the kth minimum in $I_{\omega t}$ occurs at the same Rabi frequency as the maximum in the intensity of the $(2k + 1)$th elastic peak for $k \geq 1$. The oscillations that are observed in the bichromatic case are completely absent in the case of resonant monochromatic excitation.

INTERPRETATION OF THE SPECTRUM IN TERMS OF THE DRESSED STATES

We ~~explain the origin of the features in the fluorescence spectrum by~~ develop a quantum-theoretical description of the interaction of the atom with a fully amplitude-modulated, two-frequency-component field. For $(\omega_1 + \omega_2)/2 = \omega_0$, the semiclassical Hamiltonian in the interaction picture for the atom and the fully modulated field is given by

$$H_I = -g/2[\exp(-i\Omega t/2) + \exp(i\Omega t/2)](S^+ + S^-), \tag{13}$$

and the fully quantized version of this Hamiltonian is given by

$$H = \tfrac{1}{2}\Omega b^+ b - g_0(b + b^+)S^x, \tag{14}$$

where $S^x = (S^+ + S^-)/2$. The quantization is carried out for the field with modulation frequency $\Omega/2$. If the mode b is in a coherent state $|\beta\rangle$, the coupling constant g_0 is related to the Rabi frequency g of the optical field by $g_0 = g/\beta = g/N^{1/2}$, where N is the expected number of modulated photons.[16] The photon content of the modulated field can be obtained easily by noting that the Hamiltonian given in Eq. (13) is essentially that for a displaced harmonic oscillator whose eigenstates are well known.[17]

Using the displacement operator $D(\alpha) = \exp(\alpha b^+ - \alpha^* b)$,[18] the eigenstates of the Hamiltonian can be shown to be[19]

$$|\Psi_\pm^{(n)}\rangle = D(\pm g_0/\Omega_0)|n\rangle|\psi_\pm\rangle, \tag{15}$$

where $|\psi_\pm\rangle = 1/\sqrt{2}(|1\rangle \pm |0\rangle)$ and $|n\rangle$ is the number state for the modulated field. Written in terms of the eigenstates $|\Psi_\pm^{(n)}\rangle$, the Hamiltonian with manifest eigenvalues becomes

$$H|\Psi_\pm^{(n)}\rangle = \left(\frac{n\Omega}{2} - \frac{g_0^2}{2\Omega}\right)|\Psi_\pm^{(n)}\rangle. \tag{16}$$

The matrix elements of D are given by

$$\langle m|D(\alpha)|n\rangle = \exp\left(-\frac{\alpha^2}{2}\right)\sum_q \frac{(-1)^q(\alpha)^{2q+m-n}(n!\,m!)^{1/2}}{q!(q+m-n)!(n-q)!}, \tag{17}$$

where we take α to be real. The matrix elements, Eq. (17), can be simplified in the semiclassical limit $\alpha \to 0$, $n \to \infty$, $\alpha\sqrt{n} \to$ constant and are approximately given by

$$\langle m|D(\alpha)|n\rangle = J_{m-n}(2\alpha\sqrt{n}), \tag{18}$$

where J_n is the Bessel function of order n.

The spectral features in the resonance fluorescence spectra can be interpreted as arising from transitions among the dressed states[20] given in Eq. (15). The transition matrix elements are

$$\langle \psi_{\pm}^{(m)} | S^{-} | \psi_{\pm}^{(n)} \rangle = \pm \tfrac{1}{2} \delta_{mn}, \tag{19}$$

$$\langle \psi^{(m)} | S^{-} | \psi_{\pm}^{(n)} \rangle = \pm \tfrac{1}{2} \langle m | D(\pm 2g_0/\Omega) | n \rangle. \tag{20}$$

The matrix elements of Eq. (19) contribute to the central peak at $\omega = \omega_0$, whereas the matrix elements of Eq. (20) lead to peaks at $\omega = \omega_0 + (m - n)\Omega/2$. In the semiclassical limit the matrix elements of Eq. (20) are given approximately by

$$\langle \psi^{(m)} | S^{-} | \psi_{\pm}^{(n)} \rangle = \pm \tfrac{1}{2} J_{m-n}(\pm 4g/\Omega). \tag{21}$$

The width of the transitions can be calculated from the decay of the density matrix elements in the basis, Eq. (15). For coherent transitions (elastic scattering), interference between transition amplitudes leads to the suppression of some spectral features. For example, the elastic scattering at $\omega_0 + (m - n)\Omega/2$ will be determined by

$$\langle \psi_{+}^{(m)} | S^{-} | \psi_{+}^{(n)} \rangle + \langle \psi_{-}^{(m)} | S^{-} | \psi_{-}^{(n)} \rangle = \frac{1}{2} \left\langle m \left| \left[\frac{2g_0}{\Omega} - D\left(-\frac{2g_0}{\Omega} \right) \right] \right| n \right\rangle, \tag{22}$$

which is zero when $m - n$ is even. We have verified that the matrix elements of Eqs. (19) and (20) correctly predict the intensity of the spectral features shown in Fig. 1.

It should be noted that for a fully amplitude-modulated field the field amplitude can vary as $\cos(\Omega t/2)$, a bichromatic field, or as $[1 + \cos(\Omega t/2)]$, a three-frequency field. The later case was analyzed by Blind *et al.*,[20] who showed that the atom–field eigenstates are the same as those shown in Eq. (15). In contrast, the eigenvalues for three-frequency excitation are equal to $\pm \tfrac{1}{2}g \pm \tfrac{1}{2}n\Omega - g_0^2/2\Omega$, which depend on the Rabi frequency and hence are dramatically different from those for bichromatic excitation [see Eq. (16)]. Consequently the elastic scattering for three-frequency excitation occurs at frequencies $\omega_0 \pm n\Omega/2$, whereas the inelastic scattering occurs at $\omega_0 \pm g \pm n\Omega/2$. This result shows that the fluorescence spectrum of two-level atoms that are excited by a fully amplitude-modulated field can have quite different characteristics, which are dependent on the specific form of the field. However, the variation of the total scattered intensity and the total elastic intensity as functions of the Rabi frequency are quite similar to the results for a three-frequency field.

CONCLUSIONS

In conclusion, we have developed a theoretical framework with a continued-fraction method, which is used to calculate the fluorescence spectrum of two-level atoms under strong bichromatic excitation. We have derived analytical expression for the dressed states of the system that consists of two-level atoms interacting with a fully amplitude-modulated, bichromatic field. The spectra can be interpreted in terms of the transitions among these dressed atom–field states.

Note added during publication: It has come to our attention that H. Freedhoff and Z. Chen[21] recently reported methods for calculation of the resonance fluorescence spectrum of a two-level atom in a bichromatic field. Some of the results presented in this paper appear to differ from those reported by Freedhoff and Chen.

insert

, Kumari and Tewari,[22] and Kumari[23]

ACKNOWLEDGMENTS

The work of G. S. Agarwal was partially supported by the Department of Science and Technology, Government of India. Research at the University of Oregon was financially supported by the National Science Foundation (PHY8718518) and the Air Force Office of Scientific Research (AFOSR-88-0086). This support is gratefully acknowledged.

REFERENCES AND NOTES

1. B. R. Mollow, Phys. Rev. **188**, 1969 (1969); see also A. I. Burshtein, Sov. Phys. JEPT **21**, 567 (1965) and **22**, 939 (1966) [J. Exp. Theor. Phys. (U.S.S.R.) **48**, 850 (1965) and **49**, 1362 (1965)].
2. W. Heitler, *The Quantum Theory of Radiation*, 3rd. ed. (Oxford U. Press, London, 1960), pp. 196–204.
3. The effect of nonmonochromaticity on the Mollow spectra has been investigated by G. S. Agarwal, Phys. Rev. Lett. **37**, 1383 (1976); J. H. Eberly, Phys. Rev. Lett. **37**, 1387 (1976).
4. C. Cohen-Tannoudji and S. Reynaud, J. Phys. B **10**, 345 (1977).
5. Y. Zhu, Q. Wu, A. Lezama, D. J. Gauthier, and T. W. Mossberg, Phys. Rev. A **41**, 6547 (1990).
6. Extensive research on emission and absorption in bichromatic fields has been done. For example, Refs. 7 and 8 (and references therein) examine in detail the total fluorescence and absorption as a function of one of the frequencies of the bichromatic field.
7. G. S. Agarwal and N. Nayak, J. Opt. Soc. Am. B **1**, 164 (1984); Phys. Rev. A **33**, 391 (1986); J. Phys. B **19**, 3385 (1986).
8. P. Thomann, J. Phys. B **13**, 1111 (1980).
9. S. Chakmakjian, K. Koch, and C. R. Stroud, Jr., J. Opt. Soc. Am. B **5**, 2015 (1988).
10. S. P. Goreslavsky, N. B. Delone, and V. P. Krainov, J. Phys. B **13**, 2659 (1980).
11. W. M. Ruyten, Opt. Lett. **14**, 506 (1989); Phys. Rev. A **40**, 1447 (1989); J. Opt. Soc. Am. B **6**, 1796 (1989).
12. Rich spectra associated with doubly amplitude-modulated excitation fields have been predicted by M. Wilkens and K. Rzazewski, Phys. Rev. A **40**, 3164 (1989).
13. The expectation values of the spin operators are given in terms of the expectation values of the density operator through the relations $\langle S^+(t)\rangle = \langle 0|\rho|1\rangle \exp(i\omega_1 t)$, $\langle S^-(t)\rangle = \langle 1|\rho|0\rangle \exp(-i\omega_1 t)$, and $\langle S^z(t)\rangle = \langle 1|\rho|1\rangle - \langle 0|\rho|0\rangle$.
14. See H. Risken, *The Fokker-Plank Equation* (Springer-Verlag, Berlin, 1984), Chap. 9, for an example of how Green's-function techniques can be applied to solve inhomogeneous three-term recursion relations.
15. M. A. Newbold and G. J. Salamo, Phys. Rev. A **22**, 2098 (1980).
16. Note that the number of modulated photons is equal to the number of optical photons, since the quantization is performed in the interaction picture. See, for example, B. Blind, P. R. Fontana, and P. Thomann, J. Phys. B **13**, 2717 (1980).
17. P. Carruthers and M. M. Nieto, Am. J. Phys. **33**, 537 (1965).
18. R. J. Glauber, Phys. Rev. **131**, 2766 (1963).
19. N. Polansky and C. Cohen-Tannoudji, J. Phys. (Paris) **26**, 409 (1965).
20. B. Blind, P. R. Fontana, and P. Thomann, J. Phys. B **13**, 2728 (1980), present approximate analytical results for the fluorescence spectra in an amplitude-modulated, three-frequency field under the assumption that the strength of the driving field is large enough to saturate the optical transition. They also assume that the carrier frequency of the driving field is resonant with the atomic frequency. ~~Similar approximate results for the resonant case have been obtained by M. K. Kumari and S. P. Tewari, Phys. Rev. A **41**, 5273 (1990).~~
21. H. Freedhoff and Z. Chen, Phys. Rev. A **41**, 6013 (1990).

replace with $\langle 1|\rho|0\rangle$

replace with $\langle 0|\rho|1\rangle$

22. M. K. Kumari and S. P. Tewari, Phys. Rev. A **41**, 5273 (1990).
23. M. K. Kumari, Ph.D. thesis, University of Hyderabad, 1990, unpublished.

Fig. 1. Theoretical fluorescence spectra produced by bichromatic-field excitation under the conditions $\Omega T_2 = 20$, $\Delta_2 T_2 = 10$, and $T_2 = 2T_1$. The spectra, from bottom to top, are for increasing values of the resonant Rabi frequency $g = |g_1| = |g_2|$ of the field components. gT_2 is (a1) 20, (a2) 15, (a3) 10, and (a4) 5. The curves in the left-hand column give the inelastic contributions to the fluorescence spectra, whereas the curves in the right-hand column show both elastic and inelastic contributions. The spectra are convolved with a Lorentzian transmission function with a linewidth $0.01/T_2$. The vertical axes of the figures are labeled with consistent units so that the fluorescence intensities can be compared. The average frequency $(\omega_1 + \omega_2)/2$ of the bichromatic field is equal to the atomic frequency ω_0.

Fig. 2. Calculated fluorescence spectra for bichromatic excitation. The parameters are the same as those in Fig. 1 except $(\omega_1 + \omega_2)/2 - \omega_0 = 6/T_2$, corresponding to off-resonance excitation. The relative intensity units are the same as those of Fig. 1.

Fig. 3. (a) Contributions to the fluorescence intensity versus the Rabi frequency g. The dashed curve represents the total scattering intensity I_{tot}, and the solid curve represents the total elastic scattering intensity I_{tot}^{el} for bichromatic excitation, as described in Fig. 1. The long-and-short-dashed curve and the dot-dashed curve represent the corresponding quantities for monochromatic excitation. (b) Elastic scattering intensity I_s^{el} for peaks at frequencies $\omega_0 \pm s\Omega/2$ (summed over + and −) as a function of the Rabi frequency g for the case of bichromatic excitation. Solid curve, elastic scattering intensity I_1^{el}; dotted curve, elastic scattering intensity I_3^{el}; dot-dashed curve, elastic scattering intensity I_4^{el}.

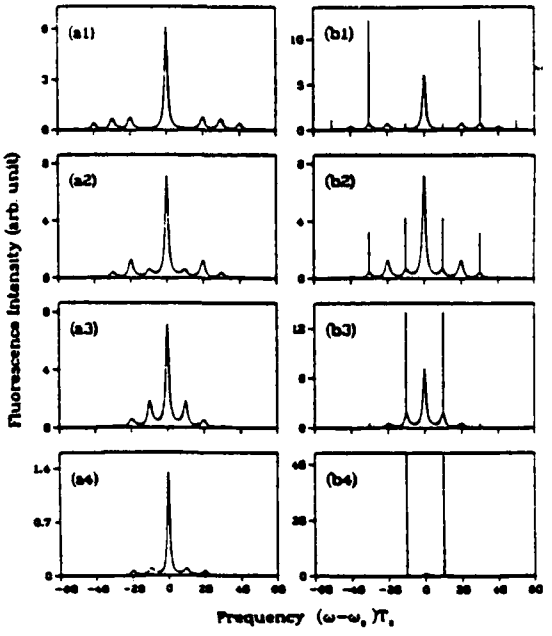
(a1)
(b1)
(a2)
(b2)
(a3)
(b3)
(a4)
(b4)
Fluorescence Intensity (arb. unit)
Frequency (ω−ω0)/Γ0

FIG. 1

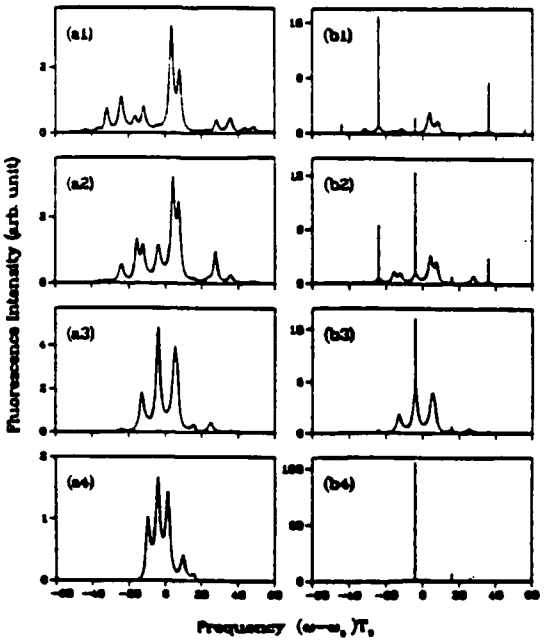
(a1)
(b1)
(a2)
(b2)
(a3)
(b3)
(a4)
(b4)
Fluorescence Intensity (arb. unit)
Frequency (ω−ω0)/Γ0

FIG. 2

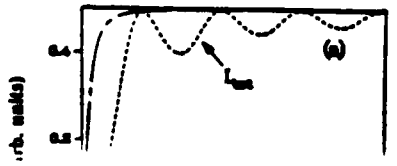
(a)
Lmax

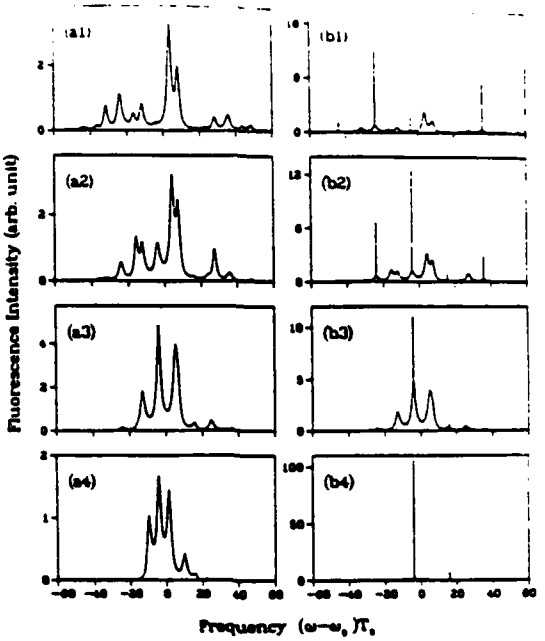

FIG. 2

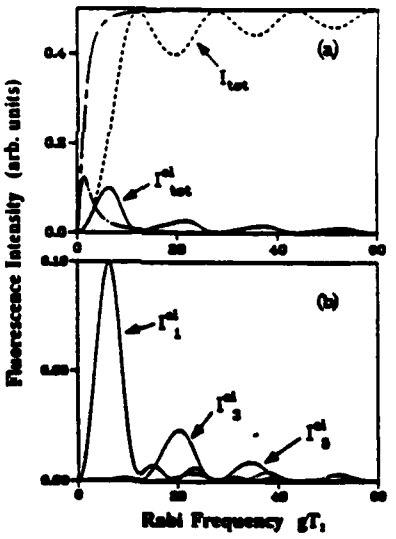

FIG. 3

JOSA B 5301